Probabilistic Run-out Modeling of a Debris Flow in Barcelonnette, France

HAYDAR YOUSIF HUSSIN

February, 2011

SUPERVISORS:
Prof. Dr. V.G. Jetten
Dr. C.J. van Westen

Probabilistic Run-out Modeling of a Debris Flow in Barcelonnette, France

HAYDAR YOUSIF HUSSIN
Enschede, The Netherlands, February, 2011

Thesis submitted to the Faculty of Geo-Information Science and Earth Observation of the University of Twente in partial fulfillment of the requirements for the degree of Master of Science in Geo-information Science and Earth Observation.
Specialization: Applied Earth Sciences

SUPERVISORS:
Prof. Dr. V.G. Jetten
Dr. C.J. Van Westen

THESIS ASSESSMENT BOARD:
Dr. D. Alkema (Chair)
Dr. L.P.H. van Beek (External Examiner, Utrecht University)
Prof. Dr. V.G. Jetten (1st Supervisor)
Dr. C.J. van Westen (2nd Supervisor)

ABSTRACT

The occurrence of debris flows have been recorded for more than a century in the European Alps forming a risk to settlements and other human infrastructure that have led to death, building damage and traffic disruptions. The aim of this study was to model the run-out of a channelized debris flow, in order to characterize the sensitivity of the outputs to the model input parameters and to spatially evaluate the possible ranges of the affected areas. A DEM was produced of the study area, which is located in the Barcelonnette Basin in the Southern French Alps, where two major debris flows had occurred in 1996 and 2003. These events were used for calibration of a debris flow with the 2D dynamic RAMMS (Rapid Mass Movements) modeling software applying the Voellmy rheology. A sensitivity analysis was carried out based on the calibrated input parameters and the available literature, resulting in 53 modeled run-outs. The resulting run-outs were applied to estimate the spatial frequency probability of the run-out distance onto the debris fan and the probability of the maximum debris flow height. The run-out distance and debris flow height was found to be most sensitive to the Voellmy turbulent coefficient ξ, while the total deposit volume was most sensitive to the RAMMS entrainment coefficient K. The estimated spatial probability of the debris flow run-out reaching the village on the debris fan was 75%. This estimation was based on the 53 modeled run-outs with an initiation volume of 16,728.4 m^3 and their corresponding input parameter values. The probability of the maximum debris height reaching 4 m at the fan apex was estimated at 26%, while a 4 m height at the village had a 2% probability. This research concluded that when an adequate DEM is used for modeling, RAMMS is capable of predicting a 4.7 km channelized debris flow from the initiation to the deposit zone. Furthermore, RAMMS can be a powerful modeling tool that can be used in the spatial estimation of the run-out probability, which forms one of the components in the hazard and risk assessment of debris flows.

ACKNOWLEDGEMENTS

In the name of God, Most Gracious, Most Merciful. All praise to the Creator of this magnificent planet we live on with its fascinating landscapes we study.

Before I start acknowledging everyone that has supported me during my research, I would like to summarize my experience at the I.T.C. in one sentence:

"I have never experienced an educational program where I have been able absorb so much knowledge in such a short period of time; it was truly a unique experience".

I would like to start off by thanking my father and mother, Dr. Yousif Ali Hussin and Mrs. Shahzanan Shaker for motivating me to complete my M.Sc. studies at the I.T.C. and their support throughout this period.

I thank the course director of the Applied Earth Sciences department Drs. Tom Loran for smoothly transitioning me into the M.Sc. program four months after it had started.

Thanks go to my supervisor Professor Victor Jetten for sharing his knowledge and comments on my thesis and how to approach the objectives and the physical modeling within my research. I have been acquainted with Professor Jetten since following his courses on land degradation at Utrecht University and he is truly a man with a lot of experience and knowledge.

Since my first years of following the B.Sc. program at Utrecht University I have been fascinated by the landslide phenomena. One morning in 2003 an expert in landslide hazard and risk assessment gave us a guest lecture on landslides. Who knew that this guest lecturer, Dr. Cees van Westen would become 8 years later my supervisor at the I.T.C. I would like to thank him for sharing his knowledge throughout the M.Sc. course and for his guidance and constructive comments on my thesis work.

I am in great debt to Mr. Byron Quan Luna. He has not only been an advisor to me but also a mentor. With his efforts I was introduced to the modeling software that made this thesis possible. His patience, lengthy discussions and comments on my thesis have further increased my knowledge on landslide mechanics and modeling. I wish him all the success in the completion of his Ph.D. at the I.T.C. and beyond.

Special thanks go to Marc Christen, Christoph Graf and Yves Bühler at the WSL/SLF Swiss Federal Institute for Snow Avalanche Research for giving me the chance to work with the powerful RAMMS (Rapid Mass Movements) modeling software they developed. I also thank them for their help on optimally using the software for my research.

I thank Dr. Jean-Philippe Malet, Prof. Theo van Asch and Dr. Santiago Beguería for sharing their knowledge and data on the study area and for their constructive meetings and advice on my research. Thanks also go to Dr. Alexandre Remaître, the Mountain Risks Project consortium and the French Forestry Office (ONF) for sharing the essential data of the study area for my research.

Thanks go to Drs. Nanette Kingma for sharing her experience, guidance and knowledge throughout the M.Sc. course and for all her help in the fieldwork in the French Alps. She seems to always care for her students and is truly the "Mother" of the Applied Earth Sciences department at the I.T.C.

I would like to thank Ir. Bart Krol, Dr. Dinand Alkema, Dr. Menno Straatsma and Mr. Wan Bakx for their discussions and insight in modeling, their information on fieldwork methods and manipulation of Digital Elevation Models. Thanks go to Dr. David Rossiter for opening my eyes to the fascinating world of statistics and also for his discussions on my work.

Further thanks and appreciation go to Mr. Benno Masselink, Mr. Job Duim and all the other staff members at the I.T.C. for the technical assistance and support.

Finally, I thank Darwin Edmund Riguer, Pooyan Rahimy, Syams Nashrrullah Suprijatna, Viet Tran, Rana Wiratama, Adeyemi Ezekiel Adetoro and all the other M.Sc. students for the good times and laughs throughout the M.Sc. program, in the fieldwork and in the final weeks of the thesis writing process in our M.Sc. room on the 5th floor of the I.T.C. building.

TABLE OF CONTENTS

LIST OF FIGURES

LIST OF TABLES

1. INTRODUCTION

1.1. Background

The term "landslide" encompasses a whole variety of slope movements and is defined by Cruden & Varnes (1996) as the "movement of a mass of rock, debris or earth down a slope" due to the slope failing under the force of gravity. A recent accepted method classifies landslides by their type of movement (fall, slide, flow) and material (rock, debris, earth) (Cruden & Varnes, 1996).

One of the most fascinating and destructive types of landslides are debris flows. A debris flow is exactly what the name suggests: a type of slope failure whereby material made up of debris ranging from unconsolidated soil particles to large boulders descends down a slope in a saturated flow like movement. They can move as granular rocky flows, muddy cement like flows, or as gradual change to floods with increasing water content such as hyper-concentrated flows (Jakob & Hungr, 2005). The debris flow phenomenon is especially challenging for researchers not only due to the wide ranging types of debris incorporated within the flow, but also due to the behavior of the debris flow run-out which can range from flowing on an open slope to being confined to a completely channelized environment.

Channeled debris flows have been extensively studied in the European Alps. One of these locations, where a large amount of data is available on past debris flow events, is the Barcelonnette basin in Southern France (Beguería et al., 2009; Flageollet et al., 1999; Malet et al., 2005; Maquaire et al., 2003; Remaître, 2006; Remaître & Malet, 2010). The basin has experienced since the 17th century extensive clear cutting of forests on slopes due to an increase in cultivation and tourism; this in turn has made the area more susceptible to debris flow hazards. The occurrence of debris flows have been recorded over more than a century in the Barcelonnette basin and form a risk to settlements and human infrastructure, leading to death, building damage and traffic disruptions (Flageollet et al., 1999). The expansion of infrastructure for tourism and winter recreational purposes has further increased the risk of people and property being affected by the debris flows. However, in the past decades the French government through the RTM (French Mountain Terrain Restoration Agency) and the ONF (French Forestry Office) have tried rehabilitating the affected areas by means of reforestation and the building of mitigation works in the form of check dams (Remaître & Malet, 2010).

The aim of this thesis is to model the run-out and debris flow height of a channeled debris flow in the Faucon catchment located within the Barcelonnette basin, in order to characterize sensitivity of the outputs to the model input parameters and to evaluate the possible ranges of the areas affected by the run-out.

The RAMMS (Rapid Mass Movements) numerical dynamic model (Christen et al., 2010c) developed by the Swiss Federal Institute for Snow Avalanche Research (WSL / SLF), which applies the Voellmy rheology will be used to model the run-out of the debris flow. Numerous studies have applied frictional and specifically the Voellmy rheology to model a wide range of mass movements like snow avalanches (Christen et al., 2010a; Christen et al., 2010c), rock avalanches (Hungr & Evans, 1996; Pirulli et al., 2004) and debris flows (Cesca & D'Agostino, 2006; Kowalski, 2008). Furthermore, the Voellmy rheological approach has found to be stable and robust when 2D modeling and back-analyzing channeled debris flows in the European Alps (Ayotte & Hungr, 2000; Rickenmann et al., 2006).

1.2. Problem Statement

Studies have been conducted in recent years on the Barcelonnette area to characterize past debris flow events (Flageollet et al., 1999; Maquaire et al., 2003). The most recent and well documented debris flows in the Faucon catchment took place in 1996 and 2003, causing significant damage to roads, bridges and property. Remaître et al. (2003) and Remaître et al. (2005a) modeled and back-analyzed the Faucon 1996 debris flow using the Herschel-Bulkley rheology with the Bing model (Imran et al., 2001). The model showed reasonably good results. However, this was a 1D model where entrainment was neglected and the velocities of the flow were overestimated.

The 2003 event was modeled in 2D by both Remaître (2006) and Beguería et al. (2009) using the Cemagref 2-D and MassMov2D models, respectively. The 2D advantage of these models was obvious, showing how the debris flow overflowed its channel on the debris fan. However, both of these studies only took the final 300 m of the debris flow run-out into consideration where the village of Domaine de Bérard was affected by the debris flow overtopping its channel.

There are several factors that determine the 'reach' of a debris flow and the associated hazard: the initial mass, the friction components during the flow and the amount of material picked up during the flow (scouring). The dynamic RAMMS model is based on the Voellmy-Salm model which assumes that the total basal friction of the flow can be split into a velocity independent dry-Coulomb friction coefficient μ and a velocity dependent turbulent coefficient ξ (Christen et al., 2010c). These rheological parameters can determine to a large part the run-out distance. Hence the so called Voellmy friction parameters are very important in run-out modeling and the associated hazard. Furthermore the DEM determines where the debris flow will occur, and in how far it will be confined to natural or artificial channels that occur in the landscape. The DEM quality therefore is important in the debris flow behavior.

This study attempts for the first time to model a complete channelized debris flow event in the Faucon catchment from the initiation zone till the run-out zone over a distance of 4.7 km in 2D with the physically based dynamic model RAMMS (Christen et al., 2010c), incorporating the process of entrainment and assessing the spatial probability of the modeled run-outs and debris flow heights. RAMMS was originally developed for modeling snow avalanches, thus making its application to debris flow modeling even more interesting. However, there have been studies that have applied RAMMS to model debris flows in the past (Cesca & D'Agostino, 2006; Kowalski, 2008).

1.3. Reasearch Objectives

The main objective of this research is to use a probabilistic method to assess the run-out and debris flow heights of a debris flow located in the Barcelonnette Basin in the Southern French Alps. Model parameterization and calibration is required to obtain run-outs and deposit heights based on real events that have occurred in the catchment. The sensitivity of the model to the input parameters will be assessed and finally the probability of the run-out and deposit heights are obtained using a simple probabilistic method. The sub-objectives of this research are:

1. To assess the applicability of the Voellmy rheology applied by the RAMMS software, originally designed for snow avalanches, to model debris flow run-outs in channelized environments

2. To calibrate the model input parameters in order to obtain debris flow run-outs and heights based on the past events in the Faucon catchment

3. To determine the sensitivity of the RAMMS dynamic model with respect to the various input parameters

4. To study the effect of the DEM used as input in the run-out model

5. To obtain the spatial probability of the modeled debris flow run-out and deposit height

1.4. Research Hypotheses

The hypotheses are based on some of the research objectives and are stated as follows:

- The Voellmy rheology should be capable of modeling debris flows in the given catchment. This Hypothesis is based on the fact that the Voellmy rheology has been used to model debris flows in other areas in recent studies (Cesca & D'Agostino, 2006; Hungr & Evans, 1996; Kowalski, 2008).

- The DEM accuracy can significantly influence the output of the run-out model.

- The RAMMS dynamic model can be used to analyze the run-out probability in the given catchment.

1.5. Thesis Structure

This thesis is structured as follows:

Chapter 1 introduces the thesis by explaining why the research should be carried out and stating the objectives of this research.

Chapter 2 is a literature review describing the debris flow phenomena and gives insight on the aspect of debris flow modeling.

Chapter 3 describes the Faucon catchment study area and summarizes the 1996 and 2003 debris flow events.

Chapter 4 is dedicated to the methods and materials used in this research, from the fieldwork phase until the final stages of modeling the debris flow. It includes the calibration and the sensitivity analysis of the model parameters and the method used to obtain the probability of the run-out and debris heights.

Chapter 5 reveals the results of the DEM creation, physical modeling of the debris flow and the associated sensitivity analysis and probability analysis.

Chapter 6 discusses each part of the results revealed in Chapter 5.

Chapter 7 finally concludes this research by stating which objectives have been met and giving recommendations for future studies.

2. LITERATURE REVIEW

2.1. The Debris Flow Phenomenon

The terminology of debris flows is wide ranging and has been updated over the years by researchers studying the phenomena. Debris is defined as a mixture of unsorted material which can contain everything from clays to cobbles, boulders and organic material. It is described has having a low plasticity and is produced by mass wasting processes (Hungr et al., 2001). The definition of debris flows by Varnes (1978), which is part of a landslide classification, is commonly used by researchers and states that "flows are rapid movements of material as a viscous mass where inter-granular movements predominate over shear surface movements. These can be debris flows, mudflows or rock avalanches, depending upon the nature of the material involved in the movement". Hungr et al. (2001) however proposed what they call "more precise terms" for the classification of flow type landslides and defined a debris flow as "a very rapid to extremely rapid flow of saturated non-plastic debris in a steep channel. Plasticity index is less than 5% in sand and finer fractions". Plasticity is the ability of a material to retain its shape attained by pressure deformation. The classification further describes debris flows as being confined to well established channels where the water content increases as the flow descends down its path (Table 1).

Whatever the definition used, it is obvious that debris flows have an interaction between fluid and solid forces (Iverson, 1997) which discriminates them from other types of landslides. Furthermore, the type of material, movement and velocity gives debris flows their distinct character.

Table 1 The classification of flow type landslides (after: Jakob & Hungr (2005))

Material	Water content[1]	Special condition	Velocity	Name
Silt, sand, gravel, and debris (talus)	Dry, moist, or saturated	No excess pore-pressure Limited volume	Various	*Non-liquefied sand (silt, gravel, debris) flow*
Silt, sand, debris, and weak rock[2]	Saturated at rupture surface	Liquefiable material[3] Constant water content	Extremely rapid	*Sand (silt, debris, rock) flow slide*
Sensitive clay	At or above liquid limit	Liquefaction *in situ*[3] Constant water content[4]	Extremely rapid	*Clay flow slide*
Peat	Saturated	Excess pore-pressure	Slow to very rapid	*Peat flow*
Clay or earth	Near plastic limit	Slow movements Plug flow (sliding)	Less than rapid	*Earth flow*
Debris	Saturated	Established channel[5] Increased water content[4]	Extremely rapid	*Debris flow*
Mud	At or above liquid limit	Fine-grained debris flow	Greater than, very rapid	*Mud flow*
Debris	Free water present	Flood[6]	Extremely rapid	*Debris flood*
Debris	Partly or fully saturated	No established channel[5] Relatively shallow, steep source	Extremely rapid	*Debris avalanche*
Fragmented rock	Various, mainly dry	Intact rock at source Large volume[7]	Extremely rapid	*Rock avalanche*

[1] Water content of material in the vicinity of the rupture surface at the time of failure.
[2] Highly porous, weak rock (examples: weak chalk, weathered tuff, pumice).
[3] The presence of full or partial *in situ* liquefaction of the source material of the flow slide may be observed or implied.
[4] Relative to *in situ* source material.
[5] Presence or absence of a defined channel over a large part of the path, and an established deposition landform (fan). *Debris flow* is a recurrent phenomenon within its path, while *debris avalanche* is not.
[6] Peak discharge of the same order as that of a major flood or an accidental flood. Significant tractive forces of free flowing water. Presence of floating debris.
[7] Volume greater than 10,000 m^3 approximately. Mass flow, contrasting with fragmental rock fall.

The other types of flow like landslides which are similar to debris flows are mud flows, debris floods and debris avalanches (Table1). According to Jakob & Hungr (2005) mud flows are flow types with more

water content and have higher plasticity (> 5%), debris floods contain even more water having a surge like motion as it flows down the channel, and debris avalanches are mainly shallow flows of partially or fully saturated debris on steep slopes that are not necessarily confined to an established channel.

Velocity is a key variable that determines the destructiveness and catastrophic influence of debris flows around the world (Table 2). They can reach extreme velocities and increase their sediment charge, picking up more sediment and larger objects down the run-out path. The debris flows discussed in this thesis are of the extremely rapid type of flows.

Table 2 Landslide rates of movement (after: WP/WLI (1995))

Movement Rate	Velocity Class	Velocity Limits	Rate (mm/sec)	Debris Flow Range
Extremely rapid	7	5m/sec	5×10^{3}	
Very rapid	6	3m/min	50	
Rapid	5	1.8m/hour	0.5	
Moderate	4	13m/month	5×10^{-3}	
Slow	3	1.6m/year	50×10^{-6}	
Very slow	2	16mm/year	0.5×10^{-6}	
Extremely slow	1			

Two main forms of debris flows can be distinguished: hillslope (open-slope) debris flows and channelized debris flows (Figure 1). Hillslope debris flows create their own path down the valley slope as tracks or sheets, depositing their material on lower slope gradients (Cruden & Varnes, 1996). Channelized debris flows follow existing channels like valleys, gullies and other types of topographic depressions. According to Cruden & Varnes (1996), the channelized flows are of high density with 80% solids by weight. Channelized debris flows further seem to have a consistency similar to that of wet concrete in many cases (Hutchinson, 1988). The studied debris flows in this research are of the channelized type.

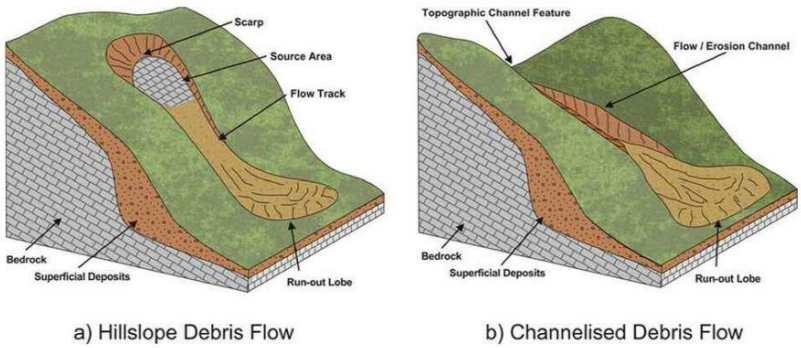

Figure 1 (a) Hillslope and (b) channelized debris flows (after: Nettleton et al. (2005))

There are three main divisions in a debris flow path: the initiation zone, the transport zone and the deposition zone (Figure 2). The initiation zone consists of a steep open slope or can contain depressions like gullies and existing stream channels. In this zone, a slope failure or an increase in discharge in a channel triggers material to loosen and descend down the slope. Debris flows at the initiation zone can first start off as other type of landslides like translational/rotational landslides, scree/rock falls, rock slides or debris avalanches and eventually form into a debris flow further down the flow path.

Heavy rainfall forms an important triggering factor which contributes to the disintegration of sediment and combines it with surface water to further mobilize the flow downstream. Channelized debris flows can be further mobilized by entrainment of unconsolidated sediment, by extreme flows following in stream valleys or other depressions. The collapse of natural or artificial dams that have blocked channels previous to the debris flow event can also trigger the initiation (Nettleton et al., 2005).

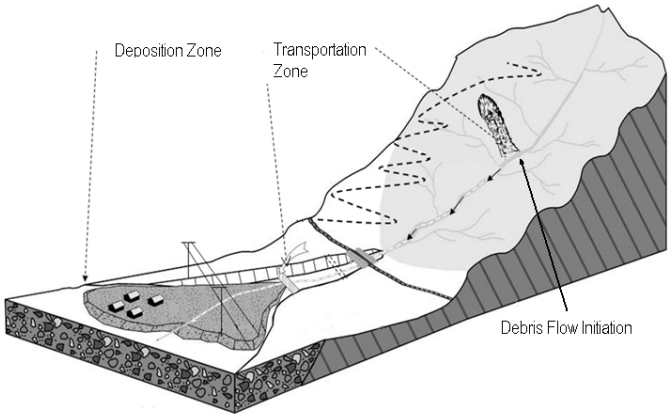

Figure 2 Schematic of a debris flow path (after: DNV (2011))

The transport zone is a transitional zone, often a steep mountain channel, where debris is incorporated by erosion (entrainment). Coarse granular avalanches can shift into a flow like motion, where volume and saturation of the debris flow is most likely to increase within the transport zone. A debris flow is able to flow as one single wave or several successive surges. In the transport zone of the flow path the decrease in slope angle once reaching below a specific value starts triggering the deposition of debris (Jakob & Hungr, 2005). Deposition within the transportation zone, when observed in the field can have the form of levees or cone-shaped lobes.

The deposition zone is in most cases a debris fan and starts at the fan apex, where the debris flow starts depositing material as the slope decreases. Possible reasons for deposition of debris onto the fan are obstructions within the channel, momentum loss on bends or decrease in channel height, causing the flow to be less confined and avulsions to take place. This zone is most likely to have elements at risk being hit by the debris flow deposits like bridges, roads, houses and electrical lines.

2.2. The Concept of Debris Flow Hazard and Risk

The assessment of the risk to mass movements (Figure 3) including debris flows is crucial for the prediction of future hazard events in order to protect people and property and to estimate any future losses. It further forms the basis for risk management which comprises of the prevention, preparedness, relief and recovery of people and property from these hazards (van Westen, 2010). Determining mitigation and prevention methods are needed to reduce the risk to debris flows (Figure 4).

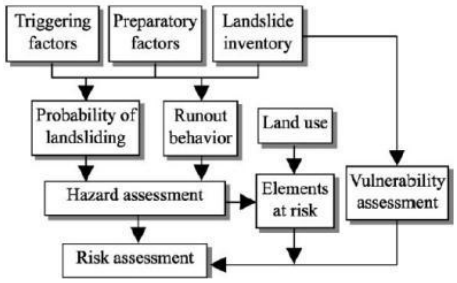

Figure 3 Framework summarizing the steps in a landslide risk assessment (adapted from: Dai et al. (2002))

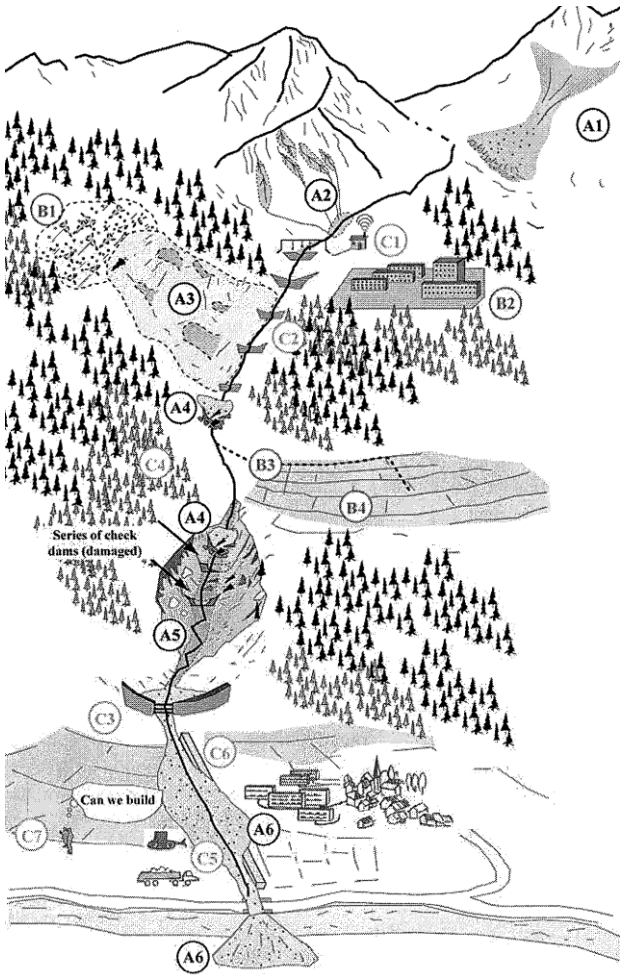

Figure 4 Aspects of debris flow risk. (A) Processes determining debris flow hazards: (A1) Landslide initiation, (A2) erosion, (A3) Shallow slides, (A4) natural dams, (A5) incision and bank erosion, (A6) overflow onto the debris fan. (B) Impact of humans to debris flow hazards: (B1) deforestation, (B2) urbanization, (B3) Drainage routing, (B4) land cultivation and degradation. (C) Mitigation: (C1) early warning, (C2) check dams, (C3) storage basins, (C4) reforestation, (C5) clearing storage systems and channels, (C6) deflection walls, (C7) land use planning (after: Remaître & Malet (2010))

Risk is defined as "the probability of losses" of elements (people or property) vulnerable to hazards and is quantitatively expressed by the following equation (van Westen, 2010):

$$\text{Risk} = \text{Hazard} * \text{Vulnerability} * \text{Value of elements-at-risk} \quad \text{(Eq. 1)}$$

When the conditional probability of landslide risk is taken into account, Equation 1 can be rewritten as follows (van Westen, 2010):

$$RS = (PT * PS * PR) * V * A \quad \text{(Eq. 2)}$$

where RS is the specific annual risk expressed in monetary values of an element at risk vulnerable to a landslide, PT is the temporal probability of the landslide occurrence, PS is the spatial probability of the landslide occurrence, PR is the conditional probability of run-out with a landslide having a specific type and volume, V is the physical vulnerability of the element at risk to the landslide event and A is the monetary value of the element at risk. (PT * PS * PR) can be described as the hazard component of risk or simply the debris flow hazard. Thus, the debris flow hazard has a time component and a magnitude component. The time component is the probability or likelihood of a debris flow occurring at a specific

time in the future and is expressed as an annual probability or the chance of an even occurring within a specific return period like 5, 10 or 50 years.

The magnitude component of the debris flow can be expressed in run-out distance, peak discharge or volume (Jakob, 2005). The run-out distance is the distance from the point of initiation until the point of complete deposition and stoppage of the flow. The peak discharge is the maximum cross-sectional area multiplied by the debris flow velocity at a specific time interval when the flow occurs at the maximum cross-sectional area. The impact pressure is also considered a magnitude component if it is used in relating it to the vulnerability of a house or other elements at risk to the actual force applied by the incoming debris flow (van Westen, 2010).

Estimating debris flow volumes is crucial for mitigation works and structurally confining the flow, whether it is building check dams or adjusting the channel at the debris fan. The total debris flow volume (Vt) reaching the fan apex is calculated by the following equation (Jakob, 2005):

$$Vt = \sum Vi + \sum Ve - \sum Vd \quad \text{(Eq. 3)}$$

where $\sum Vi$ is the total initiation volume for all the initiation zones combined, $\sum Ve$ is the total entrained volume and $\sum Vd$ is the total volume of deposition on the transport zone and deposition zone. Remote sensing (photogrammetry) and field observations can be used to estimate the average depth of debris flow scars, the initiation volumes and the deposited volumes. However, in most cases the exact information on deposit volumes after the occurrence of the event, is not well known and must be estimated using empirical relationships (Rickenmann, 1999). Estimating the entrainment volume is a more difficult task, however the simplest method is to assume all available debris and stored material is entrained by the debris flow in the transport zone. If the available debris is unknown prior to the event, than initiation volume can be subtracting from the total deposited volume.

Debris flow hazard magnitudes can be further determined by the hazard intensity. Debris flow hazard intensity parameters are: velocity, flow depth, maximum deposit thickness, impact force and the debris flow run-up onto elements at risk (Jakob, 2005).

This thesis specifically looks at the spatial probability of the run-out distance and debris flow heights. Debris volumes, velocities and deposit heights are further assessed in this research to calibrate with past events as will be discussed in Chapter 4.

2.3. Debris Flow Run-out Modeling

Prediction of debris flow run-outs are important to assess areas that will be affected by the hazard, to determine the debris flow intensity parameters and to produce hazard and risk maps (Rickenmann, 2005). Researchers have developed a considerable number of methods over the past several decades to predict the run-out of debris flows. Spatial modeling is a tool that has been used to replicate past debris flow events in order to understand their behavior and to predict future events. Brunsden (1999) explains that there is no single model that can perfectly replicate the complexity of landslides, however he mentions "considerable progress has been made in isolating many of the variables involved" in the modeling of landslides.

Methods to predict the run-out distance are generally divided into three different approaches: empirical-statistical approaches, physical scale modeling and physically based dynamic models (Figure 5).

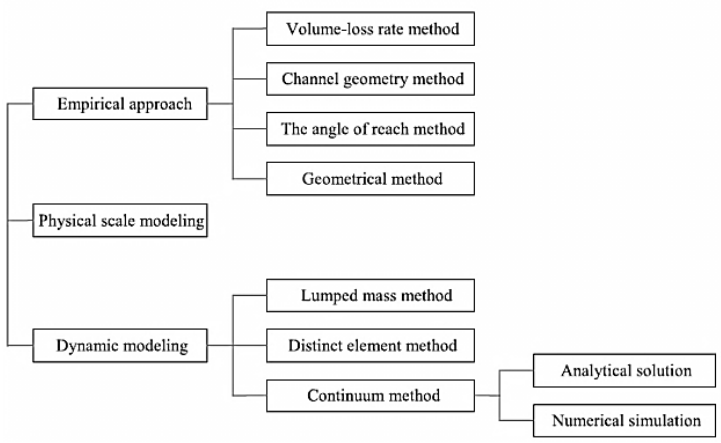

Figure 5 Summary of the run-out prediction approaches (adapted from: Chen & Lee (2004))

Rickenmann (1999) has done extensive work summarizing some of the empirical approaches. These approaches are based mainly on a great amount of collected historic data of debris flow run-outs and other parameters, producing empirical relationships. For example, the total debris flow deposit volume is considered one of the most important parameters for the prediction of other intensity parameters like the peak discharge and the velocity. Rickenmann (1999) has found that the empirical relationships between the deposit volume and the peak discharge of debris flows can be described in linear empirical equations. These equations are obtained from the estimation of debris flow volumes and their peak discharges gathered all across the world from Switzerland to Japan.

The angle of reach method is an example of an empirical approach, described by Chen & Lee (2004), used to determine the relationship between the angle of reach and landslide volumes, vertical drops and the run-out extent. This method uses regression plots and equations to predict these parameters.

Empirical approaches are simple and practical tools to estimate the travel distance of the run-out, but do not look into the rheology of the debris flow or into the mechanics of the movement. Furthermore, there needs to be sufficient field observations in order to adequately derive the empirical relationships (Chen & Lee, 2004).

Physical scale modeling applies controlled field and laboratory experiments to study debris flow mechanics. These models use debris flow flumes to simulate an event and further analyze the flow with high-speed photography or by videotaping the run-out (Iverson, 1997). However, these experiments can be expensive to carry out and can contain uncertainties do to their geometric scale. Applying these methods to field situations is not always suitable due to the difference in scale and mechanics of the modeled output (Dai et al., 2002).

Dynamic models use numerical methods applying energy and momentum conservation laws. Examples of dynamic models are: distinct element models, lumped mass models and continuum based models (Figure 5). Lumped mass models describe the motion of a flow as a single point or sheet spreading out with excess pore water pressure generated by liquefaction. The flow moves in one dimension and neglects the dissipation of the flow in more than 1 direction (Dai et al., 2002).

1D models move the flow in a single direction, assuming the flow stays in a channel and does not disperse. However, if a flow reaches a debris fan and overtops its banks then 2D models are required to

replicate the extent of the run-out onto the debris fan. Distinct element methods represent the flow as an assemblage of blocks formed as connected fractures in the separate blocks. The motion of these blocks are solved by equations of motion replicating the contact between the blocks (Hungr et al., 2005).

Continuum numerical models use fluid mechanics applying conservation equations of mass, momentum and energy for describing the debris flow dynamic motion. These models use rheology to further describe the behavior of the debris flow material (Brunsden, 1999). What is essential in dynamic continuum modeling of debris flows is the choice of the right rheology and the associated friction parameters (Rickenmann, 2005). Physically based continuum numerical models are able to determine the deposition and flow parameters along the whole debris flow path. The continuum models applying the rheological conservation laws of momentum and energy use friction parameters to explain the channel roughness and turbulence within a debris flow (Rickenmann, 2005).

There are several rheological models that have been used to describe the motion of debris flows like the Bingham fluid model, where the fluid acts as a rigid body at low shear stress and flows like a viscous fluid at higher rates of shear stress, thus described as a visco-plastic fluid (Jakob & Hungr, 2005). The Herschel-Bulkley fluid model is another non-Newtonian fluid, which gives a non-linear relationship between the stress and strain. Both the Bingham and Herschel-Bulkley models were used by Remaître et al. (2003) to model a past debris flow event in Barcelonnette, France, further discussed in Chapter 3. The Bingham model was modified to incorporate the Coulomb friction leading to the Coulomb-Viscous model which was also used to model a debris flow in the Barcelonnette area by Beguería et al. (2009).

The Voellmy rheology is another rheological model that has been extensively used to simulate debris flows (Ayotte & Hungr, 2000; Hungr & Evans, 1996; Rickenmann et al., 2006) and applies the frictional-turbulent resistance to model the resistance at the base of the flow. This research will approach the modeling of the debris flow using the dynamic continuum numerical method, applying the Voellmy rheology in the RAMMS dynamic modeling software (Christen et al., 2010c) and will be discussed in detail in Chapter 4.

2.4. Parameter Uncertainty in Rheological models

Assessing the risk of mass movements requires estimating the probability of the hazard component. There are numerous studies that have summarized the methods used to assess this probability (Dai et al., 2002; Soeters & van Westen, 1996). Dynamic continuum models are one of the most sophisticated and widely used methods applied to assess the hazard of mass movements. The rheological models used in dynamic continuum approaches require the user to estimate the corresponding values for the rheological parameters. There are three main approaches to estimate these parameters: they can be derived from laboratory tests or empirical laws from samples gathered in the field after the occurrence of an event, they can be obtained from back-calibrating a model to a past event, or can be derived from previous back-calibrated events and values published in literature (Quan Luna et al., 2010). Obtaining rheological parameters for calibrating a debris flow event is subjected to uncertainties due to the variation in the value parameters.

Probability density functions (pdf) are used to describe the likelihood of a continuous random variable to occur at a given point. They are produced by classing the frequency of the parameter value in intervals and approximating the frequency with a curve. Quan Luna et al. (2010) produced pdfs for the frictional-turbulent Voellmy parameters. These pdfs can be used in the future to assess the uncertainty of a parameter in a stochastic approach by randomly generating the rheological parameter and using it as an input into a continuum model.

The Monte Carlo approach applies random sampling (stochastic approach) of input parameters to provide estimates of their uncertainty. The approach is based on methods of random sampling of variables that have significant uncertainties in inputs, using computational algorithms to output their results and are often applied in risk assessment (Hubbard, 2007). Monte Carlo methods are capable of repeatedly generating rheological parameter values randomly from existing probability density functions. The outputs can then be used as inputs into the dynamic continuum models. Furthermore, the Monte Carlo approach has been applied in other aspects of landslide hazard and risk assessment (Calvo & Savi, 2009; Gorsevski et al., 2006; Liu, 2008).

When the probability density function is unknown or simply unavailable, other methods are needed to approximate the uncertainty of the input parameter. The FOSM (first-order second-moment) approach is used to estimate a pdf by using the first-order approximations of Taylor series expansions of the mean and the variance (second-moment parameters) of parameter values, thus estimating their uncertainty (Uzielli et al., 2006). The FOSM method has been applied for probabilistic slope stability analysis (Düzgün & Özdemir, 2006; Griffiths et al., 2008) and landslide vulnerability estimations (Uzielli et al., 2006).

The range of the rheological input parameters for calibrating the model in this research were obtained from a literature study. Based on the calibrated parameter values, a systematic sampling approach within the given range was used for the sensitivity analysis as will be described in Chapter 4. Due to the lack of time and material, the uncertainty of the parameter values could not be quantified as will be discussed in Chapter 6.

3. STUDY AREA

3.1. Overview

The study area is the Faucon catchment forming part of the Faucon commune and located in the Barcelonnette basin (Figure 6 and 7), in the department of Alpes-de-Haute-Provence in the French Alps. The basin is one of the sections of the Ubaye river valley, located in the Southern French Alps. The French commune is the lowest level of administrative division within the French Republic and their division in the Alps is based on natural boundaries or sub-catchments. The elevation in the basin ranges from 1100 to 3000 m and slope gradients vary from 20° to 50°. The landuse is mainly forest (60%), agricultural lands and bare lands with bad-lands and gullying. The basin experiences strong storm intensities (over 50 mm/h) in the summer and around 130 days of freezing per year, having a dry and mountainous Mediterranean climate.

Figure 6 Location of the Barcelonnette Basin and the Faucon catchment (traced)

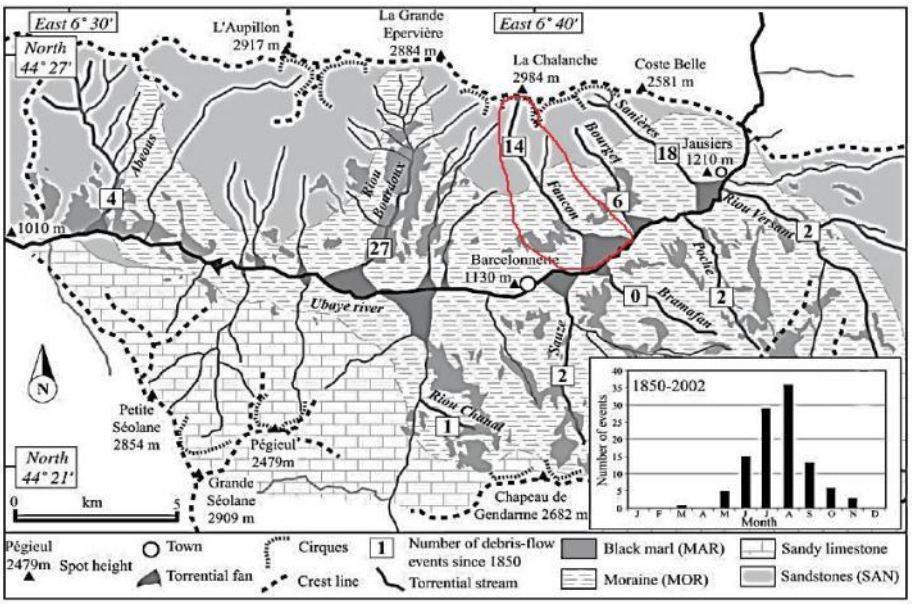

Figure 7 A sketch of the Barcelonnette basin and the Faucon catchment (red). The bottom right chart indicates monthly number of debris flow occurrences (adapted from: Remaître et al. (2005b))

The South facing slopes in the basin (Figure 7) experience most of the mass movement occurrences due to the location of springs between the permeable Autapie sheet thrust which is coarser and the Callovo-Oxfordian black marls and due to the fact that the south facing slopes are steeper than the north facing slopes (Remaître et al., 2005b).

The Faucon catchment (Figure 8) covers an area of 10.5 km², with an elevation ranging from 1150 to 2984 m. The catchment is comprised of a 5500 m long steep torrent with a steady flow of water streaming throughout the year into the Ubaye River. The peak discharge of the stream is in the spring season when snow starts melting and in the autumn when precipitation is high. The discharge in the summer can peak according to intense storm occurrences. The torrent slope ranges from 80° at the headwater of the catchment to 4° at the alluvial fan, with an average slope of 20°.

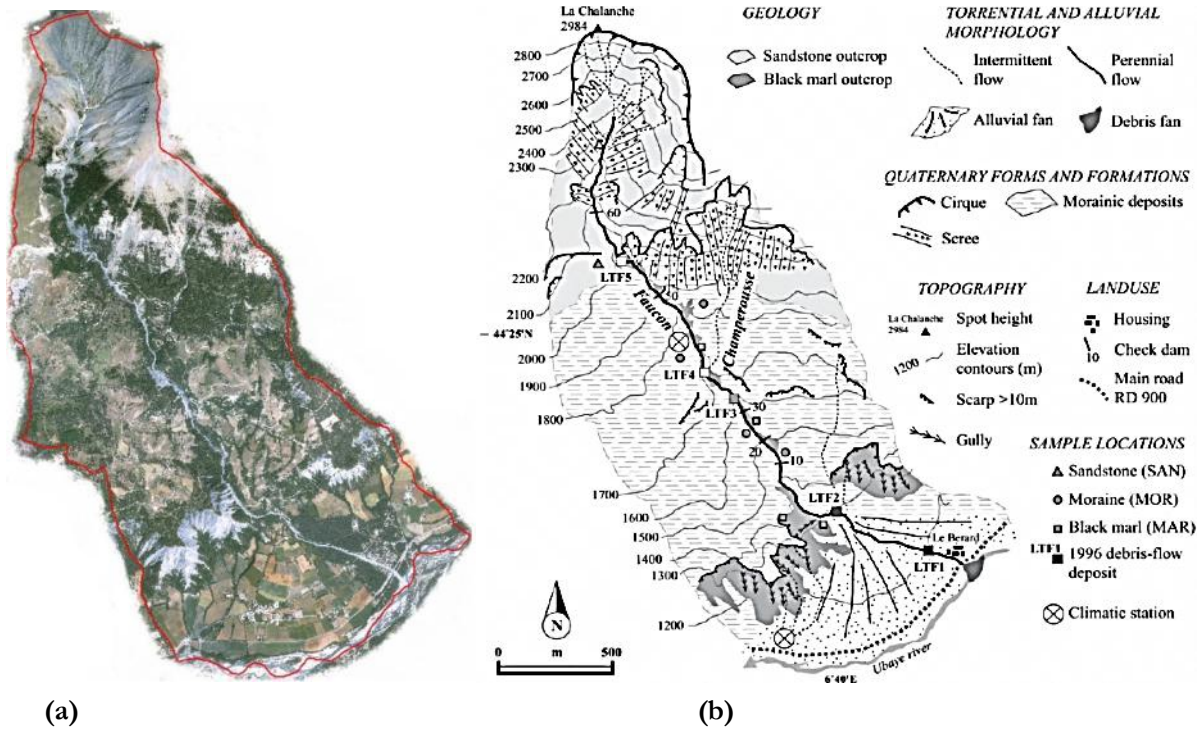

Figure 8 (a) Aerial photo of the Faucon catchment (adapted from: Malet (2010)) and (b) a morphological map of the catchment (after: Remaître et al.(2005b))

The upper part of the catchment (> 1900 m) is made up of two sheet thrusts of faulted sandstones and calcareous sandstones with extensive scree slopes. The central part (1300 – 1900 m) consists of Callovo-Oxfordian flaky clay-shales and black marls (Terre noire) outcropping at the side of the torrent. However, the marls in most of the central parts are covered by Quaternary deposits with a sandy-silt matrix such as mixtures of landslide, scree debris and moraine deposits. The debris fan (< 1300 m) has an area of approximately 2 km² and its slope ranges from 4° to 9°. Permeable and cohesionless debris make up most part of the fan (Remaître et al., 2005b).

Debris flow and flood mitigation and prevention works (Figure 9a) have been built since the 1890s, with more than 70 check dams set up from the apex up to the highest parts of the torrent. Some of these check dams have been destroyed by past debris flows (Figure 9b). The channel on the debris fan has been widened and dikes were added (Figure 10) since the last debris flow in 2003 to prevent future debris flows from spilling over into the village of Domaine de Bérard that was affected by the last event.

(a)  (b) 

Figure 9 (a) Check dam at the black marl (Terre noire) outcrops (1423 m). (b) Destroyed check dam in the upper part of the catchment (2065 m)

Figure 10 The Faucon torrent and its dikes at the debris fan (1202 m). It is managed by the French Forestry Office (ONF)

3.2. The 1996 and 2003 Debris Flow Events

The Faucon torrent is active with 31 recorded flash flood events and 14 debris flows since 1850 (Remaître, 2006). The past 2 major debris flow events which are also the most well documented occurred in 1996 and 2003.

3.2.1. 1996 Debris Flow

On the 19th of August, 1996 a debris flow had occurred in the Faucon catchment between 4:00 and 6:30 p.m. and was triggered by an intense thunderstorm. The initiation zone (Figure 11) was a shallow landslide on the Trois Hommes slope on the eastern flank of the Faucon torrent and caused extreme scouring between check dams 54 and 57.

Witnesses and the French Forestry Office (ONF) described the event occurred within 2.5 hours, with the debris flow starting as slow moving pulsating waves and then gathered speed further downstream. Damage described as low to moderate was caused by the debris flow. Further damage to the main valley road R.D. 900 (Route Departementale) (Figure 8b) on the alluvial fan blocked off traffic for several hours.

Check dam 54 (2150 m) collapsed, which according to Remaître & Malet (2010) is the breach that triggered the debris flow. Evidence of the trigger area was derived from aerial photographs, field observations of the destruction of check dams 54 to 57, including deep entrainment (up to 5 meters) and the widening of the torrent at these locations.

The Trois Hommes shallow landslide initiation volume was estimated between 5,000 and 7,500 m^3. The torrent scouring from the initiation down to check dam 54 had an estimated entrainment volume between 10,000 and 12,500 m^3. The entrainment of the torrent channel below check dam 54 caused the volume of

the debris flow to rapidly increase. Black marl outcrops between 1300 and 1900 m, further produced extensive erosion and incorporation of new material into the flow (Remaître & Malet, 2010).

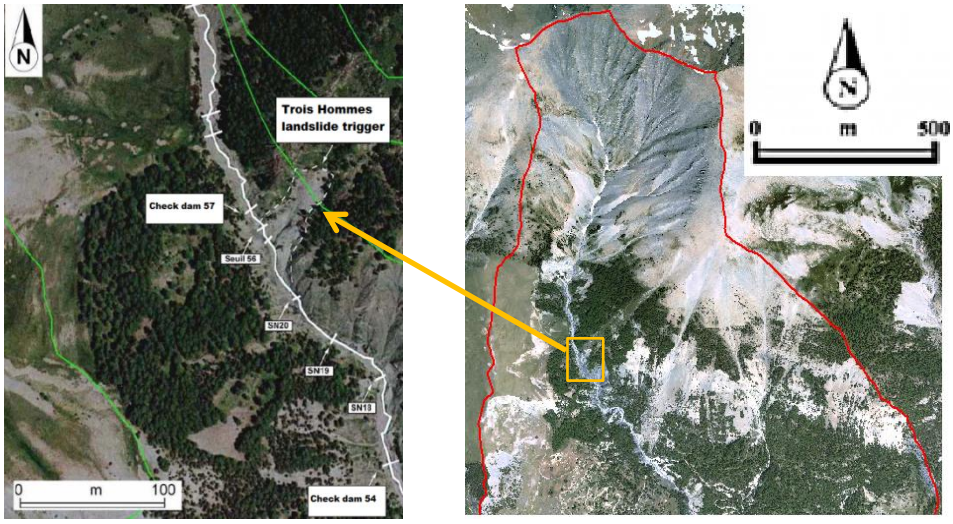

Figure 11 Location of the 1996 Trois Hommes shallow landslide initiation in the upper part of the catchment (adapted from: Remaître (2006))

Deposition within the channel torrent occurred between 1500 and 1200 m. This deposition formed lateral channel and bed deposits with narrow levees 2 to 3 m high. Channel scouring rate was estimated at 29 m^3/m. The channel width ranged from 5 to 15 m, thus a scouring rate of 29 m^3/m implies that the entrained debris heights per meter ranged from 1.9 (29/15) to 5.8 m (29/5). The average velocity estimated was 5 m/s and the peak discharge at the fan apex was estimated between 90 and 100 m^3/s. The total volume of the 1996 debris flow was estimated at 100,000 m^3 based on a solid volume concentration (C) of 0.6 (Remaître et al., 2005b). The total deposit volumes of the 1996 and 2003 events were estimated using the empirical equations found by Kronfellner-Kraus (1985), Zeller (1985) and (Rickenmann, 1999).

3.2.2. 2003 Debris Flow

The most recent debris flow event occurred on the 5th of August 2003 and caused substantial damage to residential buildings at the village of Domaine de Bérard located on the debris fan directly next to the Faucon stream channel. The trigger similar to the 1996 event was an intense rainfall after a severe drought in the area. Two areas (Figure 12) on the east flank of the Faucon torrent were initiated: the Trois Hommes area (Figure 13) and the upper part of the Champerousse torrent which is a tributary of the Faucon torrent.

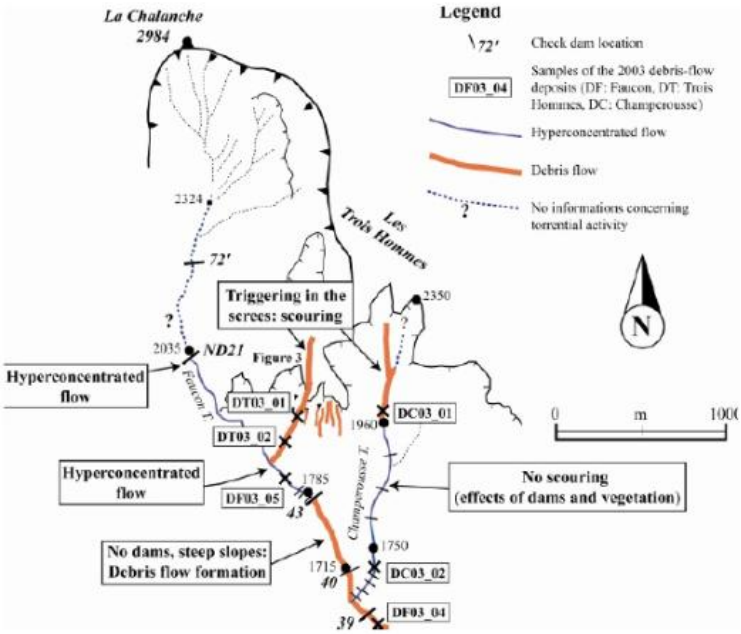

Figure 12 Sketch of the upper Faucon catchment indicating the two initiation zones of the 2003 debris flow (after: Remaître et al. (2009))

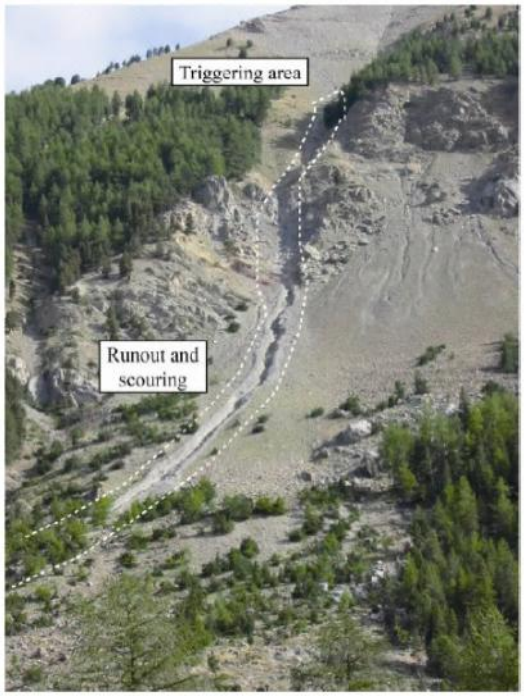

Figure 13 Trois Hommes 2003 initiation zone (after: Remaître et al. (2009))

Both initiation zones facilitated strong incision in scree slopes. The depth of this incision in the Trois Hommes is about 2 m at the headscarp and 5 m (Figure 13) at the convergence with the Faucon torrent 750 m from the point of initiation. The initiation volume of the Trois Hommes was estimated between 4,000 and 5000 m³ and flowed without obstruction into the Faucon main torrent (Remaître et al., 2009).

The Champerousse area initiated a volume ranging from 6,000 to 7,000 m³. The upper part of the area had a 2 m incision depth with the lower part having a 1 m depth. The debris path width was estimated at 3 m. Unlike the Trois Hommes trigger, not all of the estimated volume flowed down to the Faucon main torrent and approximately 3,000 m³ was trapped by the constructed series of check dams. Thus half of the

triggered volume of the Champerousse initiation ranging between 3,000 and 3,500 m³ continued to the Faucon torrent's main track.

According to Remaître (2006) a value of 8,500 m³ was considered to be the best estimation of the total solid volume of the two initiation zones. Previous studies indicate (Malet et al., 2005; Remaître et al., 2005b) that the range of the solid concentration (C) ranges from 0.50 to 0.60 in debris flows occurring in the Barcelonnette area. This implies that 8,500 m³ is the solid part of the debris flow and forms 50 to 60% of the total volume of the flow, with the rest of the 40% to 50% forming the fluid part. Thus the total volume of the initiation zone, with solids and fluids combined, ranges from 14,000 (C = 0.60) to 17,000 m³ (C = 0.50) (Remaître et al., 2009).

The torrent channel running through the debris fan was mostly filled by the 2003 event, with eye witness accounts indicating that the debris flow moved downstream in 5 separate surges. The final surge of the debris flow was 5 to 6 m high and overtopped its bank at the V.C. 3 Bridge (Figure 14). The surge caused damage to several houses and deposited 1 to 2 m of debris on the left bank, luckily with no injuries to residents in their houses at the time. The debris flow further continued downstream to block off the main R.D. 900 valley road, causing traffic to halt for several hours (Figure 15). Appendix I shows images of the aftermath of the 2003 debris flow event.

The total solid volume deposited within the Faucon torrent upper channel area was estimated to be 15,000 m³ and 45,000 m³ on the debris fan. Sampling of the deposits found the total solid fraction (C) to range between 0.58 and 0.66. Thus the total volume of the debris flow was estimated between 83,000 (C = 0.66) and 95,000 m³ (C = 0.58) (Remaître et al., 2009).

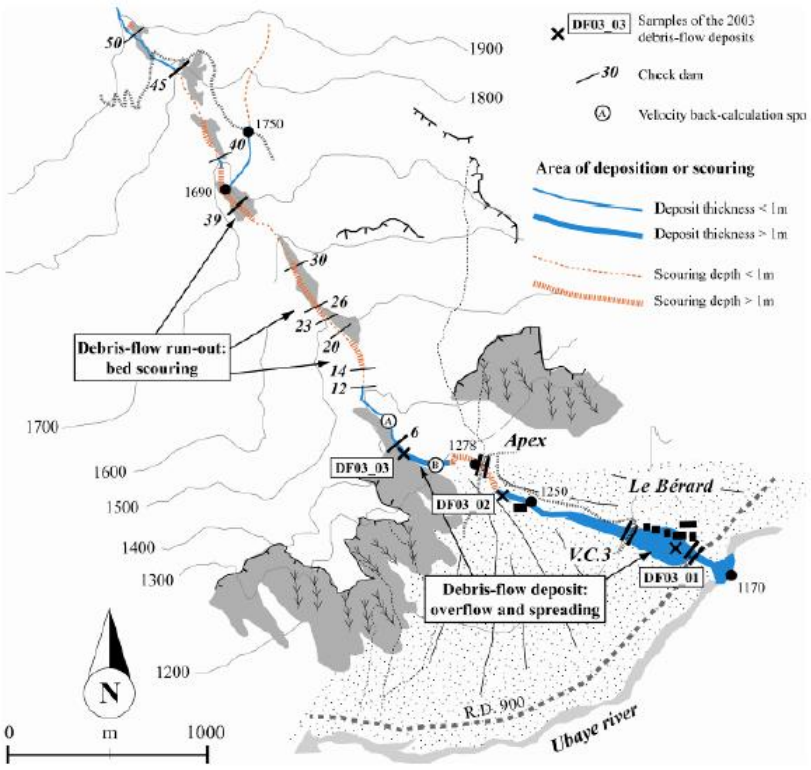

Figure 14 Morphological sketch of the entrainment and deposition zones of the 2003 debris flow (after: Remaître et al. (2009))

Figure 15 The 2003 debris flow run-out affecting Domaine de Bérard and blocking two main bridges (adapted from: Remaître (2006))

The difference between initiation volume and the total volume of the debris flow is due to extensive entrainment along the debris flow transport zone which is around 3,500 m long and has average gradients of 15°. The rate of scouring within the channel for the 2003 event was estimated at 15 m³/m. The scouring rate is similar to values observed in previous studies of debris flows occurring in similar lithological environments (Jakob et al., 2000). Further observations indicated that the entrained depth in the transport zone ranged from 0.5 to 4 m (Remaître et al., 2009).

3.2.3. The 1996 and 2003 Debris Flow Variables and Intensity Parameters

Table 3 summarizes the magnitude and intensity parameters of the 1996 and 2003 debris flow events obtained from several studies (Remaître et al., 2003; Remaître et al., 2005a; Remaître et al., 2005b; Remaître, 2006; Remaître et al., 2008; Remaître & Malet, 2010) where some have been calculated or estimated using empirical methods by Rickenmann (1999).

The initiation volume of 1996 is more than half the volume of the 2003 event. However, the total deposit volumes are comparable for both events. This is due to the fact that the 1996 shallow landslide was triggered approximately 500 m upstream from the entrainment zone of the 2003 debris flow, where the available debris height was larger. The scouring in this area was extremely deep and the breach of check dam 54 further added to the entrainment volume and momentum of the flow.

Table 3 Summary of the parameters of the 1996 and 2003 debris flows based on the literature

Parameters	1996 debris flow	2003 debris flow
Initiation volume	5,000 – 7,500 m³	14,000 – 17,000 m³
Entrainment volume	92,500 – 95,000 m³	69,000 – 78,000 m³
Total deposited volume	100,000 m³	83,000 – 95,000 m³

Run-out distance	4400 – 4500 m	4700 m
Scouring rate above fan apex	29 m^3/m	15 m^3/m
Maximum debris flow height near fan apex	1.5 – 3.0 m	5.0 - 6.0 m
Maximum debris flow height at the V.C. 3 Bridge	3.0 – 4.5 m	5.0 - 6.0 m
Velocity near fan apex	4.9 – 7.8 m/s	6.4 – 8.9 m/s
Velocity at the V.C. 3 bridge	< 4.9 m/s	2.0 – 5.0 m/s
Peak discharge at fan apex	90-110 m^3/s	150 – 200 m^3/s

3.3. Previous Debris Flow Modeling at the Faucon Catchment

As mentioned in Chapter 1, researchers have in previous studies back analyzed the past two debris flow events in the Faucon in both 1D and 2D dynamic continuum models. Remaître et al. (2003) modeled the 1996 debris flow event using the Herschel-Bulkley rheology in the 1D BING code software developed by Imran et al. (2001). Figure 16 shows the run-outs modeled by Remaître et al. (2003) and Table 4 summarizes the calibrated model parameters.

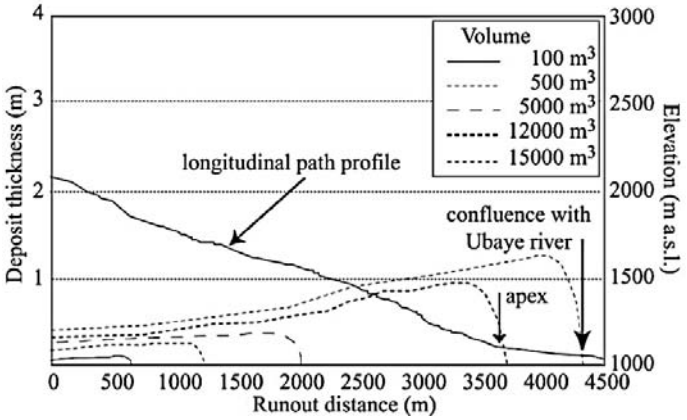

Figure 16 Modeled run-out distances with their estimated initiation volumes (after: Remaître et al. (2005a)).

Remaître et al. (2003) indicated that the Herschel-Bulkley rheology could replicate the 1996 event, however the velocities are highly overestimated (Table 4). The model could not replicate entrainment, thus a single release volume was used and modeled to see how far this volume could travel down the debris flow path. The initiation volume needed to reach the Ubaye River was approximately 13,500 m^3 and is more than twice as large as the estimated 1996 volume.

Table 4 Field observations compared with the BING model parameters (after: Remaître et al. (2003))

	Field observations and laboratory tests	BING input
Yield stress (Pa)	90 - 120 (*)	110 - 150
Viscosity (Pa s)	5 - 40	15 - 60
Total volume (m^3)	75 000 - 150 000	110 000 – 125 000
	Field observations and laboratory tests	BING ouput
Deposit thickness (m)	4.60 (**)	4.50
Velocities ($m.s^{-1}$)	4.9 – 5.1	20 - 70

* for a total solid fraction (ϕ) ranging from 40 to 50 ;
** observed at a bridge located on the alluvial fan.

The most recent debris flow modeling in the Faucon was carried out by Beguería et al. (2009). The MassMov2D script was used in the PCRaster environmental modeling software, where the Coulomb-viscous rheology was applied (Figure 17).

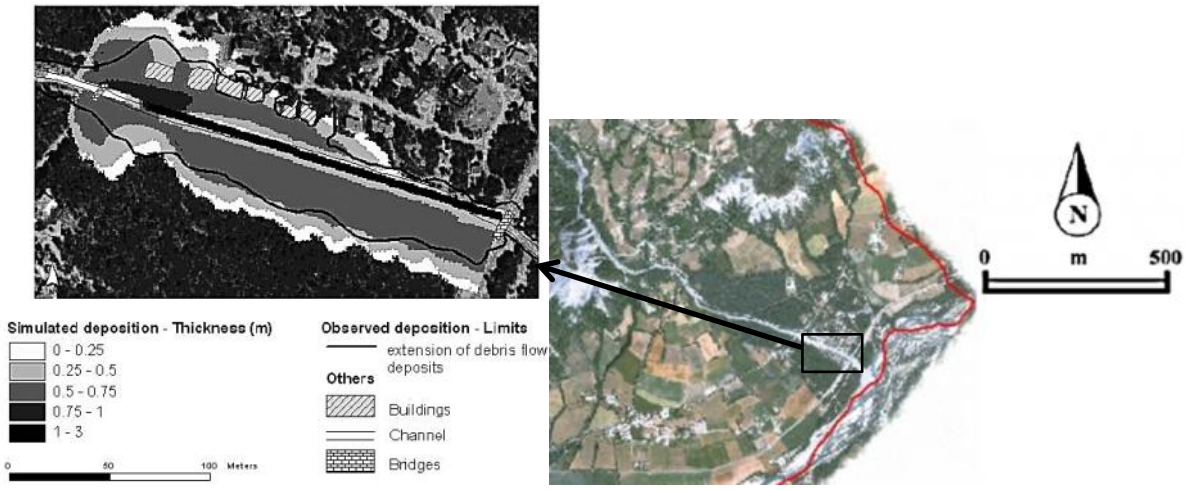

Figure 17 (Left) the 2D run-out model of the 2003 event with the Coulomb-viscous rheology (after: Beguería et al. (2009)) and (right) the location of the model on the debris fan.

Unlike the 1D modeling by Remaître et al. (2003), the advantage of the 2D modeling of the 2003 event is that the divergence and the overtopping of the debris flow over its channel banks could be spatially replicated as shown in Figure 17. The 2D model showed good results with respect to the deposit heights and their extent onto the village of Domaine de Bérard. It should be noted that the aim of Beguería et al. (2009) was not to model the total run-out distance but to replicate the run-out onto the fan. Therefore, the model only takes the final 300 m of the total run-out distance into account and does not incorporate the effects of entrainment in the transport zone of the flow path.

4. METHODS AND MATERIALS

4.1. Overview

Figure 18 gives an overview of the methods and materials used in this research. This chapter describes each part of the methodology and the results of the methods applied will be further discussed in the next chapter.

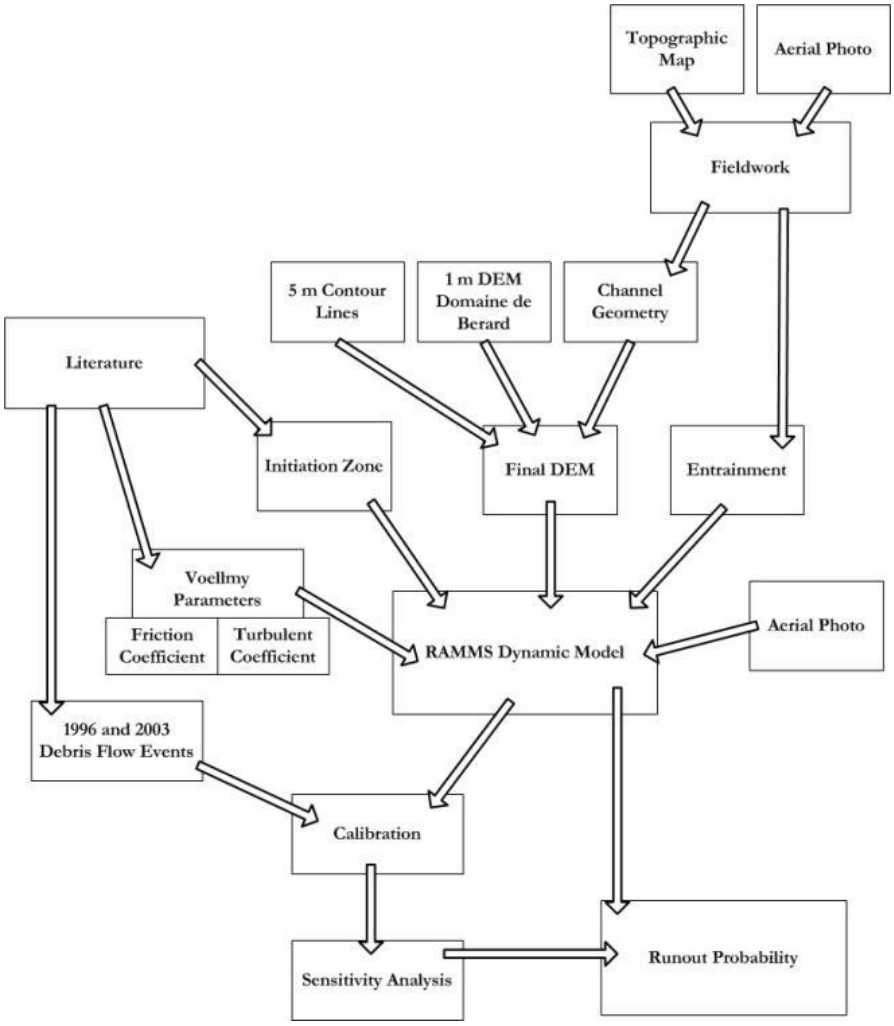

Figure 18 Flow chart of the methodology

4.2. Fieldwork

Fieldwork was carried out in the Faucon catchment during the period September/October of 2010. The central objectives of the fieldwork were:

1. To assess the topography of the Faucon main torrent, especially on the flatter debris fan in order to create an accurate Digital Elevation model (DEM) of the area for input into the debris flow modeling
2. To estimate the available material that can be entrained by future debris flows in order to incorporate the entrainment process into the physical modeling and to map the drainage channel in detail

3. To evaluate the possible initiation zones in the upstream area

A 1:15.000 scale topographic map (IGN, 2006) and a 0.5m resolution true color mosaicked aerial image of the Faucon catchment (Malet, 2010), both projected in the UTM WGS1984 zone 32 (Northern Hemisphere) projection system, were used for orientation in the field and for plotting the locations of the areas surveyed.

The fieldwork consisted of 74 points (Figure 19) surveyed in the Faucon catchment. At each point GPS measurements were conducted of the location and elevation within the torrent. Cross sections and slope of the torrent were estimated using a laser range finder. Figure 20a shows an example of the data collected in one of the surveyed areas. Handheld photographs were also taken throughout the torrent and at the surveyed areas (Figure 20b). The cross-sections of the channel measured at the debris fan are shown in Appendix II.

Debris heights within the torrent were visually estimated and recorded, including the occurrence of levees, check dams and secondary debris that has flowed in from the flanks of the channel. All loose unconsolidated debris, from silt and sandy heaps to big boulders were considered part of the debris height. After the debris heights were estimated and recorded in the field, a database (Figure 21) was created in the ArcGIS software comprised of polygons with each an assigned debris height and area.

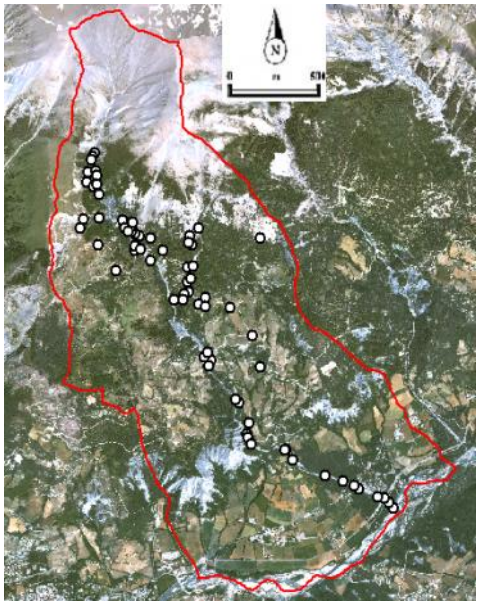

Figure 19 Areas surveyed in the Fieldwork of September/October 2010

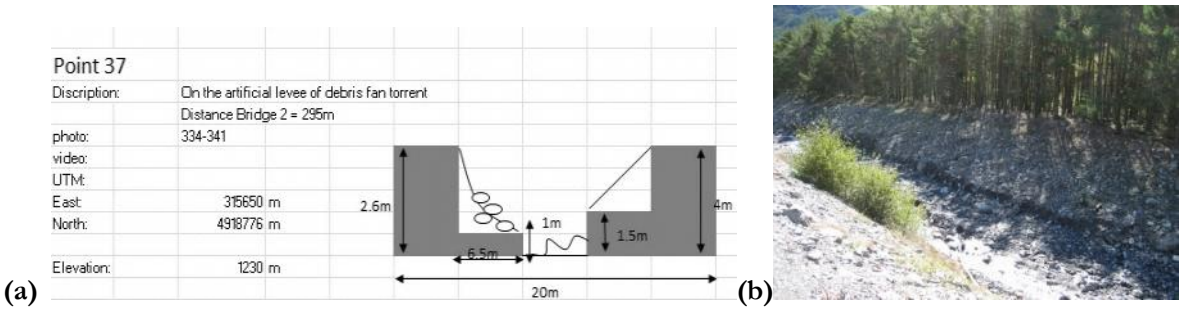

Figure 20 (a) Point 37 surveyed at the debris fan torrent and a (b) photograph of fieldwork point 37

Shape *	ID	debris_hei	Area
Polygon	46	1.8	998
Polygon	19	2	291
Polygon	20	2	1193
Polygon	21	2	894
Polygon	53	2	574
Polygon	58	2	669
Polygon	66	2	1203
Polygon	89	2	1692
Polygon	105	2	655
Polygon	106	2	368
Polygon	43	2.5	520
Polygon	68	2.5	630
Polygon	92	2.5	1105
Polygon	101	2.5	1320
Polygon	13	3	569
Polygon	14	3	481
Polygon	15	3	460

Figure 21 Part of the database on debris heights in the Faucon catchment

4.3. Determining the Initation Zone

After the latest debris flow event in 2003, Remaître (2006) studied the occurrence of debris flows in the Barcelonnette basin in general, and in the Faucon catchment in specific. One of the conclusions of his work was the outlining of the area that is most susceptible to future debris flow initiations (Figure 22a) based on expert evaluation, field observations and geomorphological analysis. The Faucon torrent slopes on the eastern side and specifically the Trois Hommes slopes are seen as the most susceptible to translational/rotational landslides, scree falls and avalanches as the slopes are the steepest within the catchment and with the most activity. The 1996 and 2003 events both were initiated in this area.

According to this information on susceptibility, the initiation zone chosen to be modeled in this research is located in the Trois Hommes slope and within the same channeled depression that triggered the 2003 event (Figure 13). The length of the initiation zone is approximately 615 m, slightly shorter than the 2003 initiation zone of 750 m. The width however is larger than the 2003 zone, ranging from 8 to 16 m. The zone was demarcated by a polygon (Figure 22b) drawn in the ArcGIS software using the aerial photo available on the area. The initiation polygon is located inside the most susceptible area (Figure 22). A wider initiation zone was chosen in order to increase the total initiation volume and to concentrate that volume on one particular area instead of multiple initiation zones. RAMMS requires a single polygon for each initiated area. Section 4.6 of this chapter will further discuss how the height and volume of the initiation zone was determined for modeling the debris flow.

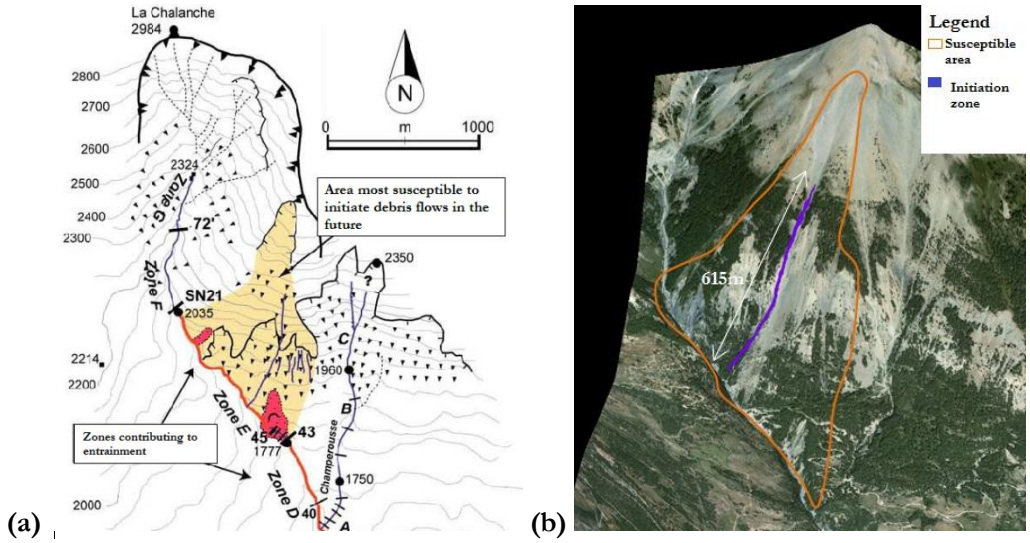

Figure 22 (a) The Trois Hommes area determined to be the most susceptible to future debris flow initiation (adapted from: Remaître (2006)). (b) A 3D visual representation of the Trois Hommes slope indicating the susceptible area (orange) and the initiation zone used in the modeling (purple)

4.4. Generating a DEM for Modeling

4.4.1. Available Elevation Data

Accurate topographic information is a crucial input into any 2D modeling of channeled debris flows. Elevation differences within a model will determine the slope and thus the direction of movement of the debris flow. The available data on the elevation of the Faucon catchment are:

- 5 m contour lines (ArcGIS shapefile) of the Faucon catchment digitized from a topographic map (Malet, 2010)
- IFSAR 5 m resolution DSM and DTM (Malet, 2010) of the Faucon catchment produced by Intermap Technologies (2010)
- 1 m resolution DEM of the area along 300 m of the channel at the Domaine de Bérard village used by Beguería et al. (2009). This model was created using the available 5 m contour lines mentioned above, and further enriched with GPS points (Beguería et al., 2009)

4.4.2. Topographic Data Analysis

The suitability of the elevation data was tested in the RAMMS dynamic model in order to see how well the data represents the actual topography of the torrent when modeling the debris flow. The RAMMS model itself will be discussed in detail in Section 4.5.

The available 5 m contour lines were interpolated to create a 5 m resolution DEM using the ArcGIS topo-to-raster function, based on a thin plate spline technique (ArcGIS Resource Center, 2010). This 5 m DEM was imported into RAMMS and a preliminary model run was conducted. The preliminary run shows that the debris flow does not stay in the torrent as it nears the apex and shoots off the bend just above the apex (Figure 23). The debris flow further spreads laterally onto the fan, without any consideration of a channel running to Domaine de Bérard and the Ubaye River. The same problem was found with the IFSAR DTM and DSM.

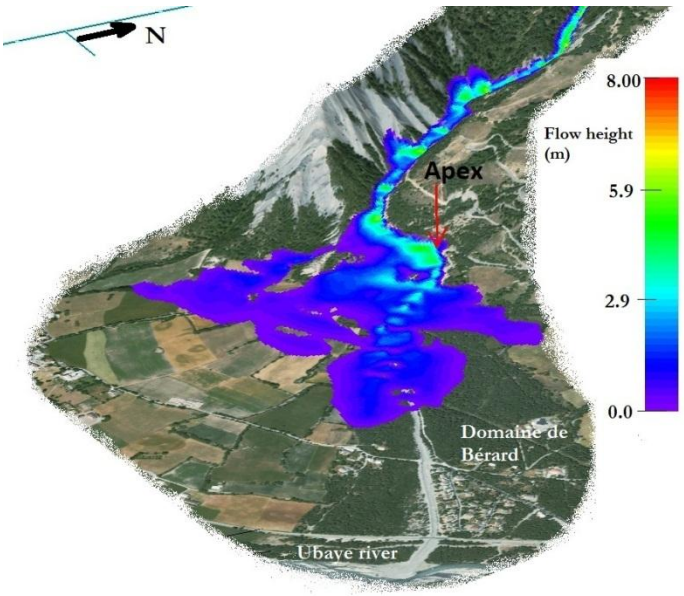

Figure 23 3D visualization of the preliminary model run in RAMMS using the 5 m DEM interpolated from the available 5 m contour lines

The preliminary model runs show that the available elevation data is not sufficient to replicate a realistic debris flow event. The channel depth was extremely low to nonexistent in some parts of the fan, when compared with the observations in the field.

4.4.3. Creating the New DEM

The channel topography and geometry (elevation, slope and cross sections) on the debris fan obtained from the field observations (Section 4.2 and Appendix II) were converted into an ArcGIS shapefile (Figure 24). The 1 m DEM from Beguería et al. (2009) was converted into 1 m contour lines (Figure 25a). The 1 m DEM is incorporated in the production of the new DEM of the study area due to its higher accuracy and resolution. Beguería et al. (2009) mention that this part of the fan has been made using differential GPS points and combined with the 5 m contour lines already available, thus creating a small 1 m DEM of the final run-out path that gives a more accurate depiction of the topography near Domaine de Bérard. The channel and dikes in the 1 m DEM are of the 2003 situation. This research is interested in the topography of the fan and not in the 2003 channel geometry. Therefore, after producing contour lines of the 1 m DEM, the lines were then smoothed to remove the old 2003 channel (Figure 25b).

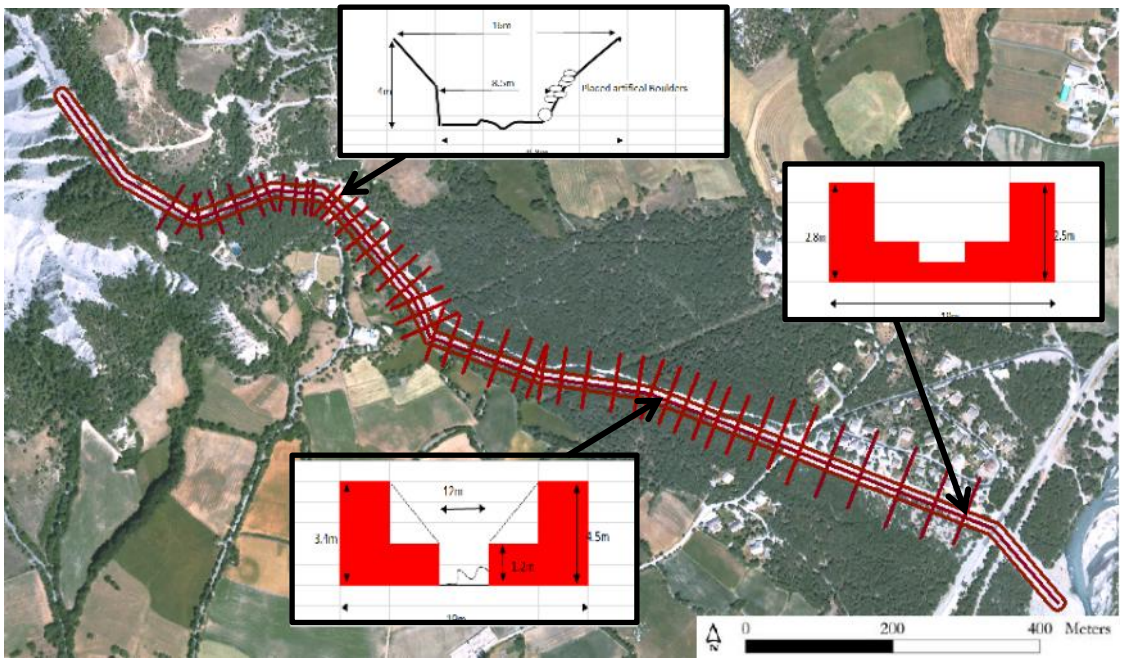

Figure 24 Shapefile of the channel geometry based on field observations

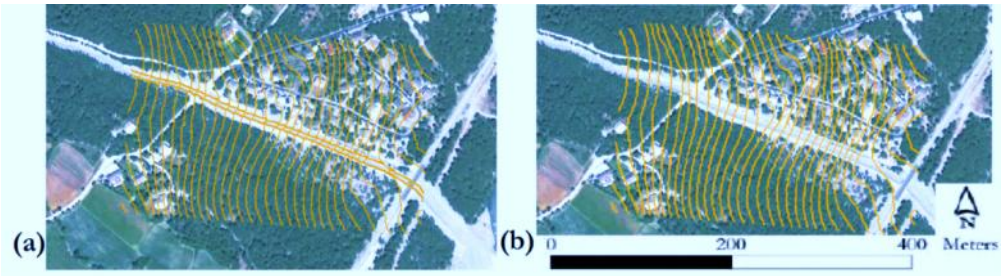

Figure 25 (a) 1 m contour lines derived from the 1 m DEM before channel removal and (b) the contour lines after removing the channel

The 5 m contour lines had their channel removed as well by smoothing the contours and were then interpolated with the 1 m contour lines using the ArcGIS topo-to-raster function. The topo-to-raster function is an iterative finite difference interpolation technique using discretized thin plate splines (ArcGIS Resource Center, 2010).

The channel geometry (Figure 24) was then burned into the debris fan including the area above the apex where the preliminary model run overtopped its banks at the channel bend. Finally, the available 5 m contour lines, the new constructed channel geometry and the 1m contour lines were all interpolated

(Figure 26) together into a single 5 m resolution DEM, again using the topo-to-raster function in ArcGIS. The resulting DEM is discussed in Chapter 5. It would have been better and less time consuming if a DEM with higher accuracy and resolution was available, for example a LIDAR DEM. Such a DEM could give a more accurate depiction of the channel throughout the area, compared to contour lines derived from topo maps. However, such a DEM was unfortunately unavailable in this research.

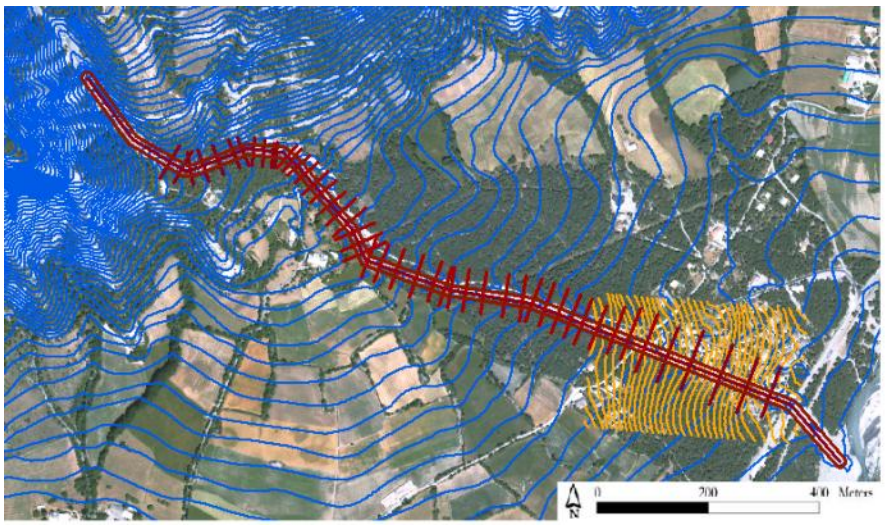

Figure 26 Datasets interpolated to create the final DEM: (blue) 5 m contour lines, (red) corrected channel geometry and (yellow) 1 m contour lines

4.5. The Dynamic RAMMS Modeling Software

4.5.1. Description of the RAMMS Software

RAMMS (Rapid Mass Movements) is a dynamic numerical modeling software package originally designed to model snow avalanches (Christen et al., 2010c), but has been applied in the past to model other types of mass movements like lahars (Quan Luna, 2007) and debris flows (Cesca & D'Agostino, 2006; Kowalski, 2008). RAMMS is developed by the Swiss Federal Institute for Snow Avalanche Research (WSL / SLF) and is a user friendly, powerful software tool for predicting mass movements. It further gives quick results, with a GIS-environment linked with the open source software GRASS and a user interface (iTools) based on the IDL programming language.

The RAMMS software is a 2D model capable of predicting the run-out path, velocities, flow heights and impact pressures in a two and three dimensional environment. Although initially designed for snow avalanches it has also been used for debris flow modeling. It is further capable of modeling entrainment throughout the debris flow path. The visualization in RAMMS is very sophisticated, where aerial photos, satellite images or topographic maps can be draped over a three dimensional terrain and analyzed from all angles. The applications of RAMMS range from studying the dynamics of snow avalanches and other mass movements to hazard mapping and zoning for risk assessment.

The RAMMS model is a generalization of the quasi one-dimensional model as discussed by Bartelt et al. (1999). RAMMS uses the Voellmy-Salm fluid flow continuum model (Salm, 1993) based on the Voellmy-fluid flow law and describes the debris flow as a hydraulic-based depth-average continuum model. The flow resistance is divided into a dry-Coulomb friction and a viscous resistance turbulent friction as will be explained in the next section. RAMMS further contains an entrainment model discussed by Sovilla et al. (2006).

The model solves the governing mass and momentum equations using a second-order, cell-centered, positivity conserving HLLE (Harten, Lax, van Leer and Einfeldt) finite volume scheme, which is a numerical method to solve a Riemann problem (Christen et al., 2010c). Time integration within the model is given by the Runge-Kutta-Heun method (Christen et al., 2010c), which is an extension of the Euler's method into a two-stage Runge-Kutta method and is a numerical procedure for approximating differential equations.

4.5.2. Governing Equations

All the equations mention below are derived from the research conducted by Christen et al. (2010c). The RAMMS environment is based on three dimensions (Figure 27): x and y are the directions of the mass movement flowing down the surface and the elevation is given by $z(x, y)$ which is perpendicular to the profile. Based on this three component coordinate system used on the surface, the gravitational acceleration vector in the three directions is $g = (g_x, g_y, g_z)$ and the time component is defined as t (Christen et al., 2010c).

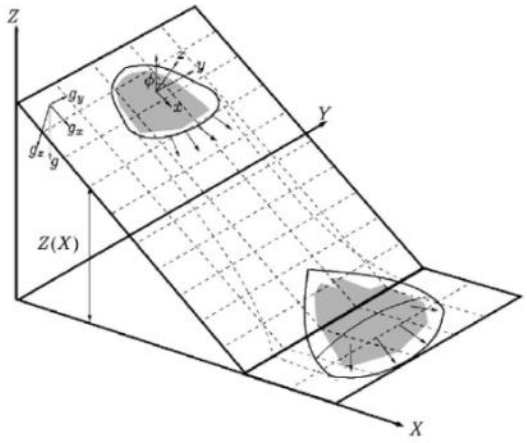

Figure 27 The Cartesian coordinate system in the RAMMS software, where Z is the topography and the horizontal coordinates are X and Y (after: Christen, 2010b).

RAMMS moves the flow in an unsteady and non-uniform motion and is characterized by two main flow parameters which are the flow height $H(x, y, t)$ (m) and the mean velocity $U(x, y, t)$ (m/s) (Christen et al., 2010c):

$$U(x, y, t) = (U_x(x, y, t), U_y(x, y, t))^T \quad \text{(Eq. 4)}$$

where U_x and U_y are the velocities in the x and y directions respectively, and T is used to transpose the matrix of the mean velocity. The magnitude of the velocity is given by:

$$\left||U|\right| = \sqrt{U_x^2 + U_y^2} \quad \text{(Eq. 5)}$$

where the double lines ($\|\cdot\|$) indicate the norm on the velocity U, making $\left||U|\right|$ a strictly positive velocity with a certain size in a vector space, which is the Cartesian coordinate system. The direction of the flow velocity is given by a unit vector (n_U):

$$n_U = \frac{1}{||U||}(U_x, U_y)^T \quad \text{(Eq. 6)}$$

The Voellmy-Salm model uses the following mass balance equation:

$$\partial_t H + \partial_x(HU_x) + \partial_y(HU_y) = Q(x, y, t) \quad \text{(Eq. 7)}$$

where H is the flow height (m) and $Q(x, y, t)$ (kg/m²s) is the mass production source term, also called the entrainment rate $(Q > 0)$ or deposition rate $(Q < 0)$ (Christen et al., 2010c). $Q = 0$ if there is neither entrainment nor deposition of mass. The depth-averaged momentum balance equations in the x and y directions are respectively given by:

$$\partial_t(HU_x) + \partial_x\left(c_x HU_x^2 + g_z k_{a/p}\frac{H^2}{2}\right) + \partial_y\left(HU_x U_y\right) = S_{gx} - S_{fx} \qquad \text{(Eq. 8)}$$

and

$$\partial_t\left(HU_y\right) + \partial_y\left(c_y HU_y^2 + g_z k_{a/p}\frac{H^2}{2}\right) + \partial_x\left(HU_x U_y\right) = S_{gy} - S_{fy} \qquad \text{(Eq. 9)}$$

where c_x and c_y are profile shape factors and g_z is the gravitational acceleration in the vertical direction. The vertical information within the Voellmy-Salm model is given by an anisotropic Mohr-Coulomb relation, using the earth pressure coefficient $k_{a/p}$ as a proportionality factor for the vertical and normal stresses (Christen et al., 2010c). The earth pressure coefficient $k_{a/p}$ is given by the following equation:

$$k_{a/p} = tan^2\left(45° \mp \frac{\varphi}{2}\right) \qquad \text{(Eq. 10)}$$

where φ (degrees) is the angle of internal friction of the debris flow. The earth pressure coefficient can be either active (k_a):

$$k_{a/p} = tan^2\left(45° - \frac{\varphi}{2}\right) \qquad \text{(Eq. 11)}$$

where the flow is dilatant and contracting causing an increase in the change of the velocity $(\nabla \cdot U \geq 0)$, or passive (k_p):

$$k_{a/p} = tan^2\left(45° + \frac{\varphi}{2}\right) \qquad \text{(Eq. 12)}$$

where the flow is compressive and the change in velocity of the flow decreases $(\nabla \cdot U < 0)$. The earth pressure coefficient $k_{a/p}$ in the RAMMS software is given the name "Lambda", which is the name that will be further used in this thesis. The right hand side of Equations 8 and 9 give the effective accelerations, and are noted as:

$$S_{gx} = g_x H \qquad \text{(Eq. 13)}$$

and

$$S_{gy} = g_y H \qquad \text{(Eq. 14)}$$

where S_{gx} and S_{gy} are the driving gravitational accelerations in the x and y directions, respectively. Equations 8 and 9 further contain on the right hand side frictions that add up to a total friction (S_f):

$$S_f = \left(S_{fx}, S_{fy}\right)^T \qquad \text{(Eq. 15)}$$

where S_{fx} and S_{fy} are the frictions in the x and y directions respectively and are given by:

$$S_{fx} = n_{U_x}\left[\mu g_z H + \frac{g||U||^2}{\xi}\right] \qquad \text{(Eq. 16)}$$

and

$$S_{fy} = n_{U_y}\left[\mu g_z H + \frac{g||U||^2}{\xi}\right] \quad \text{(Eq. 17)}$$

where n_{U_x} and n_{U_y} are the velocity directional unit vectors in the x and y directions respectively. The total basal friction in the Voellmy-Salm model is split into a velocity independent dry-Coulomb friction coefficient μ (Mu) and a velocity dependent turbulent friction coefficient ξ (Xi) (m/s^2) (Christen et al., 2010c). For the sake of simplicity μ is named the "friction coefficient" and ξ the "turbulent coefficient".

RAMMS uses a rate-controlled entrainment method which regulates the mass being up taken by the incoming debris flow and regulates the time delay to accelerate this mass to the debris flow velocity. The entrainment rate $Q(x, y, t)$ is given by (Christen et al., 2010c):

$$Q(x,y,t) = \begin{cases} 0 & for \quad \left[h_s(x,y,0) - \int_0^t Q(x,y,\tau)d\tau\right] = 0 \\ \frac{\rho_i^s}{\rho} K_i U & for \quad \left[h_s(x,y,0) - \int_0^t Q(x,y,\tau)d\tau\right] > 0 \end{cases} \quad \text{(Eq. 18)}$$

where ρ (kg/m³) is the density of the initiated debris flow, τ is the shear stress and $h_s(x, y, 0)$ (m) is the initial height of the entrainment layer given by the total height of the debris cover at position (x, y) and time $t = 0s$. The total height of the entrainment layer in RAMMS can be divided into three separate entrainment layers: $i\,\{1, 2, 3\}$, so that $h_s = \sum h_i$ and the density of the each layer is given by ρ_i^s (kg/m³). Finally, K_i is the dimensionless entrainment coefficient for each layer. However, if a single entrainment layer is chosen, K_i can be simply defined as K. Christen et al. (2010c) mention that the entrainment rate depends on the speed of the incoming flow, but when $K > 1.0$ than entrainment is near instantaneous. Furthermore, Christen et al. (2010c) have found that if $K < 0.5$, entrainment continues but at a lower rate with basal erosion taking place, and if $K > 0.5$ than frontal plowing takes place at the head of the flow.

4.5.3. RAMMS Model Inputs

Figure 28 summarizes the main inputs of the RAMMS modeling software. A quick guide on how to model a run-out in RAMMS has been made available in Appendix III. The DEM (Digital Elevation Model) forms the basis on where all the modeling takes place. It is imported into RAMMS in the ESRI ASCII Grid format, which can be exported from the ArcGIS software. The header of the ASCII Grid file must contain the number of columns, rows, the x and y coordinates of the lower left corner and the cell size. RAMMS can resample the original input DEM into another resolution. However, if the DEM is imported in the same resolution no resampling takes place according to the latest version (RAMMS v.1.3.16) of the software.

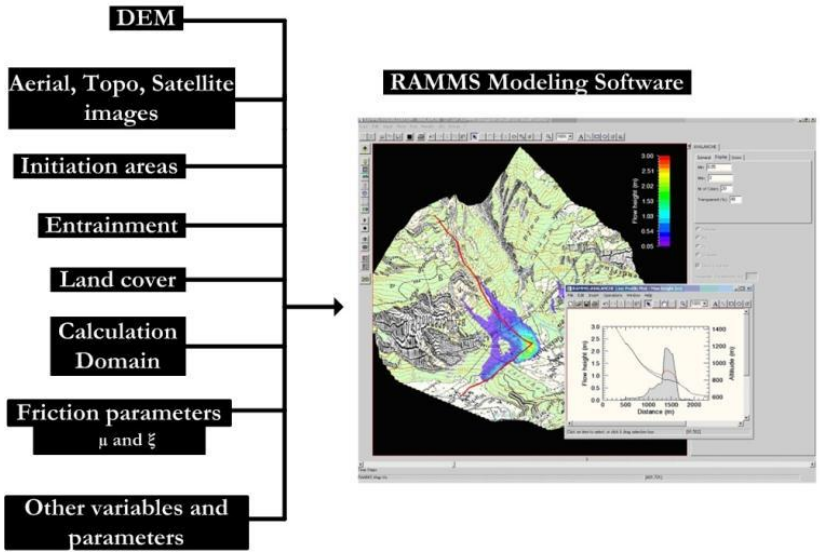

Figure 28 RAMMS inputs and the user interface

As mentioned before, RAMMS has powerful visual capabilities where aerial photos, satellite images and topographic maps can be imported and draped over the DEM. However, the imagery must be first geo-referenced and then imported in the TIF image file format with a corresponding TFW-file (world-file).

After the DEM and images are imported, a user defined calculation domain is drawn in RAMMS in the area of interest which is the complete debris flow path. The smaller the domain, the faster the calculation time will be for a single model run. Another input that effects the calculation time is the grid resolution (m) of the model and is one of the simulation input parameters (Figure 29a). The other simulation parameters are: the end time of the simulation (s), the number of dump steps (time steps), the constant density ρ (kg/m^3) of the debris flow and the earth pressure coefficient Lambda.

Initiation areas and land cover information (forests) can be either imported from polygon shapefiles created in ArcGIS or by manually drawing polygons in RAMMS using the imagery available. Initiation polygons need to be assigned release heights that are either defined by the user or by RAMMS which determines the heights based on the topography (Figure 29b). Once a height is entered by the user, RAMMS automatically estimates the initiation volume.

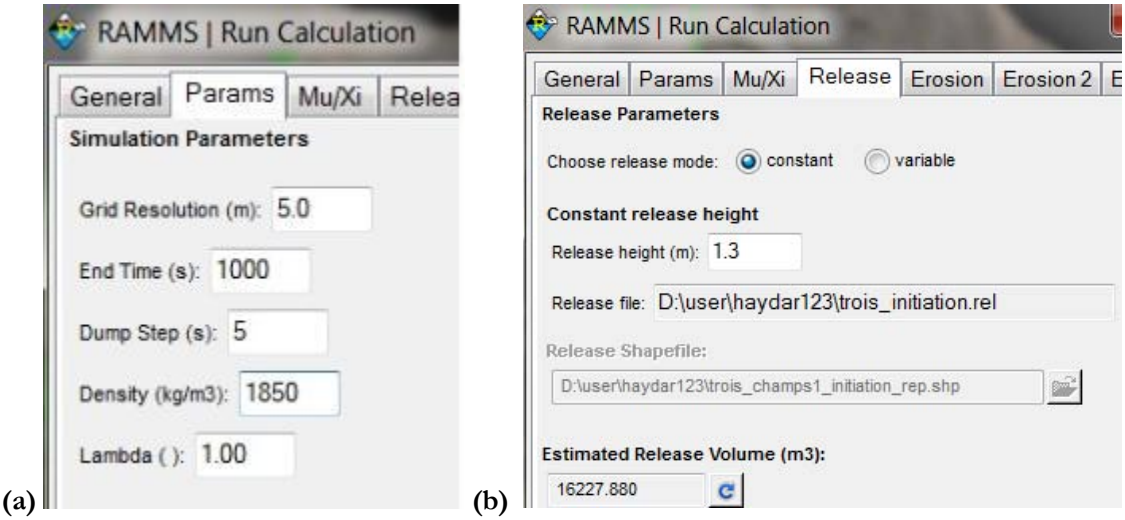

Figure 29 (a) Simulation parameters and (b) release information in RAMMS

The friction parameters used as inputs in RAMMS are: the friction coefficient μ (Mu) and the turbulent coefficient ξ (Xi). These parameters are either kept constant (Figure 30) over the whole terrain or are variable throughout the terrain based on user defined polygons or user defined friction values combined with the RAMMS automated topographic classification. In this research the friction parameters are kept constant for each debris flow model run in order to assess the overall sensitivity of the output to the friction parameters as will be discussed later on in this thesis.

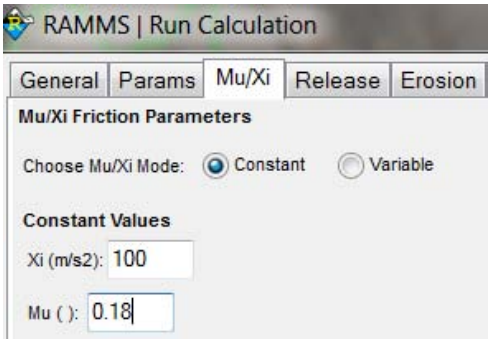

Figure 30 Assigning the friction parameters in RAMMS

There are two methods in RAMMS for the entrainment of debris in the transport zone by the flow. The first method is entrainment using 3 separate vertical layers as described in Section 4.5.2. The second method applies user defining polygons in the transport zone where entrainment should talk place (Figure 31). These polygons, similar to the initiation polygons, can be imported as shapefiles from ArcGIS or drawn within RAMMS. The user defined polygon method allows for two separate shapefiles to be imported into RAMMS, where each shapefile can contain its own set of polygons representing two different entrainment heights. Three parameters are assigned to each shapefile that represent the entrainment zone: the height of the entrainment layer (m), the density of the layer (kg/m^3) (Rho) and the entrainment coefficient K.

The simulated debris flows in RAMMS are stopped either by the user defining the end time (s) of the simulation or by using the stop criteria which is based on the momentum (kgm/s). RAMMS sums the momenta of all the grid cells and compares it with the maximum momentum sum. If the percentage difference in momentum is lower than the percentage defined by the user, than the flow is regarded as stopped (Christen et al., 2010b).

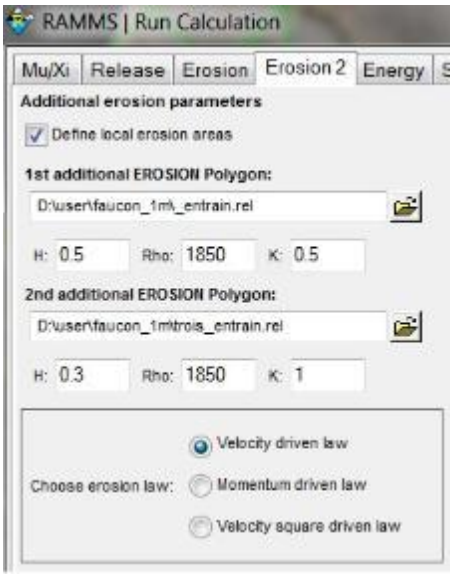

Figure 31 User defined entrainment polygons in RAMMS

4.5.4. RAMMS Model Outputs

RAMMS run-out simulations can vary between 100 seconds to 15 minutes, depending on the domain size and the chosen grid resolution. The run-out can be viewed in 2 or 3 dimensions and from any angle. Once the simulation has been completed RAMMS automatically crops the DEM and the draped image according to the chosen domain to save processing and loading times of the simulations. Results can be exported to ArcGIS or other GIS software as ESRI shapefiles or in the ASCII grid format. The main outputs in RAMMS are:

- Initiation, entrainment and deposit volumes (m^3) at any moment of the flow
- The surface area of the flow (m^2) at any moment
- Deposit heights (m), velocities (m/s), impact pressures (kPa), entrainment rates (kg/m^{2}s) and eroded mass (kg) at any moment of the flow, including their overall maximum values
- Longitudinal path profiles and cross sections of the debris flow
- Animations of the entire flow in the GIF file format

4.6. Model Calibration

Calibration is an important part of modeling debris flows or any other type of modeling trying to spatially replicate past events or predict future ones. The aim of calibrating models is to adjust the parameters of the model so that modeled results replicate real observed events and thus determining the range of values of the parameters. This research calibrates a debris flow run-out event in the Faucon catchment using the information of two well documented events from 1996 and 2003.

4.6.1. Calibration Inputs

The input parameters that are needed to calibrate the debris flow run-out with past events can be divided into two types of parameters: constant parameters that have values based on information of past events and calibration parameters for which their ranges in value or their effect on the run-out is not exactly known. Parameters that are kept constant throughout the calibration are:

- The grid resolution (m)
- The density (kg/m^3) of the initiation and entrainment layers
- The height (m) of the initiation and entrainment zone

The more accurate the information is on these constant parameters, the more accurate the calibration results will be. The grid resolution in RAMMS is kept to 10 m to reduce calculation times to 10 to 15 minutes per simulation. Density of both the initiation zone and entrainment layers are set to 1850 kg/m^3 following Remaître (2006) and Beguería et al. (2009). The input parameters chosen to be calibrated are:

- The friction parameters μ (Mu) and ξ (Xi)
- The entrainment coefficient K
- The earth pressure coefficient Lambda

4.6.2. Initiation Zone

Section 4.3 discussed the basis on which the choice was made for the initiation zone. The assigned height of the initiation zone is 1.5 m with an average width of 14 m. RAMMS calculated an initiation volume of 16,728.4 m^3, based on the 1.5 m height and shape of the initiation polygon (Figure 32). Table 5 compares the 2003 initiation with the one modeled in this research. A 1.5 m initiation height was chosen in order to obtain a volume that fits within the range of the 2003 event.

Figure 32 The initiation zone

Table 5 2003 debris flow initiation versus the new initiation zone

Parameters	2003 event	Initiation zone
Height	2 – 5 m	1.5 m
Volume	14,000 – 17,000 m^3	16,728.4 m^3

4.6.3. Entrainment Zone

As mentioned before RAMMS takes 2 separate shapefiles for the entrainment zone. This means that only two entrainment heights can be assigned within the whole transport zone when using the polygon entrainment method. However, a single shapefile can contain a set of multiple polygons. The ArcGIS polygons in the debris height database collected from the fieldwork (Section 4.2) were averaged out into 2 entrainment heights of 0.5 m and 2 m. The first shapefile contains a set of 3 polygons with each a 0.5 m height, and the second shapefile contains 2 polygons with each a debris height of 2.0 m. The transport zone is then made up of a total of 5 polygons. The 0.5 m area starts at the end of the initiation zone until an elevation of approximately 1700 m. From 1700 m to 1400 m the 2.0 m zone is more dominant and there are thicker debris heights available to entrain. These areas are also more notable for the Terre Noire outcrops. The two entrainment zones were imported as shapefiles into RAMMS (Figure 33). The total distance of the entrainment zone is approximately 3500 m.

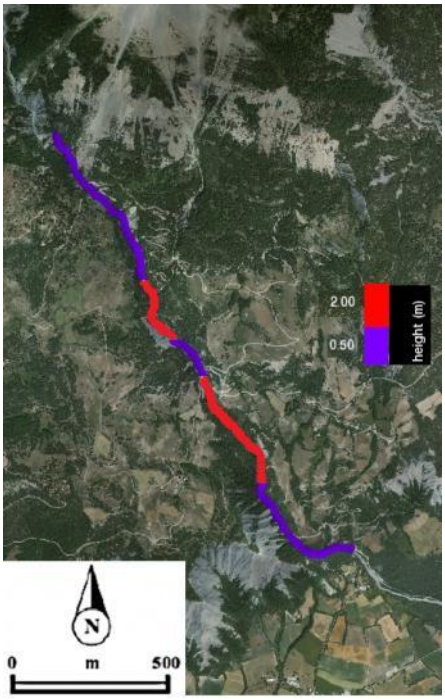

Figure 33 Entrainment zones in RAMMS. Red indicating 2.0 m entrainment height, and purple indicating a height of 0.5m.

4.6.4. Friction Parameters

Calibrating the friction parameters μ (Mu) and ξ (Xi) starts by reviewing the literature on these two parameters used in the Voellmy rheology. As mentioned in Chapter 1, the Voellmy rheology has been used to model a variety of mass movements. Therefore, the ranges of friction parameter values obtained from the literature should be specifically determined for debris flows.

Sosio et al. (2008) have summarized from several important studies the ranges of the Voellmy friction parameters (Table 6). These studies are based on the back-analysis of hundreds of debris flow and avalanche events. The work conducted by Hungr & Evans (1996) is one of the studies included in Table 6. Hungr & Evans (1996) back-analyzed 23 well documented debris flows and avalanches, finding the optimal values for μ (Mu) and ξ (Xi) to be 0.1 and 500 m/s^2, respectively.

Scotto di Santolo & Evangelista (2009) carried out a back-analysis of 57 debris flows in Italy using the Voellmy rheology in the 2-D DAN-W modeling software. The landslides include open slope, channeled and mixed slope debris flows. The friction parameters ranged from 0.01 to 0.2 for μ (Mu) and 100 to 200

m/s² for ξ (Xi). When ξ (Xi) was set to 100 m/s², most of the channeled debris flows had a μ (Mu) value of 0.06 and a μ (Mu) value of 0.18 for open slopes. Their study further mentions that as a debris flow runs through a channel the μ (Mu) is lower due to the flow's greater mobility than in an open slope environment where the flow dissipates and spreads out latterly causing greater shear stresses, frictions and lower velocities.

Table 6 Summary of value ranges for the Voellmy rheology parameters based on a wide variety of studies (adapted from: Sosio et al. (2008))

	Internal rheology	Frictional rheology	Voellmy rheology	
	Friction angle, ϕ_i	Bulk friction angle, ϕ_b	Frictional coefficient, μ	Turbulent coefficient, ξ
	[°]	[°]	[-]	[ms^{-2}]
Rock avalanches	35–40	10–30	0.1–0.25	450–1000
Debris avalanches	35	23–30	0.07–0.1	200–250
Rockslide-debris avalanches	35	8–31	0.05–0.2	200–400
Ice-rock avalanches	20–35	10–20	0.03–0.1	1000
Debris flows	35	22–29	0.05–0.2	200–500
Volcanic-rock avalanches	30–35	9–13	0.05–0.1	100–140

Quan Luna et al. (2010) compiled a database of the back-analysis of 253 past landslide events, where 61% of these events are debris flows. 152 of the 253 events were back-analyzed using the Voellmy rheology. Their study produced probability density functions of the Voellmy parameters (Figure 34). The most frequent occurring values for μ (Mu) in the back-analysis of the past events range between 0.05 and 0.2, where the probability curve reaches its peak (Figure 34a). The turbulent coefficient ξ (Xi) is most frequent between 150 and 600 m/s², reaching its peak at 500 m/s² (Figure 34b).

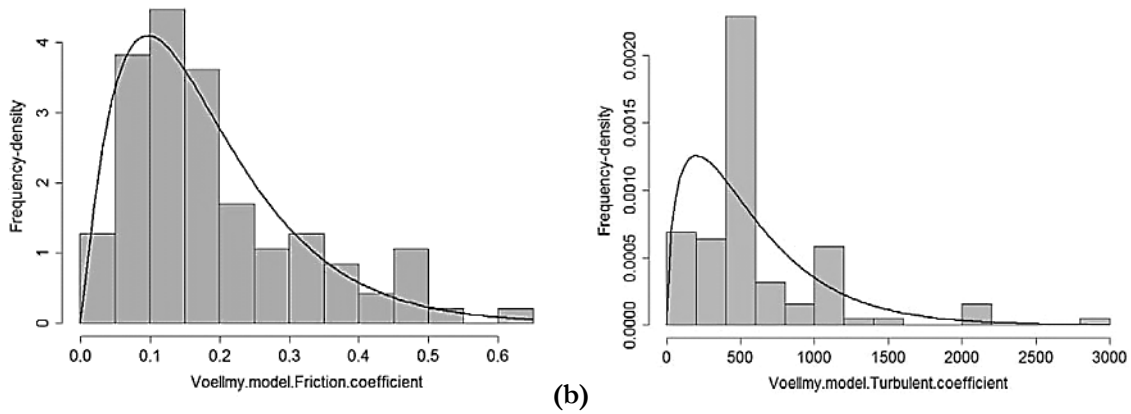

Figure 34 Frequency density histograms and curves of (a) the friction coefficient μ (Mu) and (b) the turbulent coefficient ξ (Xi) (after: Quan Luna et al. (2010))

4.6.5. Entrainment Coefficient K

As mentioned in Section 4.5.2. Christen et al. (2010c) studied the effects of the entrainment coefficient K on the entrainment process in RAMMS. For K = 0 there is no entrainment of a given debris height by the flow and when K = 1 entrainment is near instantaneous. However, their study further tested entrainment rates on K values above 1 and found the entrainment rate to increase even more up to K = 5. Therefore, a calibrated debris flow event that takes entrainment into consideration in RAMMS, must have a calibrated K value ranging $0 < K \leq 5$.

4.6.6. Earth Pressure Coefficient Lambda

The earth pressure coefficient is related to the angle of internal friction φ (Eq. 10 in Section 4.5.2.). The internal friction angle is a measure of the ability of a unit of rock or soil to withstand a shear stress. If Lambda = 1 then $\varphi = 0$, and the flow is considered hydrostatic, flowing as water. Beguería et al. (2009) modeled the run-out at the Faucon using $\varphi = 3.8°$, which gives a Lambda of approximately 0.9. However, φ can vary depending on the fluid content and material of the debris flow. Lambda is considered in the calibration to range between 0.3 and 1, with a Lambda of 0.3 giving a φ of 33°.

Pirulli et al. (2007) have studied the effects of the earth pressure coefficient on the run-out of landslides, incorporating information on the earth pressure coefficient from Savage & Hutter (1989) Their work has found that a decrease in the earth pressure coefficient, and thus increasing the angle of internal friction, causes the flow in the flat areas (debris fan) to decrease in run-out and to increase its spreading laterally.

4.6.7. Calibration Outputs

Five calibration criteria have been set based on the intensity parameters of the 1996 and 2003 events. The intensity parameters have been discussed in Chapter 3 (Table 3). The calibrated modeled debris flow should meet these five criteria in order to be defined as a successful calibration. The calibration criteria are as follows:

1. The calibrated model should reach a similar run-out distance as the past events
2. The initiation volume should be within the range of the past events
3. Modeled deposited volume should be within the range of the past events
4. Modeled velocities at the fan's apex and the V.C. 3 Bridge at the village of Domaine de Bérard should be within the velocity ranges of the past events
5. Modeled deposit heights at the apex and V.C. 3 Bridge should be within the range of the past events

It should be noted that the channel and dikes of the 2003 event are not the same as the calibrated model. Therefore, when similarities are compared the difference in channel geometry should be taken into account and will be further discussed in Chapter 6.

The intensity parameters mentioned in each criterion are the output parameters of the debris flow modeling. The result of the calibrated debris flow, its intensity parameters and the number of criteria met are discussed in Chapter 5.

4.7. Sensitivity Analysis

A sensitivity analysis quantifies the variation in a model output due to variations in the model inputs. It shows how sensitive the output of the model is to changes in the input and gives an indication which input parameter weighs more on the model.

The sensitivity analysis is carried out on four input parameters which were also used for calibration of the final debris flow model in the Faucon catchment. These parameters are:

- The friction coefficient μ (Mu)
- The turbulent coefficient ξ (Xi)
- The entrainment coefficient K
- The earth pressure coefficient Lambda

Each single input parameter was increased or decreased by a certain percentage from its original calibrated value (Appendix IV), while the other three input parameters were kept constant at their calibration values

in order not to affect the sensitivity of the parameter being tested. Table 7 gives the ranges used in the sensitivity analysis for each input parameter based on value ranges obtained from the literature (Table 6 and Figure 34). A total of 53 run-outs were modeled using these ranges and their results are assessed in Chapter 5. The assessed outputs of the sensitivity analysis are:

- The total deposited volume (m^3)
- The Run-out distance (m) and the percentage difference from the calibrated run-out
- The debris flow height at the V.C. 3 Bridge and the percentage difference from the calibrated debris height

Table 7 The ranges used in the sensitivity analysis

Input parameters	Ranges of value
Friction coefficient μ (Mu)	0.01 – 0.2
Turbulent coefficient ξ (Xi)	100 – 800 m/s^2
Entrainment coefficient K	0 – 5
Earth pressure coefficient Lambda	0.3 – 1.0

4.8. Probability Analysis

There are several probabilities (temporal, spatial, etc.) that are combined in order to assess the hazard component of debris flow risk as mentioned in Chapter 2. Besides the hazard, the risk itself has its own probability which is made up of the probabilities of all the hazard components and the probability of damage to elements at risk (also referred to as vulnerability). Therefore, when probability is mentioned, it must be well defined which probability is being assessed, what method is being applied to estimate the probability and how this probability fits into the risk assessment framework.

This research looks specifically at estimating the spatial probability of the debris flow run-out distance onto the debris fan of the Faucon catchment. In other words, the chance that a debris flow, with a known and well defined initiation (16,728.4 m^3) and entrainment zone (3500 m long), will reach a specific point or area on the debris fan. The second spatial probability estimated is the debris height at the apex and V.C. 3 Bridge. The information on debris flow heights can be used to assess the probability of the debris flow overtopping its banks. The debris heights can be further combined with velocities to assess the impact pressure on elements at risk, which is a hazard intensity used in vulnerability assessment.

The probability of the run-out depends highly on the number of friction parameter values sampled and the method used to sample these values. The Monte Carlo method mentioned in Chapter 2 is used to sample hundreds if not thousands of values randomly in order to estimate uncertainty in the input parameters and can be further used in a probabilistic hazard assessment. However, due to the lack of time, the Monte Carlo Method could not be applied in this study.

The method used to calculate the run-out probability onto the fan and the debris heights at their locations is a simple frequency probability method. The probability $P(x)$ of a debris flow run-out reaching area x is approximated by:

$$P(x) \approx \frac{n_x}{n_t} \qquad \text{(Eq. 19)}$$

where n_t is the total number of modeled run-outs and n_x is the number of modeled run-outs where the area x has been affected. Thus, the probability is approximated using the relative frequency, and for this reason given the name Frequency Probability method.

All 53 run-outs that have been modeled for the sensitivity analysis, including the calibrated run-out model, were used to calculate the frequency of the run-out on areas on the debris fan until the Ubaye River. This was done by dividing the length of the channel in the debris fan into 10 m intervals. A total distance of 2000 m was chosen in order to represent the whole channel on the debris fan including everything in between the apex and the Ubaye River. A total of 200 intervals (2000 m/10 m) are represented within this 2000 m zone of the channel.

The number of modeled debris flow run-outs that reached each interval was counted, thus obtaining the frequency of run-outs at each 10 m interval. The probability of a debris flow reaching each interval on the debris fan is then calculated by dividing the frequency with the total number of debris flow run-outs. Figure 35 illustrates an example of how the probability of the run-out distance was estimated.

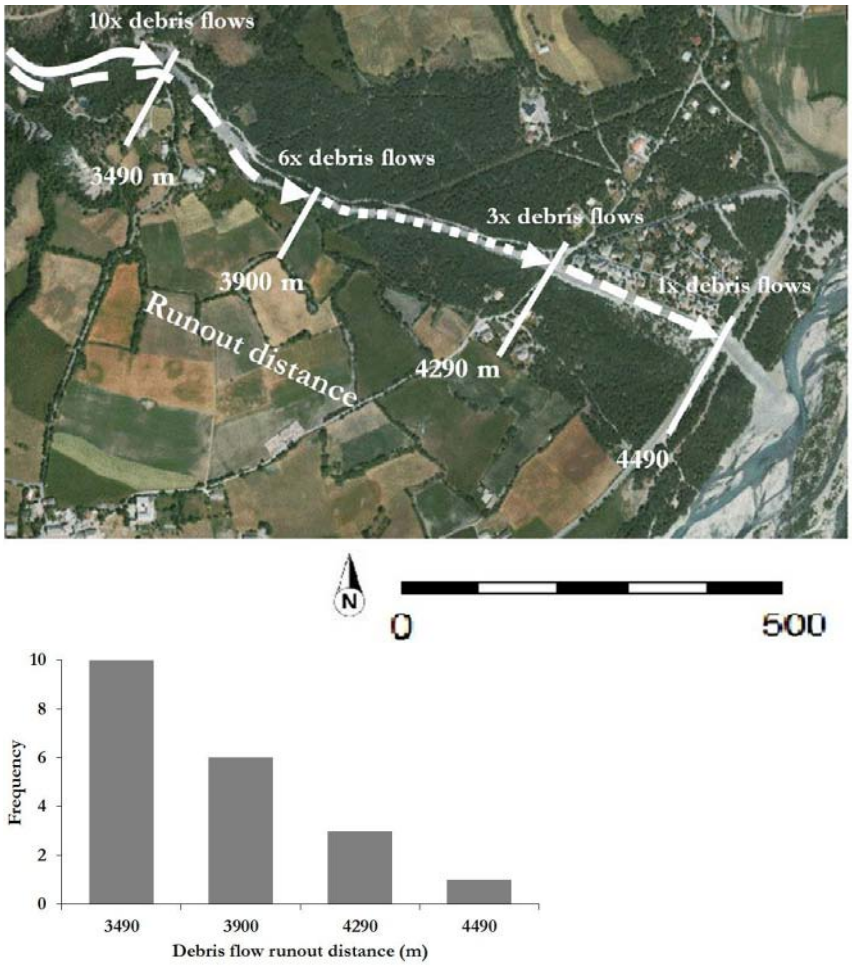

Figure 35 (Top) Using distance intervals to obtain the frequency of the debris flow run-out. The frequencies in this illustration are only an example and not the actual frequencies found in the research. (Bottom) Example of the frequency distribution of the run-out distance according to the information on the left image.

The run-out frequencies (Figure 35) are divided by the total number of run-outs and the final outcome is a graph showing the run-out distance from the apex until the Ubaye River versus the spatial probability of the debris flow run-out reaching a particular area within the debris fan. Thus, giving the chance of a debris flow with an initiation volume of 16,728.4 m³, passing through a transport zone (3500 m) with 0.5 m and

2.0 m debris heights (Figure 33), reaching an area on the debris fan, given that 53 run-outs are modeled with their corresponding input parameter ranges (Table 7). What is of particular interest is the probability of the debris flow reaching the V.C. 3 Bridge which is the start of the Domaine de Bérard deposit zone and where most of the elements at risk are located.

The same method (Eq. 19) used to calculate the run-out probability is applied to calculate the spatial probability of the debris height at the apex and the V.C. 3 Bridge, which are considered two points of interest. The height at these two locations is divided into intervals of 10 cm, from 0 m to the highest debris height modeled in the 53 runs.

When a modeled run-out reaches a point of interest, the maximum height is taken of that flow and the number of 10 cm intervals is counted between 0 m and the maximum height of the modeled flow. For example if the maximum debris height at the apex is 3 m, then (300 cm/10 cm) 30 intervals would each receive 1 count (occurrence). The frequency is then calculated by summing the number of occurrences for each 10 cm, after 53 run-outs are modeled. The result is the probability of the maximum debris flow height, given as a relative frequency distribution for each 10 cm interval from the channel bed to the maximum height reached by all the 53 models. By dividing this frequency with the total number of models (53), the probability is then estimated. Figure 36 is an example illustrating how the frequency for the debris flow height was estimated.

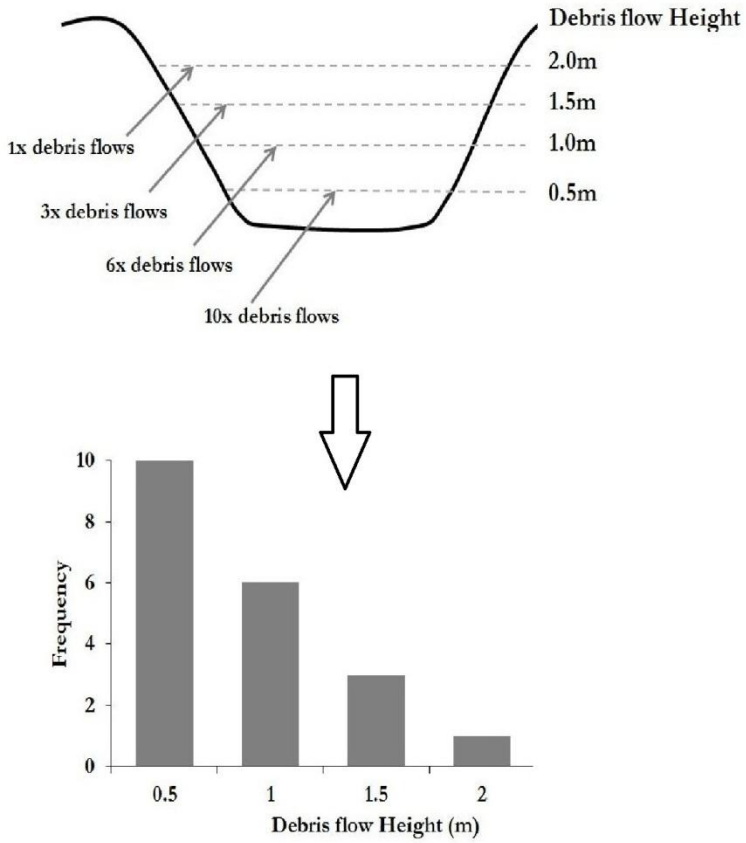

Figure 36 (Top) The number of debris flows reaching an interval height is counted and (bottom) the frequency is plotted versus the debris flow height. This example uses 0.5 m intervals; however in this research 10 cm intervals were used.

5. RESULTS

5.1. Introduction

The objective of this chapter is to explain the results found based on the applied methodology in the previous chapter. The outcome is an improved DEM which was used to calibrate the run-out model. After calibration, the findings of the sensitivity analysis are further explained including the results of the probability analysis of the run-out and maximum debris flow height at the fan apex and the V.C. 3 Bridge.

5.2. The Produced DEM

The ArcGIS topo-to-raster function tries to create a hydrologically correct surface model (ArcGIS Resource Center, 2010), taking drainage into account. Figure 37 shows the contour lines derived from the new created DEM. This area is the transition zone between the 5 m contours including the new channel geometry and the 1 m contour area at Domaine de Bérard. The final DEM used as the main input in the RAMMS modeling has a resolution of 5 m and only represents the initiation zone, the torrent in the transport zone and the deposit zone at the debris fan (Figure 38a). In order to save calculation time of the interpolation of the contour lines and the importing of the DEM to RAMMS, areas that are of no interest to the debris flow were cropped out in ArcGIS. Figure 38b further shows the complete study area of the Faucon catchment in 3D after the new DEM was imported into RAMMS.

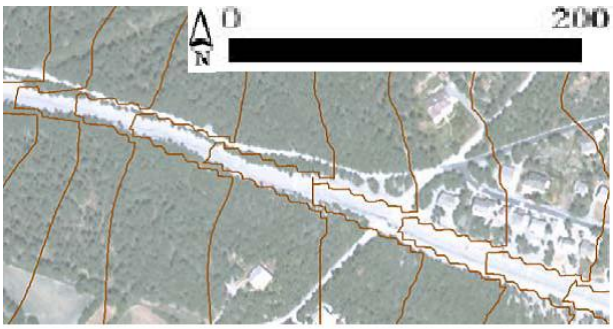

Figure 37 Resulting contour lines of the final interpolation at the transitional zone between the corrected channel geometry and the 1m DEM

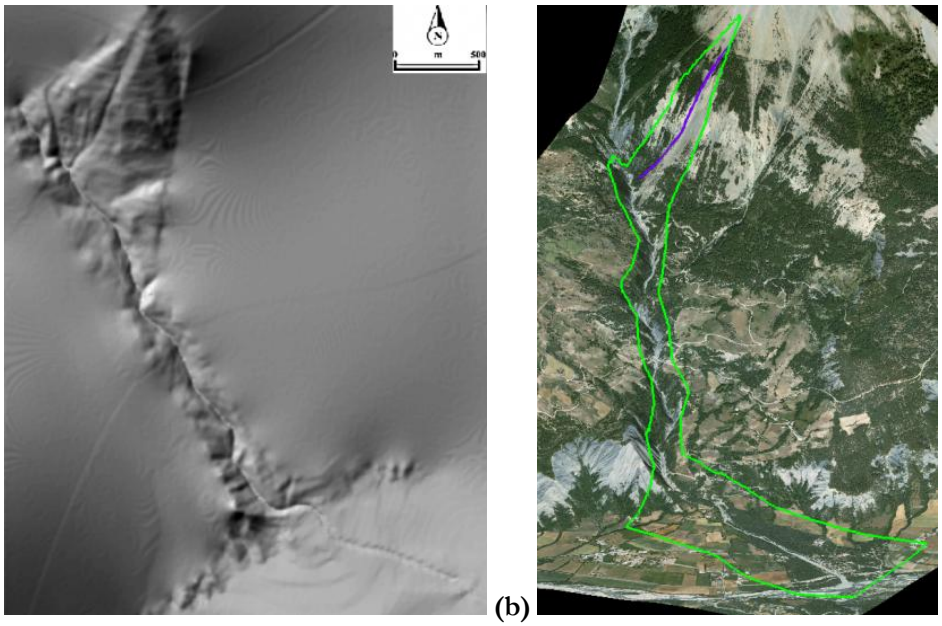

(a) (b)

Figure 38 (a) Hillshade of the final 5 m DEM. (b) 3D visualization of the terrain after the DEM is imported in RAMMS including the calculation domain.

The new DEM was tested with the calibrated model run-out in RAMMS to compare with the preliminary model run which used the previous DEM made from the 5 m contours. The results of this comparison are shown in Figure 39. There is a considerable improvement in the new DEM, the debris flow stays within the channel and reaches the Ubaye River.

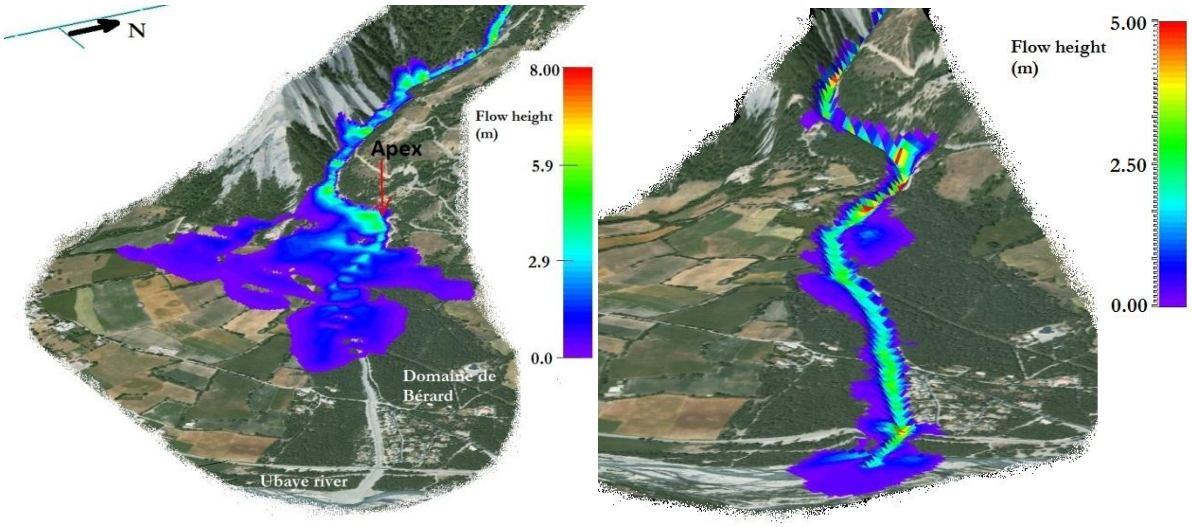

Figure 39 (Left) Model run of the maximum debris heights with the old 5 m contour derived DEM and (right) the result of modeling with the new created 5 m DEM

5.3. Calibration Results

5.3.1. Calibrated Inputs

The method of trial and error combined with calibration criteria was used to calibrate the debris flow model based on data from past events (initiation zone), fieldwork (entrainment zone) and literature (model parameters). Table 8 summarizes all the input values that resulted from the model calibration.

Table 8 Summary of the Calibrated inputs

Simulation Parameters	**Values**
Grid resolution (m)	10
End time (s)	800
Dump step (s)	10
Total dump steps	80
Initiation Zone	
Release Height (m)	1.5
Calculated Release Volume (m^3)	16,728.40
Density Release (kg/m^3)	1850
Entrainment Zone	
Density Entrainment (kg/m^3)	1850
Entrainment Height	
zone 1 (m)	0.5
zone 2 (m)	2
Model Input Parameters	
μ (Mu)	0.06
ξ (Xi) (m/s^2)	500
Entrainment coefficient K	1
Earth pressure coefficient Lambda	1

The simulation parameters, initiation parameters and entrainment parameters were all used as constants. The optimal calibrated values of the input model parameters that were found are 0.06, 500, 1 and 1 for μ (Mu), ξ (Xi), K and Lambda, respectively.

When calibrating a model that can have continuous variations in the values of input parameters, one must consider the principle of equifinality. Equifinality states that there are many ways or paths that can lead to the same end (von Bertalanffy, 1968). Therefore, there is a possibility of reaching the same calibrated output using different combinations of input values.

In order to avoid equifinality and come up with a single set of parameter values for the calibration, the values were constrained to their limits (ranges) based on the literature. The model was run many times using trial and error methods in order to optimize each parameter. However, the most important method used to avoid equifinality was the use of the calibration criteria. These are 5 different criteria as mentioned in the previous chapter and further discussed in the next section. There was not a single run that could meet all 5 criteria, including the calibrated model. Therefore, the possibility of another set of parameter values replicating the same calibrated run-out is very slim.

5.3.2. Calibrated Outputs

Table 9 summarizes the intensity parameters of the calibrated model and their deviation from the 1996 and 2003 debris flow parameters estimated by the studies discussed previously in Chapter 3. Most of the intensity parameters of the past events have specific ranges. For example the initiation volume of the 1996 event was estimated by Remaître (2006) to range between 5,000 and 7,500 m². Thus, the deviation from past events is calculated in percentage difference from the lowest or highest range depending on whether the calibrated values are underestimated or overestimated.

Table 9 Past events versus calibrated intensity parameters

Intensity Parameters	1996 Debris Flow	2003 Debris Flow	Calibrated Model	Deviation from 1996	Deviation from 2003
Initiation volume	5,000 – 7,500 m³	14,000 – 17,000 m³	16,728.4 m³	+ 223 %	0 %
Entrainment volume	92,500 – 95,000 m³	69,000 – 78,000 m³	75,052 m³	- 18.9 %	0 %
Total deposited volume	100,000 m³	83,000 – 95,000 m³	91,780.4 m³	- 8.2 %	0 %
Run-out distance	4400 – 4500 m	4700 m	4765 m	+ 5.9 %	+ 1.4 %
Maximum debris flow height near fan apex	1.5 – 3.0 m	5.0 – 6.0 m	3.38 m	+ 26.7 %	- 32.4 %
Maximum debris flow height at the V.C. 3 Bridge	3.0 – 4.5 m	5.0 – 6.0 m	2.76 m	- 8 %	- 44.8%
Velocity near fan apex	4.9 – 7.8 m/s	6.4 – 8.9 m/s	7.19 m/s	0 %	0 %
Velocity at the V.C. 3 bridge	< 4.9 m/s	2.0 – 5.0 m/s	2.59 m/s	0 %	0 %

The difference between the volumes of 1996 and of the calibrated model is due to the difference in the initiation. The 1996 debris flow was initiated by a shallow landslide next to the torrent, unlike the 2003

event and the modeled debris flow which initiated in the scree slopes. The 1996 event was used in the calibration due to the similarity of the entrainment and depositional processes with the 2003 event. Thus, the calibrated model is more similar to the 2003 event in all aspects.

The following calibration criteria (Section 4.6.7) have been met (Table 9):

- The calibrated initiation volume of 16,728.4 m³ falls within the 2003 initiation volume range
- The calibrated deposited volume of 91,780.4 m³ is very close to the 1996 event and falls within the 2003 deposit volume range
- The calibrated run-out distance is only overestimated by 1.4 % from the 2003 debris flow
- The calibrated velocities at the apex and at the V.C. 3 Bridge both fall within the 1996 and 2003 range

The final criterion of the debris heights could not be met. The model underestimates the debris flow heights at both the apex and V.C. 3 Bridge by 30 to 45 % when compared with the 2003 event, and slightly overestimates the debris height by 26.7 % at the apex when compared with the 1996 event. Possible reasons for this underestimation are discussed in the next chapter.

Figure 40 shows the results of the calibrated model from the initiation until the deposit zone in a 3D environment. The average maximum flow heights range between 1.5 to 3 m and increase rapidly just before the fan apex. The final debris flow deposit is approximately 3500 m long from the head to the tail of the debris flow.

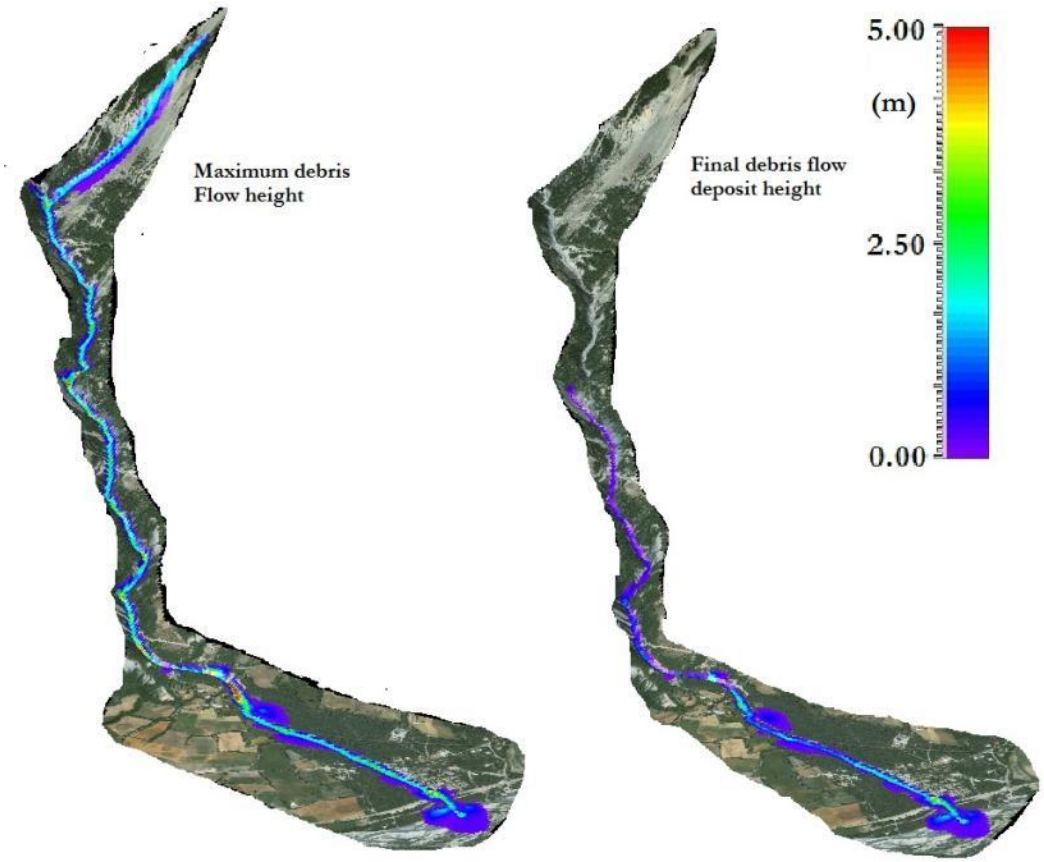

Figure 40 (Left) Maximum debris flow height of the calibrate model and (right) the deposit thickness at the end of the flow.

The debris fan is especially important due to the elements at risk that are affected by the debris flow. Figure 41 reveals the deposit height on the debris fan of the calibrated debris flow. Starting at the fan apex the flow increases in height and overtops its channel banks just below the apex, with maximum deposits of 50 cm on the banks. As the flow approaches the V.C. 3 Bridge, the height increases and deposits a few centimeters of debris just next to the channel. The largest increase in height occurs before the R.D. 900 Bridge, reaching almost 5 meters and covering an area approximately 70 m wide around the main road. Finally the Ubaye River is only partially blocked by the debris where the flow starts dispersing on the banks of the Ubaye River.

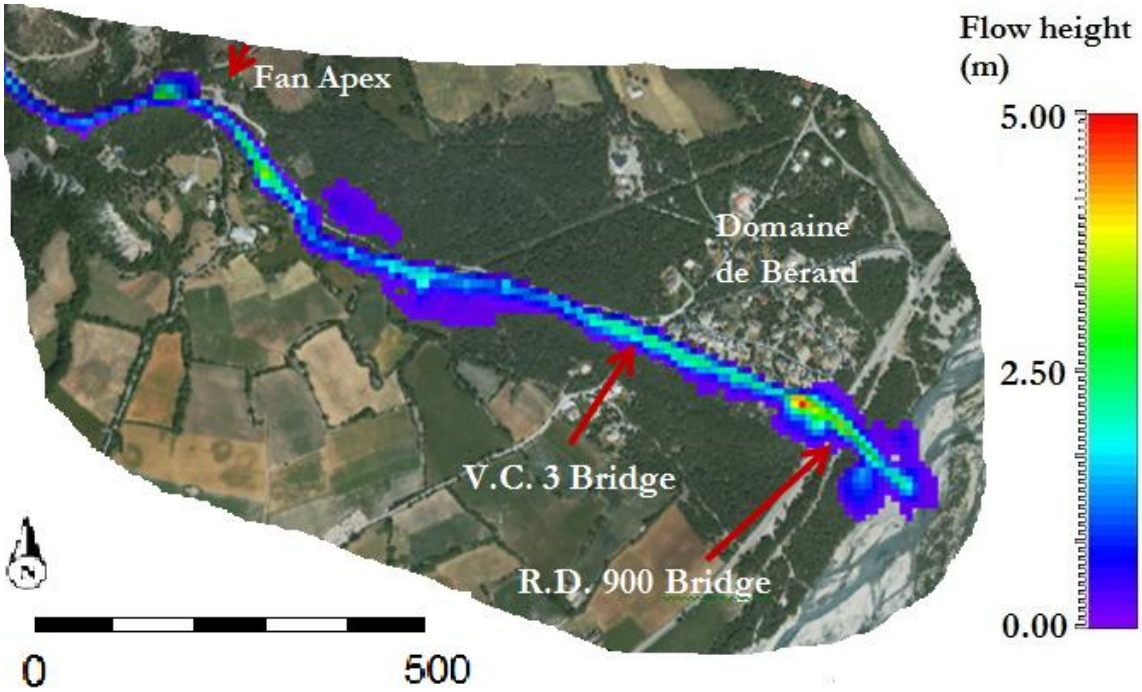

Figure 41 Deposit height of the calibrated debris flow at the debris fan.

When looking at the run-out of the deposit height in a longitudinal profile, there are sudden peaks visible (Figure 42a). The peaks correspond to an increase of height ranging from 1.5 to 2.5 m at several areas in the torrent. After a run-out distance of 2500 m in the flow path, five peaks occur. The final peak coincides with the flow being plugged before the R.D. 900 Bridge. Figure 42b shows the cross section of the channel near the V.C. 3 Bridge and the corresponding deposit height (red) of the debris flow. The figure indicates that the channel banks are covered by less than 0.5 m of debris.

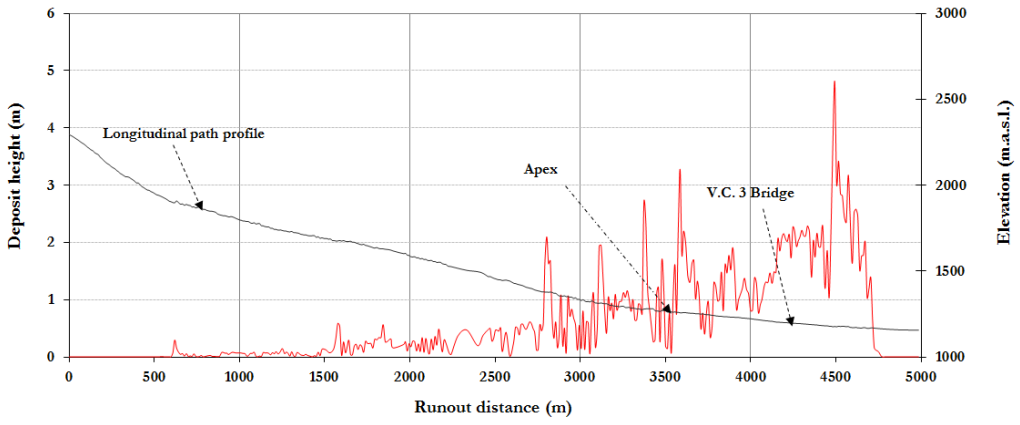

(a)

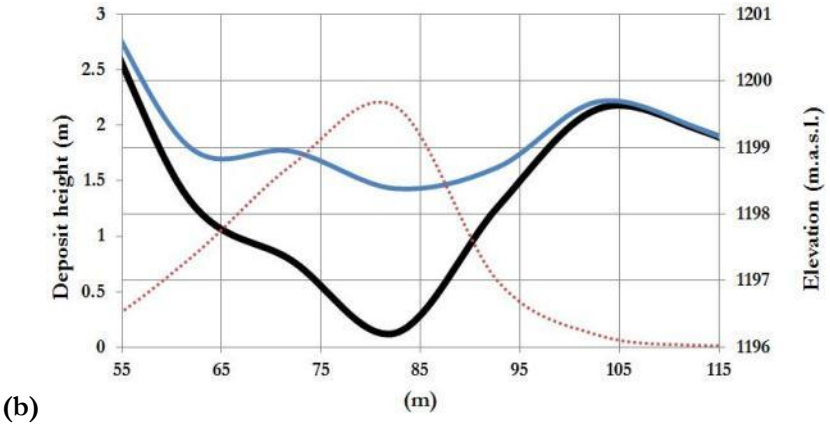

(b)

Figure 42 (a) Run-out profile of the calibrated debris flow. (b) The cross section of the debris flow deposit (blue) and the corresponding height (red) near the V.C. 3 Bridge location.

The velocity substantially decreases as the debris flow continues on the debris fan from the apex (Figure 43). Before the apex, velocities range between 10 to 15 m/s. Average velocities after the apex range between 4 and 6 m/s in most parts of the channel until reaching the R.D. 900 Bridge, where the flow starts dispersing and velocity rapidly decreases into the Ubaye River.

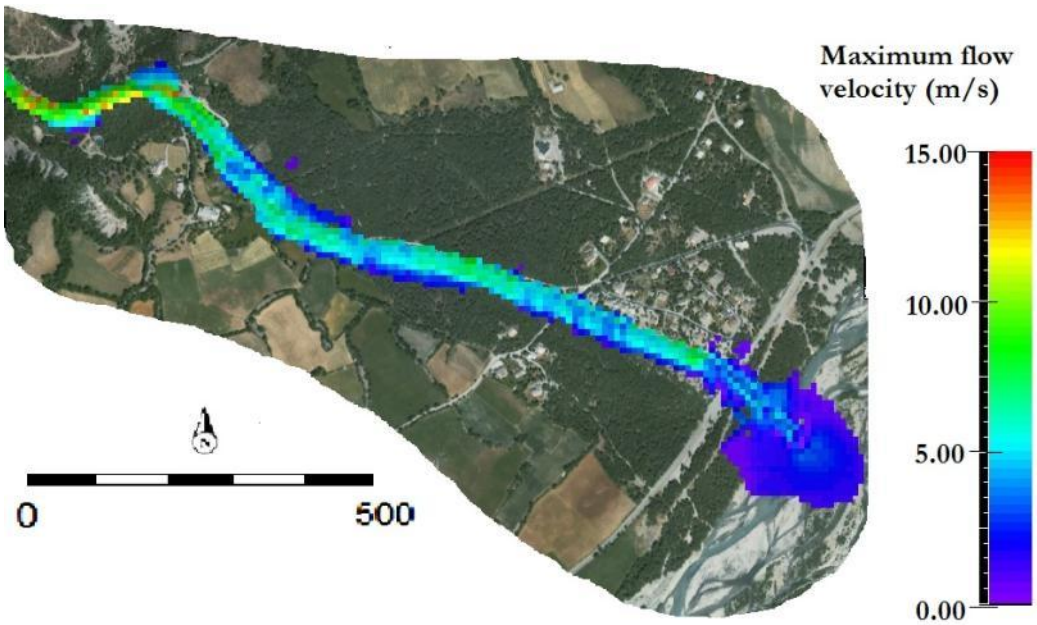

Figure 43 Maximum calibrated velocities at the debris fan

5.4. Results of the Sensitivity Analysis

Table 10 is an example of how one of the parameters, in this case the friction coefficient Mu, was varied from the calibrated value (0.06) for the sensitivity analysis. The corresponding change in deposit volume, run-out distance and debris height and their deviation from the calibrated output values are all calculated. This was done for each of the four input parameters tested and tables of all the modeled results are available in Appendix IV.

Table 10 Sensitivity of the deposit volume, run-out and debris height to changes in the friction coefficient Mu. The calibrated outputs are shaded in grey.

Mu	Mu (%)	Volume (m3)	Volume (%)	Runout (m)	Runout (%)	Height VC3 Bridge (m)	Height VC3 Bridge (%)
0.01	-83.33	62,973.60	-31.39	4,970.00	4.30	3.06	10.94
0.02	-66.67	71,590.20	-22.00	4,965.00	4.20	3.10	12.30
0.03	-50.00	77,585.40	-15.47	4,925.00	3.36	2.59	-6.27
0.04	-33.33	58,474.30	-36.29	4,815.00	1.05	2.16	-21.93
0.05	-16.67	57,117.70	-37.77	4,755.00	-0.21	2.06	-25.44
0.06	0.00	91,780.40	0.00	4,765.00	0.00	2.76	0.00
0.07	16.67	55,111.20	-39.95	4,515.00	-5.25	1.83	-33.58
0.08	33.33	54,169.40	-40.98	4,311.00	-9.53	1.19	-56.78
0.09	50.00	72,020.90	-21.53	4,215.00	-11.54	0.00	-100.00
0.10	66.67	68,021.30	-25.89	4,034.00	-15.34	0.00	-100.00
0.15	150.00	47,820.20	-47.90	3,565.00	-25.18	0.00	-100.00
0.16	166.67	48,157.10	-47.53	3,448.00	-27.64	0.00	-100.00
0.20	233.33	59,398.90	-35.28	3,036.00	-36.29	0.00	-100.00

5.4.1. Sensitivity to the Friction Coefficient μ (Mu)

An increase in the friction coefficient μ (Mu) causes a decrease in the run-out distance (Figure 44 and Table 10). This is expected, due to the increase in the basal friction of the flow with increase in Mu. The debris flow does not reach the Ubaye River or the R.D. 900 Bridge above a Mu value of 0.08.

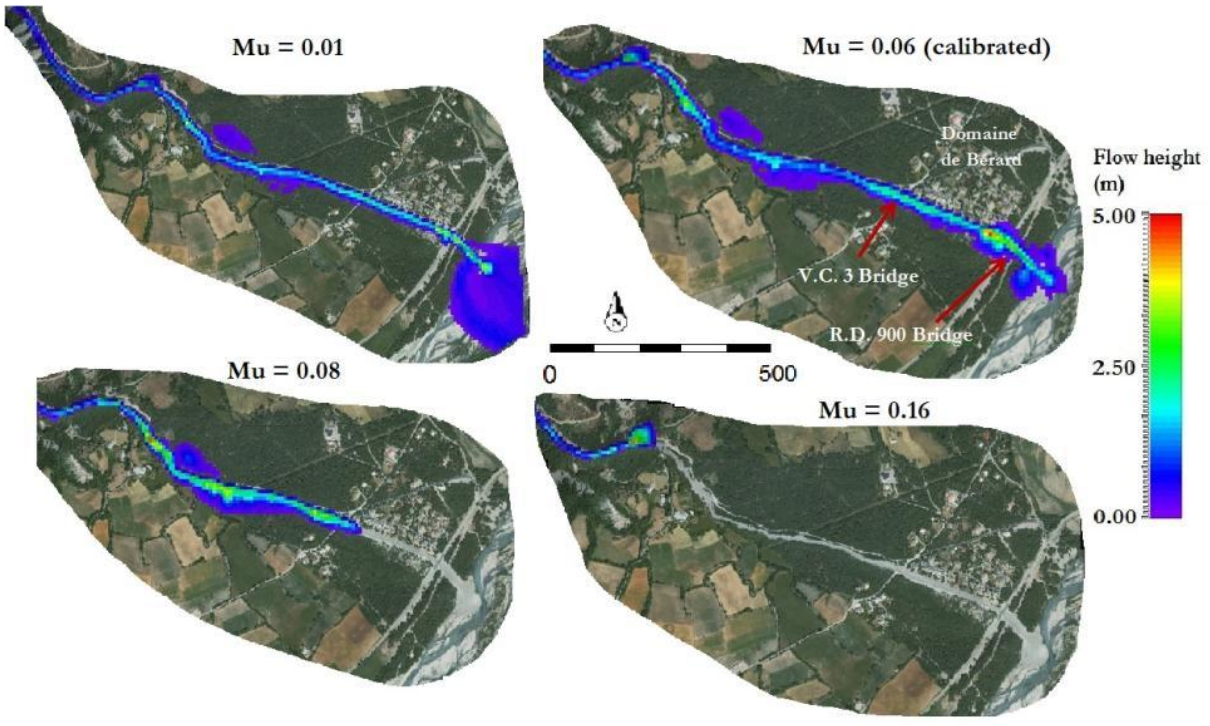

Figure 44 Extent of the debris flow run-out for different friction coefficient (Mu) values

Mu values from 0.16 and onwards causes the flow to stop before the apex. Mu values higher than the calibrated 0.06 also generate higher deposit heights (> 4 m) around the fan apex and an increase in deposits on the channel banks due to the divergent spreading of the flow as it slows down. The velocities decrease when Mu is lower, however the biggest velocity difference with the calibrated model is found at the V.C. 3 Bridge. A Mu value of 0.07 gives a velocity at the bridge of 1.1 m/s, compared with the calibrated 2.6 m/s, which is a twofold decrease in velocity.

When Mu is lower than the calibrated 0.06, the debris flow increases its run-out distance into the Ubaye River, causing extra deposits of sediment (10 to 50 cm) inside the Ubaye River channel. Lower Mu values further generate lower deposit heights (1 – 2 m) in the channel on the debris fan and there are less deposits on the channel banks. However, there seems to be a reversing trend in heights between 0.06 and 0.03 Mu, where the heights first decrease, than increase after 0.03. The flow is further more confined to its channel and the velocities increase. The velocity at the fan apex for a Mu of 0.01 is 9.7 m/s compared to the calibrated 7.2 m/s.

Figure 45 shows the debris flow profiles for Mu values higher than 0.06. The difference in run-out distance between 0.06 and 0.16 is approximately 1750 m. The peaks of the deposit height before the fan apex (run-out distance of 3490 m) are almost twice as high for a Mu of 0.16; the difference in deposit height is similar throughout the deposition until the tail of the debris flow.

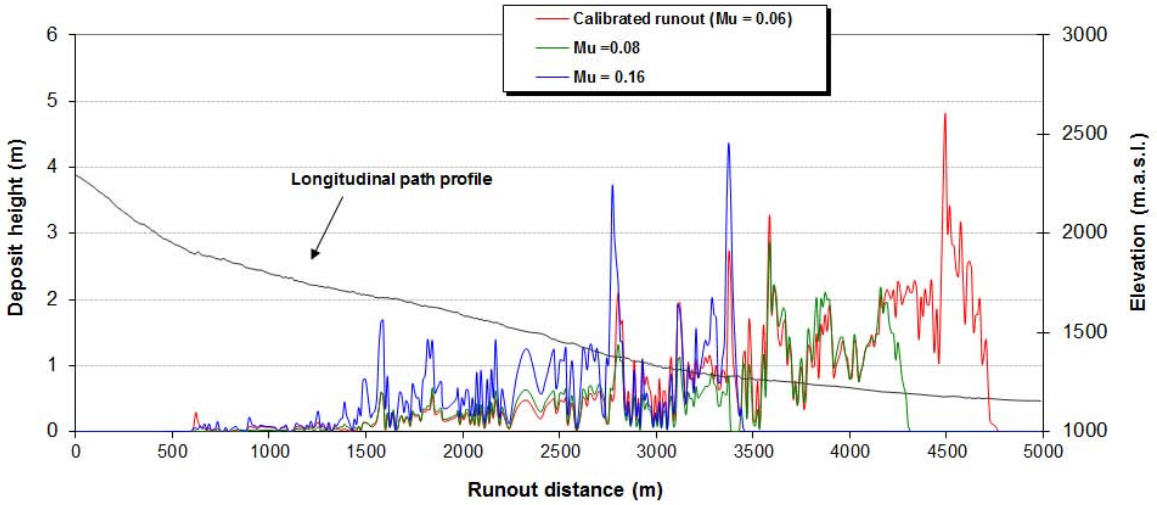

Figure 45 Longitudinal profile of the calibrated run-out versus run-outs calculated with higher friction (Mu) coefficient values

5.4.2. Sensitivity to the Turbulent Coefficient ξ (Xi)

Table 11 and Figure 46 show the extent of the run-out with changes in the turbulent coefficient ξ (Xi). A decrease in Xi causes a decrease in run-out distance. The head of the debris flow leaves a higher deposition as it stops near the apex. Below a Xi value of 300 m/s², the flow does not reach the V.C. 3 Bridge and below 150 m/s² the flow stops before the fan apex. There is further little dispersal of the flow onto the channel banks. The velocity is also affected by changes in Xi, where a Xi of 200 m/s² corresponds to a velocity of 4.2 m/s compared to the calibrated 7.2 m/s at the apex. A Xi of 300 m/s² gives a velocity of 1.42 m/s compared to the calibrated 2.6 m/s at the V.C. 3 Bridge.

Table 11 Sensitivity of the deposit volume, run-out distance and debris height to changes in the turbulent coefficient Xi. The calibrated outputs are shaded in grey.

Xi (m/s^2)	Xi (%)	Runout (m)	Runout (%)	Deposit volume (m^3)	Deposit volume (%)	Max height VC3 (m)	Max height VC3 (%)
100.00	-80.00	2961.00	-37.86	48616.40	-47.03	0.00	-100.00
125.00	-75.00	3384.00	-28.98	45050.20	-50.92	0.00	-100.00
150.00	-70.00	3586.00	-24.74	48277.30	-47.40	0.00	-100.00
200.00	-60.00	3828.00	-19.66	55225.80	-39.83	0.00	-100.00
250.00	-50.00	3806.00	-20.13	53284.10	-41.94	0.00	-100.00
300.00	-40.00	4290.00	-9.97	51880.20	-43.47	1.27	-53.89
350.00	-30.00	4311.00	-9.53	56121.40	-38.85	1.49	-45.90
400.00	-20.00	4399.00	-7.68	56775.10	-38.14	1.84	-33.24
450.00	-10.00	4573.00	-4.03	56669.80	-38.26	1.91	-30.75
500.00	0.00	4765.00	0.00	91780.40	0.00	2.76	0.00
550.00	10.00	4805.00	0.84	97778.40	6.54	2.74	-0.92
600.00	20.00	4835.00	1.47	89472.10	-2.52	2.75	-0.39
650.00	30.00	4845.00	1.68	87836.00	-4.30	2.63	-4.64
700.00	40.00	4875.00	2.31	92428.50	0.71	3.01	9.18
800.00	60.00	4895.00	2.73	92772.70	1.08	3.08	11.46

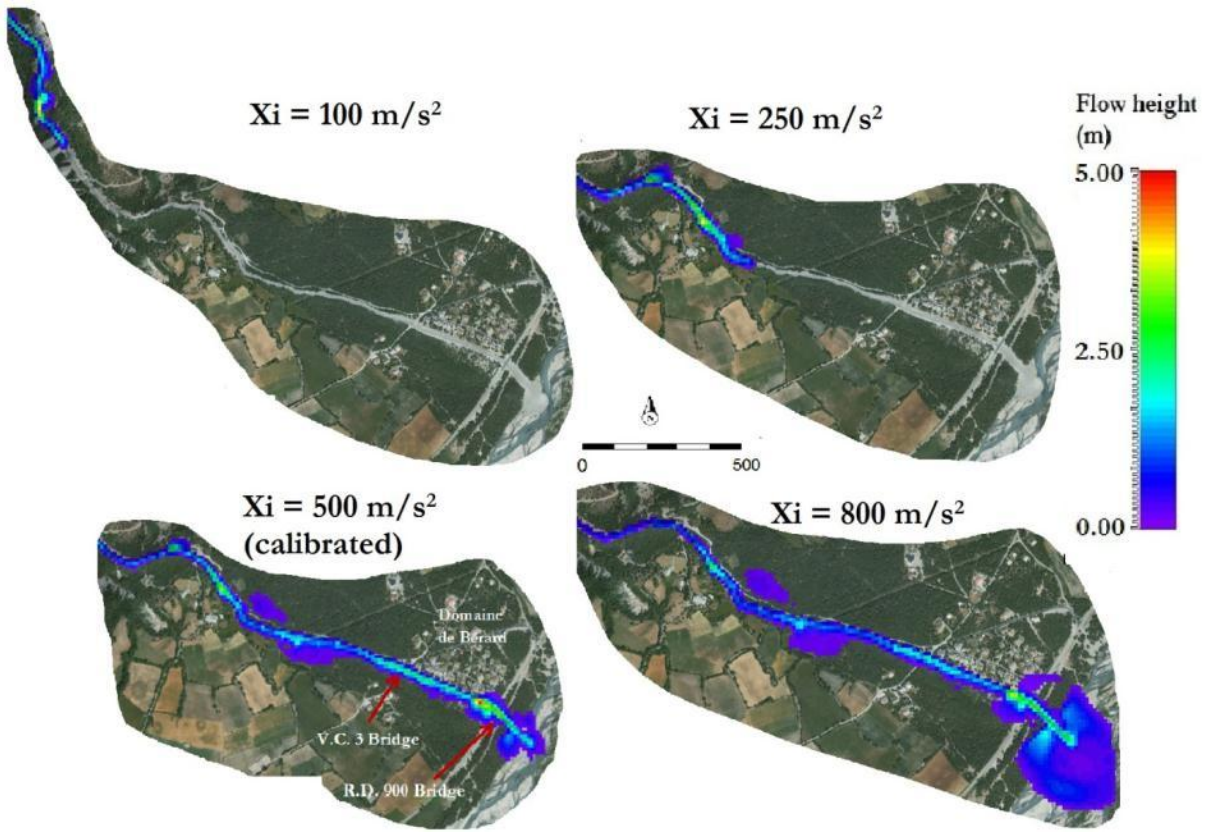

Figure 46 Extent of the debris flow run-out for different turbulent coefficient (Xi) values

An increase in Xi generates an increase in the run-out distance (Figure 46), so that the head of the flow is farther extended into the Ubaye River. However, the deposit heights on the fan are fairly similar to the calibrated heights when the Xi is increased, unlike the velocities which do show a considerable increase. A Xi of 800 m/s^2 generates a velocity of 9 m/s at the fan apex, compared to the calibrated 7.2 m/s.

Figure 47 shows that a Xi of 250 m/s² has a run-out distance 1700 m shorter than the calibrated run-out, with slightly higher depositions before the apex. A Xi of 100 m/s² shows similar results to the calibrated model (Xi = 500 m/s²), with a slight decrease in deposit heights.

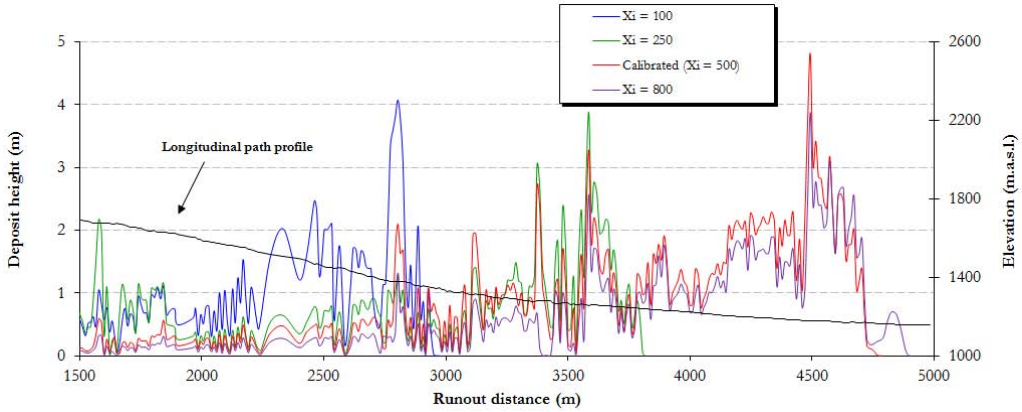

Figure 47 Longitudinal profiles for different turbulent coefficient (Xi) values

5.4.3. Sensitivity to the Entrainment Coefficient K

Figure 48 reveals the extent of the run-out with changes in the entrainment coefficient K. The debris flow does not reach the V.C. 3 Bridge with K values 0.3 or lower. The only K value that stops the flow before the apex is 0, where no entrainment takes place at all. A K of 0.1 still causes the flow to pass the apex, however the debris flow heights are extremely low (50 to 80 cm). A K of 0.4 generates a debris height of 1.8 m at the apex and 1.6 m at the V.C. 3 Bridge, compared with the calibrated values of 3.4 m and 2.6 m, respectively. The overall decrease in run-out distance with decrease in the entrainment coefficient is expected, due to the fact that less debris is entrained. The debris flow velocities corresponding to lower K values are slightly lower compared with the calibrated values. A 0.1 K generates a velocity of 5.4 m/s at the apex, compared to the calibrated 7.2 m/s.

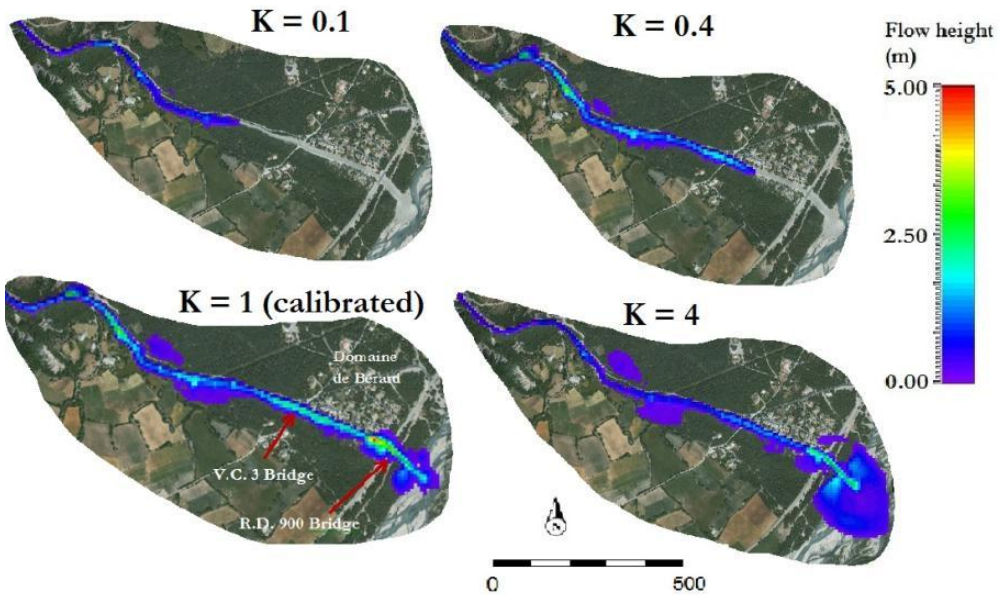

Figure 48 Extent of the debris flow run-out for different entrainment coefficient (K) values

Higher K values show only a slight increase in velocity and debris height. A K value of 4.0 has a slightly longer run-out (± 150 m) distance than the calibrated model (Figure 48). There is further very little deposition on the channel banks, with just a few centimeters below the apex.

Figure 49 shows that the modeled run-out with K value 4.0 resembles the calibrated model. The debris height however is lower, especially at the R.D. 900 peak, where the calibrated model has a debris height almost 2 m higher. A higher entrainment coefficient is expect to generate higher deposits, however this is not the case. A K of 0.4 has a shorter run-out distance than the calibrated run-out but the deposit heights are similar to the calibrated heights.

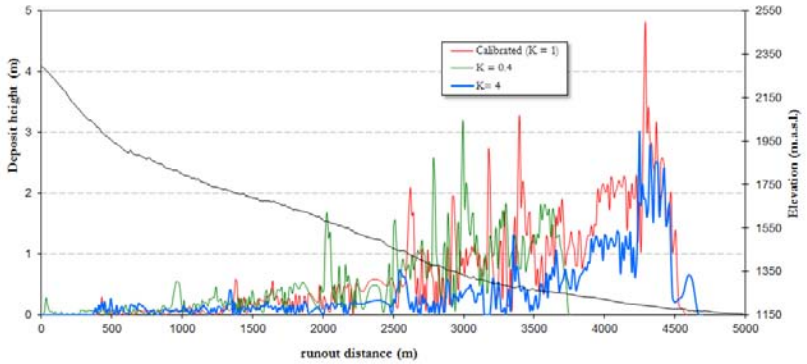

Figure 49 Longitudinal profiles for different entrainment coefficient (K) values

5.4.4. Sensitivity to the Earth Pressure Coefficient Lambda

A lower earth pressure coefficient value is expected to cause a higher dispersion of the flow at areas where the velocities decrease, like on the debris fan as mentioned in the previous chapter. This is indeed the case when looking at Figure 50.

The calibrated value for the earth pressure coefficient Lambda is 1.0. The rest of the Lambda values in the sensitivity analysis were set below 1.0, because Lambda cannot be higher than 1.0. Figure 50 shows that as the Lambda decreases, the debris flow slightly increases in height at the head and increases in run-out distance. The lateral divergence of the flow into the channel of the Ubaye River also increases with the run-out. The run-out distance is not affected as compared to the effects of the other parameters in the sensitivity analysis. The decrease in Lambda further causes more debris deposits to overtop the channel banks.

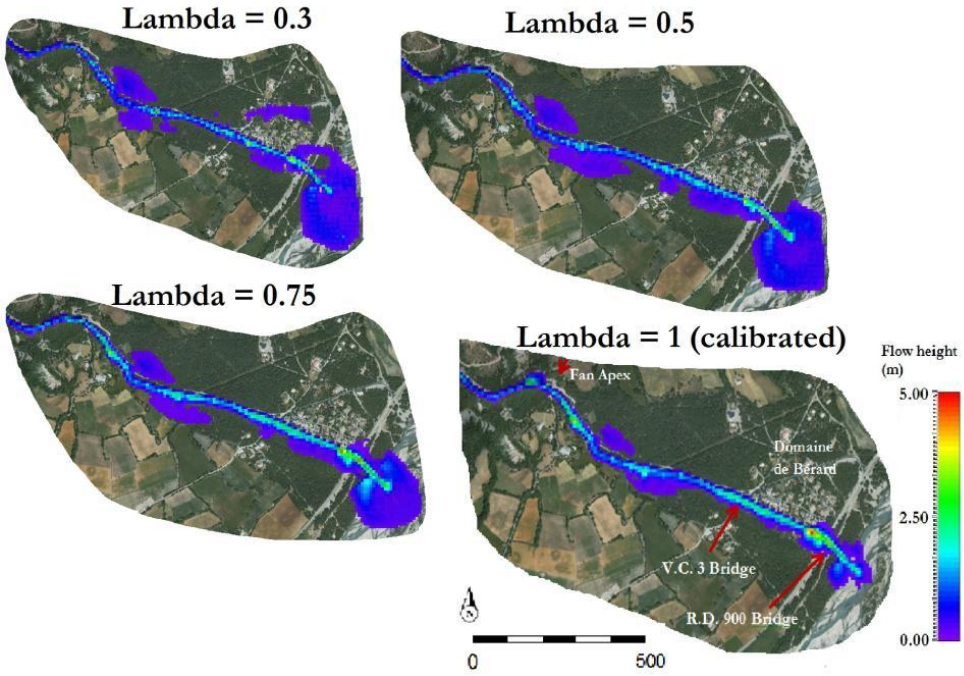

Figure 50 Extent of the debris flow run-out for different earth pressure coefficients (Lambda) values

The velocities slightly increase as the Lambda decreases, with a Lambda value of 0.5 corresponding to a velocity of 8.0 m/s at the apex and 2.9 m/s at the V.C. 3 Bridge, compared to the calibrated 7.2 m/s and 3.4 m/s respectively.

Figure 51 shows that the debris flows of lower Lambda values are very similar in run-out compared to the calibrated run-out, with slight increase in distance. The debris heights above the apex also show similarities. Thus, the earth pressure coefficient has little effect on the run-out distance or deposit heights.

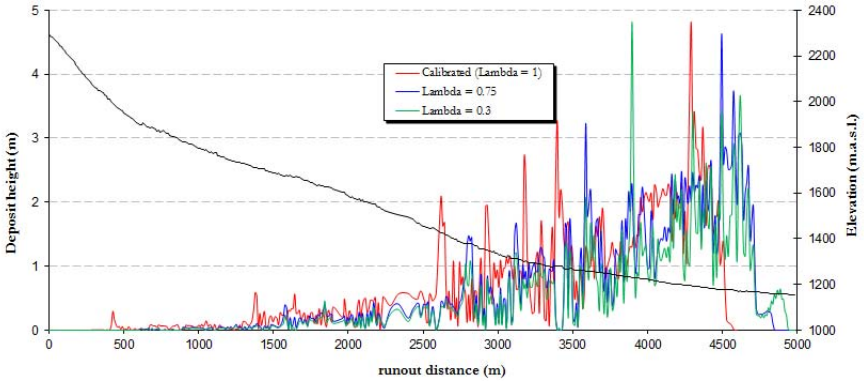

Figure 51 Longitudinal profiles for different earth pressure coefficient (Lambda) values

5.4.5. Sensitivity of the Deposit Volume to the Input Parameters

The total deposited volumes for friction coefficient (Mu) values other than the calibrated 0.06, are all lower than the calibrated volume (91,780.4 m^3). Figure 52a shows an almost symmetrical graph around Mu 0.06, as if a slight decrease or increase from 0.06 seems to have similar effects on the deposit volume. However, increasing the Mu above 0.1 causes a further drop in the volume, with the lowest deposit volume (47,820.2 m^3) found at Mu = 0.15.

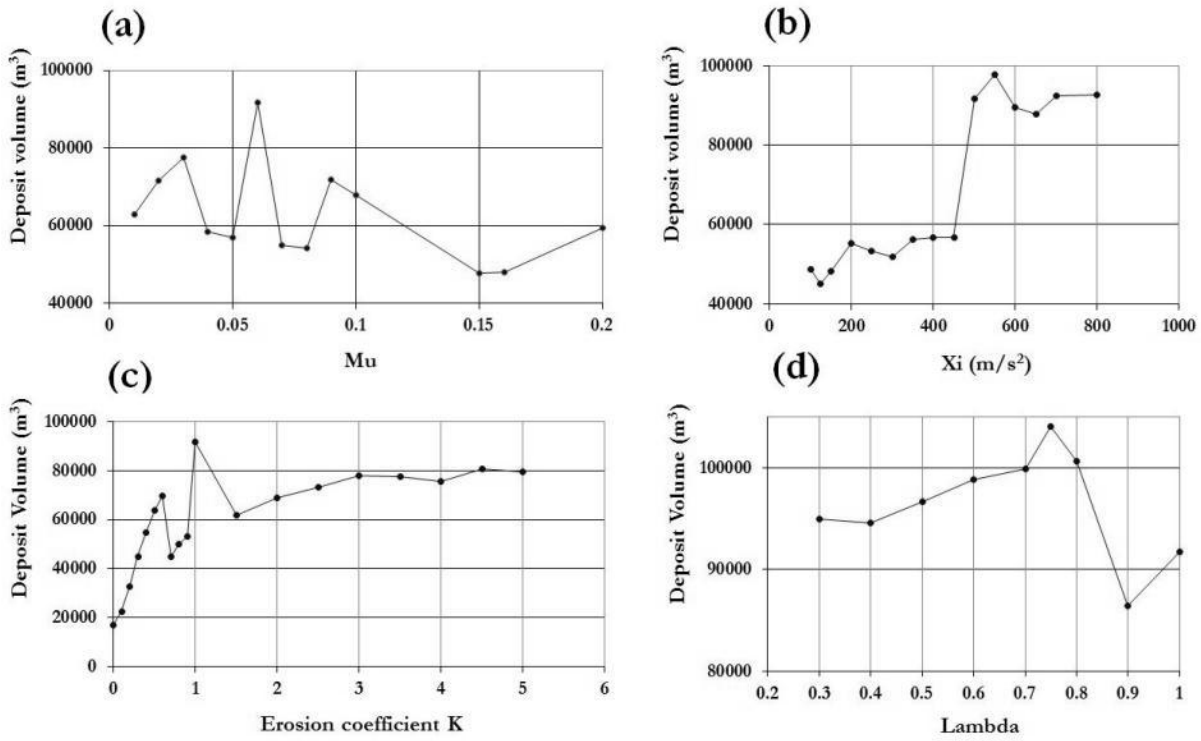

Figure 52 (a) Sensitivity of the deposit volume to the friction coefficient Mu, (b) turbulent coefficient Xi, (c) entrainment coefficient K and (d) the earth pressure coefficient Lambda.

The effect of the turbulent coefficient Xi on the deposit volume is remarkable (Figure 52b), with a large decrease in volume between the calibrated Xi value of 500 m/s² and 450 m/s². The decrease in volume is approximately 34,000 m³. Volumes corresponding to a Xi below 450 m/s² continue to decrease but at a steady state. Above a Xi of 500 m/s² the volume seems to be nearly constant.

The calibrated volume with an entrainment coefficient (K) value of 1.0 is the highest modeled deposit volume out of the whole range of K values (Figure 52c). A decrease in K from the value 1.0 causes a substantial decrease in the deposit volume. An increase from 1.0 decreases the volume to approximately 60,000 m³ and afterwards slightly increases to 80,000 m³. The decrease of the entrainment coefficient has a stronger effect on volume than an increase.

An earth pressure coefficient (Lambda) of 0.9 decreases the total deposited volume to approximately 87,000 m³. Decreasing Lambda further causes the volume to range between 95,000 and 114,000 m³ (Figure 52d). These values indicate that the effect on volume is not as strong as compared to the effects of the other input parameters mentioned in this chapter.

5.4.6. Sensitivity of the Run-out Distance to the Input Parameters

Figure 53 indicates that the run-out distance is more sensitive to an increase in the friction coefficient Mu than to a decrease. A 50 % increase in Mu causes a 10% decrease in the run-out, while a 50% decrease generates only an increase of the run-out distance by 5%. The effect seems twice as large, with the increase in Mu seeming almost linear to the decrease in run-out.

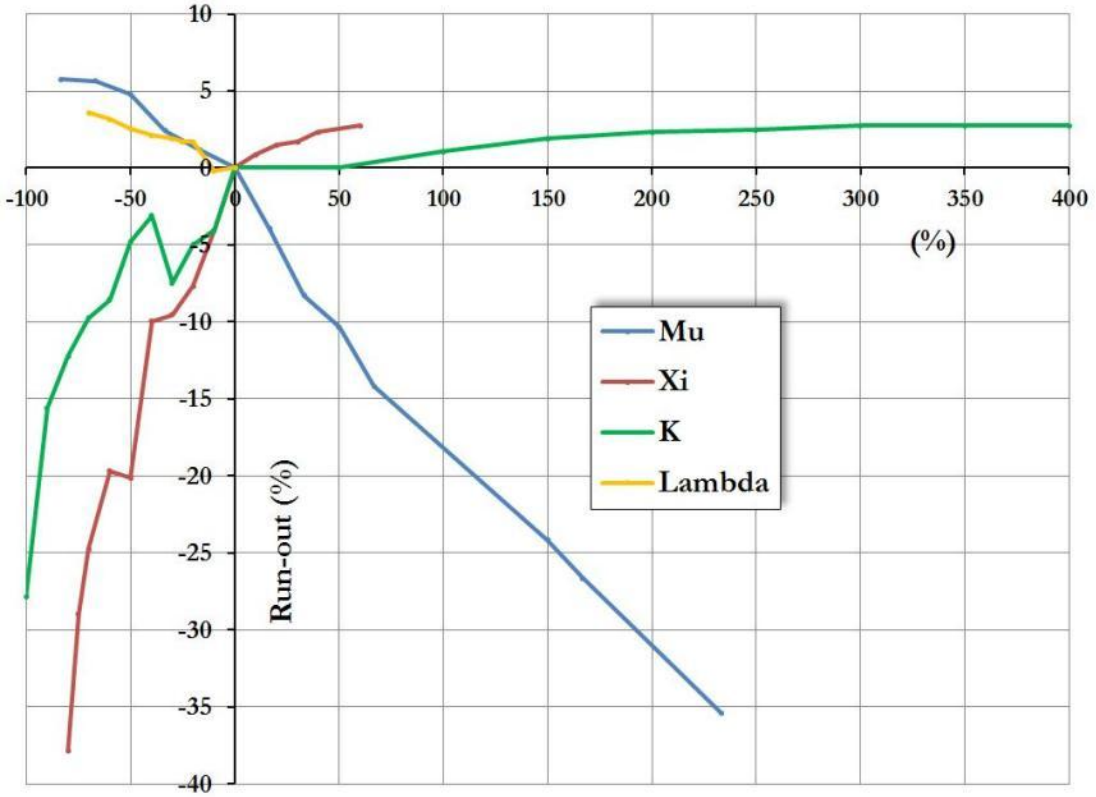

Figure 53 Sensitivity of the run-out distance to the four input parameters: friction coefficient (Mu), turbulent coefficient (Xi), entrainment coefficient (K) and the earth pressure coefficient (Lambda)

The change in run-out distance with the change in turbulent coefficient Xi (Figure 53) seems to follow the trend found in the change of the deposit volume (Figure 52b). A 50 % increase in Xi causes the run-out to increase by only 2.5%, but a decrease by 50% generates a 20% decrease in the run-out distance of the flow.

The decrease in the turbulent coefficient has a stronger effect on the run-out than the decrease in the friction coefficient. However, the increase in the friction coefficient has a stronger effect than the increase in the turbulent coefficient.

Increasing the entrainment coefficient K has very little effect on the increase in run-out distance (Figure 53). The increase is gradual and becomes constant (2.5 % increase of run-out) at around a 300% increase of K. However, after a 70 % decrease in K, the decrease in run-out distance becomes substantial and starts dropping below 25%. When K equals 0 (no entrainment) the modeled run-out falls behind the apex and decreases by approximately 27%.

The decrease in earth pressure coefficient Lambda only slightly increases the run-out distance (Figure 53). A maximum decrease of 70 % causes a 3.5 % increase in the run-out distance. Interesting to note is that a decrease in Lambda by 10% which corresponds to a Lambda of 0.9 slightly decreases the run-out. The earth pressure coefficient seems to have the least effect on the run-out distance.

5.4.7. Sensitivity of the Debris Flow Height to the Input Parameters

Decreasing or increasing the friction coefficient Mu by 20% causes a drop in debris height at the V.C. 3 Bridge (Figure 54). The effect of Mu on the debris height looks similar to the effects on the deposit volume (Figure 52a). A 50% increase in the friction coefficient generates no height (-100%) due to the fact that the flow does not reach the bridge. Remarkably, a reversing trend can be seen between a 10% to 50% decrease in Mu, the height starts increasing after a 50% increase.

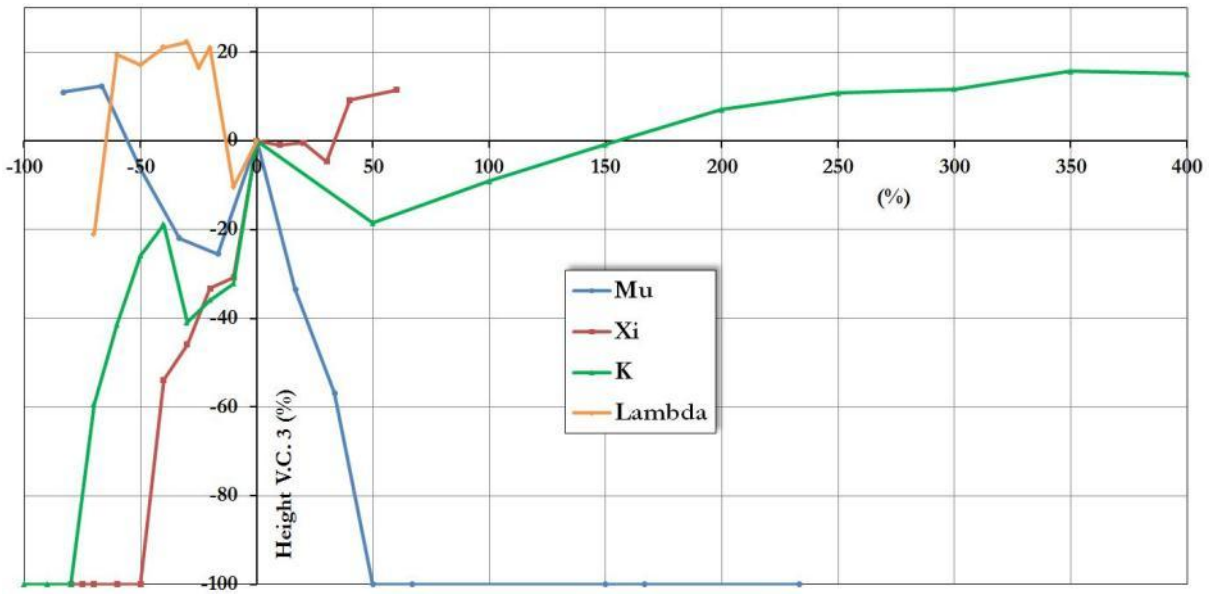

Figure 54 Sensitivity of the debris flow height at the V.C. 3 Bridge to the four input parameters: friction coefficient (Mu), turbulent coefficient (Xi), entrainment coefficient (K) and the earth pressure coefficient (Lambda)

The resulting change in debris height with change in the turbulent coefficient Xi values (Figure 54), are also similar to the change in volume and run-out distance. A 20 % increase in Xi does not affect the debris height, with a further increase by 60% generating a debris height 10% larger than the calibrated value. However, a 50% decrease in Xi causes the height to decrease by 100% (no height). Thus, the decrease in Xi greatly affects the run-out distance, deposit volumes and the debris flow height, with only slight changes of these parameters to an increase in the Xi value. The decrease in the turbulent coefficient (Xi) and the increase in the friction coefficient (Mu) have similar effects on the debris height, almost symmetrical when looking at Figure 54.

The increase in entrainment coefficient K until 150 % actually causes a decrease of the debris height (Figure 54). An increase in the K value higher than 150%, only slightly increases the debris height. This is interesting because, it was expected that an increase in the entrainment coefficient would cause an increase in the entrained volume and thus increasing the debris flow height. However, this is not the case.

A decrease in the entrainment coefficient K greatly affects the debris flow height (Figure 54), with a 100% drop in debris height with a 75% decrease in K. The debris height is clearly the most affected when K is set lower than the calibrated value of 1.0.

The debris height at the V.C. 3 Bridge increases between 15 % to 25% when the earth pressure coefficient Lambda is decreased by 20% or more (Figure 54). As with the run-out distance, the Lambda value of 0.9 causes a slight decrease in height by 10%. From Lambda 0.8 the height stabilizes until Lambda 0.4, where the height starts to drop below the calibrated value.

5.4.8. Summary of the Sensitivity Analysis

According to Figures 52, 53 and 54, the effects of each parameter on the sensitivity of the deposit volume, run-out distance and the debris flow height depends on whether the parameter value is being increased or decreased from the calibrated value. When combining the effects of the increase and decrease of each parameter, an overall effect can still be assessed.

The total deposit volume is most sensitive to a decrease in the entrainment coefficient K followed by the turbulent coefficient Xi and then by the friction coefficient Mu (Figure 52). The deposit volume is the least sensitive to the earth pressure coefficient Lambda.

The parameter that shows the highest effect on the run-out distance to an increase in its value is the friction coefficient Mu. The other parameters do not affect the run-out distance more than 5% when increased. The parameter that shows the highest effect on the run-out distance to a decrease in its value is the friction coefficient Xi.

The run-out distance is most sensitive to the overall effect of the turbulent coefficient Xi followed by the friction coefficient Mu and then by the entrainment coefficient K (Figure 53). The run-out distance is least sensitive to the earth pressure coefficient Lambda.

Finally the debris flow height at the V.C. 3 Bridge is most sensitive to the turbulent coefficient Xi followed by the friction coefficient Mu and then by the entrainment coefficient K (Figure 54). The earth pressure coefficient Lambda has the least effect on the debris flow height.

5.5. Results of the Probability Analysis

5.5.1. Run-out Probability

Table 12 indicates all the run-out distances modeled in the sensitivity analysis and includes the calibrated run-out distance (shaded in grey). These run-outs were used to calculate the spatial frequency and probability of the run-out onto the debris fan as explained in the previous chapter.

Table 12 The 53 modeled run-out distances including the calibrated model run shaded in grey

Mu	Runout (m)	Xi	Runout (m)	K	Runout (m)	Lambda	Runout (m)
0.01	4970	100.00	2961.00	0	3438	0.3	4935
0.02	4965	125.00	3384.00	0.1	4022	0.4	4915
0.03	4925	150.00	3586.00	0.2	4182	0.5	4885
0.04	4815	200.00	3828.00	0.3	4300	0.6	4865
0.05	4755	250.00	3806.00	0.4	4357	0.7	4855
0.06	4765	300.00	4290.00	0.5	4538	0.75	4845
0.07	4515	350.00	4311.00	0.6	4618	0.8	4845
0.08	4311	400.00	4399.00	0.7	4410	0.9	4755
0.09	4215	450.00	4573.00	0.8	4527	1	4765
0.1	4034	500.00	4765.00	0.9	4573		
0.15	3565	550.00	4805.00	1	4765		
0.16	3448	600.00	4835.00	1.5	4765		
0.2	3036	650.00	4845.00	2	4815		
		700.00	4875.00	2.5	4855		
		800	4895	3	4875		
				3.5	4882		
				4	4895		
				4.5	4895		
				5	4895		

Given the limited time for this research, it was not possible to carry out more than 53 runs. The run-outs modeled for the sensitivity analysis were very useful. However, they only contain the variation of one parameter at a time. Thus, the effect of changing two or more parameters in a single run is not taken into account. In order to carry out such an approach, where multiple parameters are changed accumulating to several hundred model runs with corresponding parameter combinations, would need a Monte Carlo approach. Not only was there a lack of time for such an approach, but the necessary tools were unavailable.

Figure 55 shows the spatial probability distribution of the run-out onto each 10 meters between 3000 and 5000 m of the debris flow path, within the debris flow channel. The probability is assessed on four areas of interest due to their proximity to elements at risk: the fan apex, the V.C. 3 Bridge, the R.D. 900 Bridge and the outlet of the Faucon torrent to the Ubaye River. The spatial probabilities of the run-out reaching the four areas of interest are indicated in Table 13.

The spatial run-out probability is calculated using 53 modeled debris flows with the constant parameter values of an initiation height of 1.5 m with a total volume of 16,728.4 m^3, an entrainment zone with debris heights of 0.5 m and 2.0 m and an initiation and entrainment material density of 1850 kg/m^3. The 53 models were kept to the calibrated constant values while shifting the value of each of the four input parameters within the sensitivity analysis parametric range (Table 7).

Given the above mentioned information used in calculating the probability, the chance of the debris flow reaching the apex is 91%. The chance that the debris flow reaches the V.C. 3 Bridge and the village of Domaine de Bérard is estimated at 75%, with a 62% chance of the flow hitting the R.D. 900 Bridge and a 51% chance of the flow continuing to the Ubaye River.

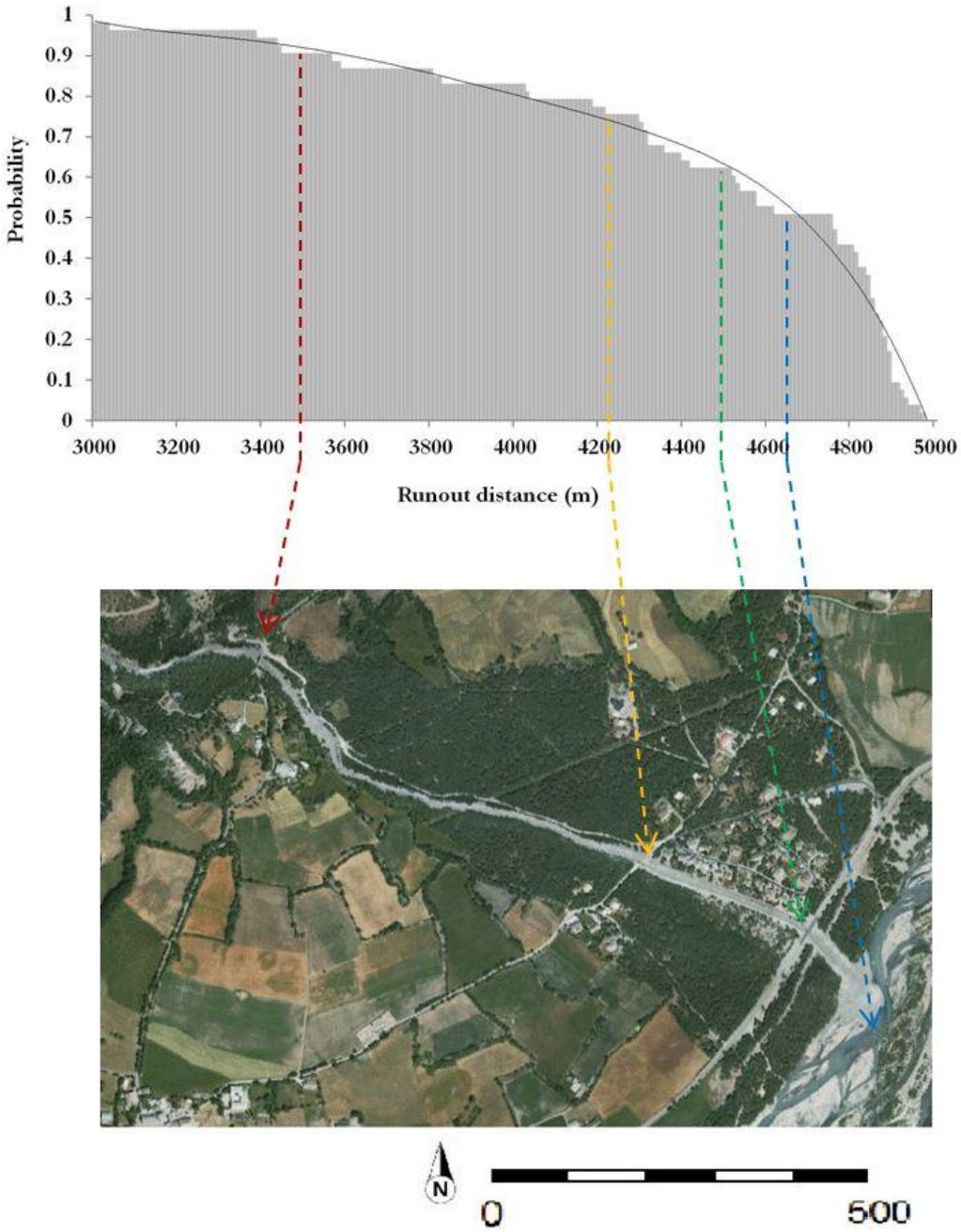

Figure 55 (Top) Probability of the run-out between 3000 and 5000 m of the run-out path. (Bottom) locations of the points of interest.

Table 13 Probability of run-out onto the locations of interest

Points of interest	UTM East (m)	UTM North (m)	Elevation (m)	Runout distance (m)	Frequency (nr. of flows)	Probability
Fan Apex	315274.51	4919022.5	1269	3490	48	0.91
V.C. 3 Bridge	315935.56	4918684.8	1197	4240	40	0.75
R.D. 900 Bridge	316210.43	4918567.9	1176	4490	33	0.62
Ubaye River	316331.41	4918431.7	1167	4650	27	0.51

5.5.2. Probability of the Maximum Debris Height

The probability of the maximum debris height is assessed for two locations: the apex and the V.C. 3 Bridge. These locations are chosen due to the bridges (elements at risk) they contain and the fact that the V.C. 3 Bridge is the start of the depositional zone at Domaine de Bérard. Figure 56 and 57 show the distribution of the probability of the maximum debris flow height at the apex and the V.C. 3 Bridge, respectively. There is approximately a 15% probability that the debris height equals 0 m at the apex and a probability of 18% of a 0 m height at the V.C. 3 Bridge, which corresponds to debris flows that never reached the apex or the V.C. 3 Bridge.

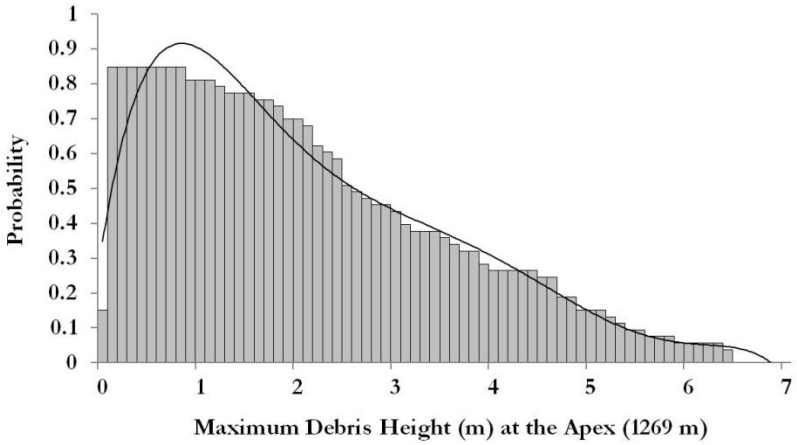

Figure 56 Probability of the maximum debris height at the fan apex

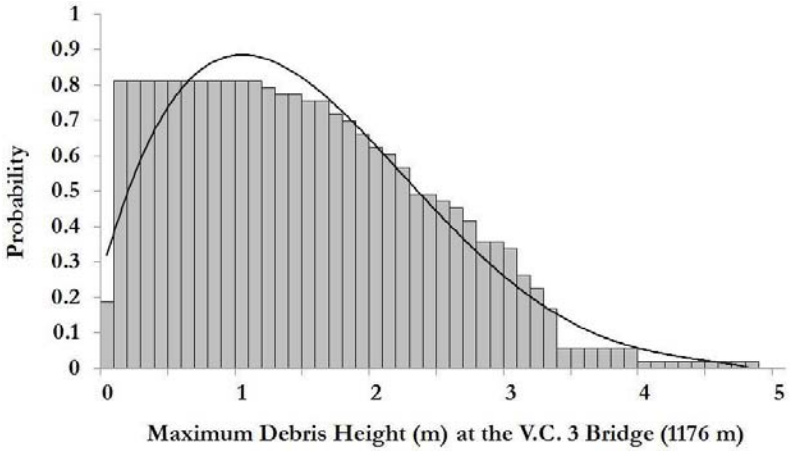

Figure 57 Probability of the maximum debris height at the V.C. 3 Bridge

The probability distribution for both locations is right skewed, with the distribution at the apex having a longer tail due to the number of debris flows stopping near the apex. As the debris flow stops near the apex, the head of the flow is higher than the rest of the body, giving the probability of higher debris flow heights near the apex. When the debris flow does reach the V.C. 3 Bridge, the head is mainly located after the R.D. 900 Bridge or partly inside the Ubaye River channel. Therefore the highest part of the debris flow does not occur at the V.C. 3 Bridge.

The mean probabilities of the height at the apex and the V.C. 3 Bridge are 0.43 and 0.42, respectively and correspond to a height of 3.0 and 2.65 m, respectively. The probability of the debris flow height at both locations is similar until 2.5 m. Above a 2.5 m height the probability at the V.C. 3 Bridge decreases from 0.4 to 0.01 at a 5 m height (Figure 57).

6. DISCUSSION

6.1. DEM Accuracy

The DEM is an essential input into the modeling of debris flows. The available topographic data for this research was shown to be unsuitable to directly use as input into the modeling process. Without creating a new DEM, the debris flow in the Faucon catchment could not have been realistically modeled and calibrated to past events. The important question is: how accurately does this new created DEM depict the reality of the topography of the area?

The ArcGIS topo-to-raster function used to interpolate the available contour lines and the channel geometry tries to create a hydrologically correct elevation model (ArcGIS Resource Center, 2010). However, when comparing the results of the newly created debris fan channel in the DEM with the actual channel geometry measured in the field, differences can be seen in the shape of the channel (Figure 58).

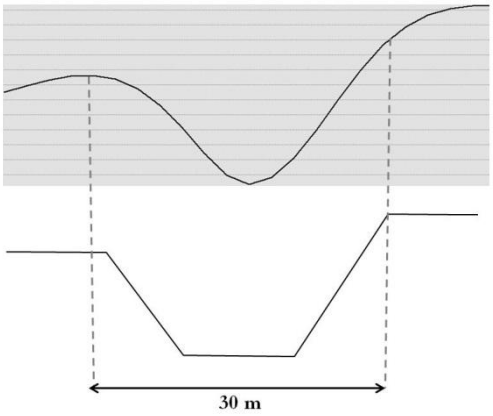

Figure 58 (Top) Smoothed channel geometry at the debris fan in the created DEM. (Bottom) The actual trapezoidal shape of the channel as observed in the field.

The width and depth of the channel in most areas in the new DEM are similar to the real channel; however the interpolation of the elevation data seems to smooth the channel cross section. The trapezoidal geometry of the channel constructed and maintained by the RTM (French Mountain Terrain Restoration Agency) is estimated with a smooth curve due to the interpolation (Figure 58). This effect can alter the flow of the model. The smooth transition onto the channel banks can cause the flow to overtop more easier, while in the trapezoid channel the sides are more steeper causing the discharge of the flow to continue down its path within the channel (Gostner et al., 2008).

This study shows that modeling channelized debris flows is extremely sensitive to the accuracy of the DEM. If the channel is not accurately depicted by the DEM, the modeled flow can be greatly affected. A LIDAR DEM can possibly give a more accurate depiction of the topography of the entire study area including the flat areas on the debris fan. LIDAR can acquire high density 3D terrain surfaces with higher accuracy for detailed representation of the study area (Liu et al., 2007). However, such a DEM was not available for this research.

It is important to note that a DEM depicts the topography at a particular point in time. The actual topography can change over a period of time by deposition and erosion of subsequent debris flows or by

human modifications to the channel, such as the construction of dikes along the channel. This research has tried to incorporate these changes. However, the effect of check dams in the upper catchment is very difficult to incorporate in the model. An important question to ask in future studies on the area: will the check dams hold when the debris flow occurs or will they be breached? Such a study can use the impact pressure on the check dams which RAMMS is able to calculate.

6.2. Initiation Zone

The calibrated debris flow that was modeled had a comparable initiation (16,728.4 m^3) to that of the 2003 event (14,000 – 17,000 m^3), which was a type of debris avalanche in scree slopes. This is different than the 1996 event that had a completely different type of initiation (shallow landslide). The 2003 event initiated in two different areas, but the modeled event was chosen to be only modeled from one single initiation zone, based on the susceptibility assessed by Remaître (2006), leaving out the areas determined to be less susceptible to the initiation of debris flows.

A thorough susceptibility analysis of the slopes in the upper part of the catchment can give more accurate information on future initiation zones in the area. Such a study would produce a detailed susceptibility map that can be used in the future as a basis for modeling debris flows or other mass movements in the catchment.

However, the prediction of future initiation zones, initiation modes and especially initiation volumes, are extremely difficult to model. This thesis has not looked into the uncertainty in initiation modeling, but other studies (e.g. Kuriakose et al., 2010) have shown that the initiation also has a very high degree of uncertainty. Especially the relationship between return period of triggering events (rainfall duration and intensity) and initiation volumes is still a largely unsolved problem, partly due to the unavailability of detailed spatial information on material properties (strength and depth of soils) and spatially distributed detailed rainfall data. In terms of run-out probability the effect of the uncertainty in initiation volume could be more important than those related to the parameters used in the run-out modeling.

6.3. Entrainment Zone

The entrainment of material in the transport zone is extremely important to the production of the deposit volume on the debris fan. The modeled initiation volume of 16,728.4 m^3 entrained a volume of 75,052 m^3 of debris to produce a final deposition of 91,780.4 m^3. Thus, the entrainment volume is approximately 4.5 times larger than the actual initiation volume.

The entrainment method used in RAMMS of dividing the transport zone in two averaged debris heights (0.5 and 2.0 m) (Figure 33) can also be subjected to an inaccuracy in the total amount of entrained debris. If the entrainment height did not have to be averaged to 0.5 m and 2.0 m and if more than two entrainment shapefiles could be added to RAMMS, than the entrainment volume would possibly have a different value.

As with the channel at the debris fan, the steeper channel of the entrainment zone is also subjected to inaccuracies in the DEM. A V-shaped channel geometry observed in several parts of the zone, was interpolated into a U-shaped channel, similar to the one shown in Figure 58. Thus, affecting the behavior of the flow in the transport zone. A narrower channel can increase the discharge and velocities of the debris flow (Gostner et al., 2008). Another point to note is that the modeled entrainment is only focused on the base of the channel and not on the side walls. Therefore, changes in the entrainment height are very important.

Entrainment in the model is dealt with in a simple manner (two entrainment zones). In reality entrainment is often simply assessed for historical events by comparing the deposited volume with the initiation volume. The effect of possible destruction of check dams and the uncertainty related to these kinds of events also plays a major role. This is something that needs further studying in the future.

6.4. Model Calibration

The application of calibration criteria has shown to be very useful in replicating a debris flow similar to the past events in the Faucon catchment. The method applies strict goals that must be met in order for a calibration to be successful. However, it must be mentioned that the calibration was conducted under an environmental setting that has been altered since the last 2003 event. The channel geometry used in the calibration is not identical to the 2003 geometry. Therefore, it cannot be expected that the modeled debris flow will have the exact same run-out as the 2003 event. The difference in the run-out between the 2003 event and the modeled debris flow is illustrated in Figure 59 and 60.

The effects of channel widening are obvious, where the model has a wider flow and deposit inside the channel (Figure 60) than the 2003 event. The modeled flow does not affect Domaine de Bérard as it did in 2003. The modeled deposit height near the houses is no more than 20 to 40 cm, slightly touching the first few houses next to the flow path.

The modeled flow in Figure 59 further shows two locations before the flow reaches the village where very thin deposits (10 – 30 cm) occur in forested areas. These deposits coincide with changes in the slope of the channel. As the channel decreases in slope, the velocity rapidly decreases and the model compensates this change by increasing the height of the flow causing the flow to overtop its banks; the rheology is thus plugged by rapid decrease in flow velocity. The maximum debris flow deposit (± 5 m) is located approximately 50 m from the R.D. 900 Bridge. This area also seems to have a decrease in slope as the channel proceeds to the Ubaye River. The reason for this rapid decrease in slope in several areas within the channel can be caused by the inaccuracies in the measured field observations or in the interpolation of the topographic data which produced the final DEM.

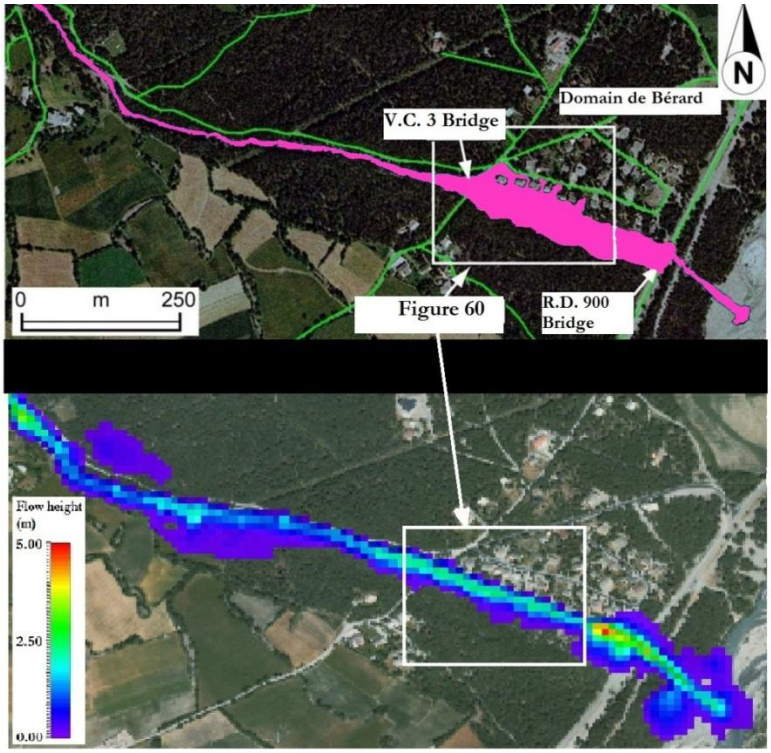

Figure 59 (Top) The 2003 debris flow run-out extent onto the debris fan (adapted from: Remaître (2006)) and (bottom) the calibrated model run-out.

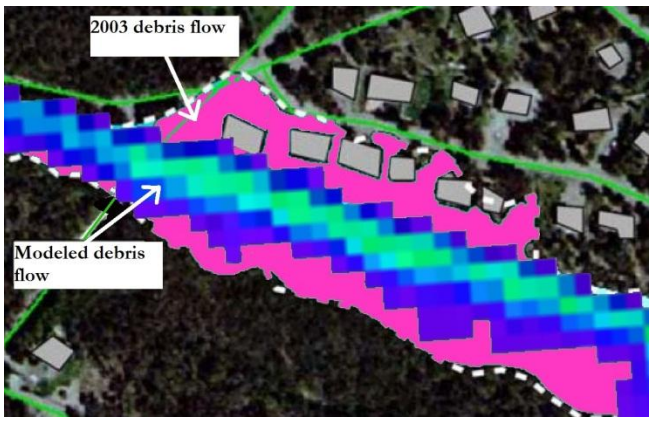

Figure 60. The 2003 event versus the modeled debris flow at Domaine de Bérard

6.5. Sensitivity Analysis

6.5.1. Deposit Volume

The total deposit volume was found to be most sensitive to the entrainment coefficient K (Figure 52c). The change in K values between 0 and 1 greatly influence the entrainment rate and thus the deposit volume. Interesting to note is that the entrainment coefficient has little effect on the deposit volume above a value of 1 (Figure 52c). According to Christen et al. (2010c), as the K value increases from 1 to 5, the debris flow height and the entrainment rate increases (Figure 61). This research indeed shows that higher entrainment coefficient values increase the debris flow height (Figure 54). However, K values higher than 1 do not produce larger deposit volumes than the calibrated 91,780.4 m³. Even if the calibrated entrainment volume of 75,052 m³ is assumed to be the maximum available entrainment volume, why do entrainment coefficient values of 2 or 5 do not pick up this entire volume, like the K value of 1? This question remains to be answered. Further studies are needed in the future to see how exactly the entrainment coefficient used in RAMMS effects the total entrained and deposited volumes

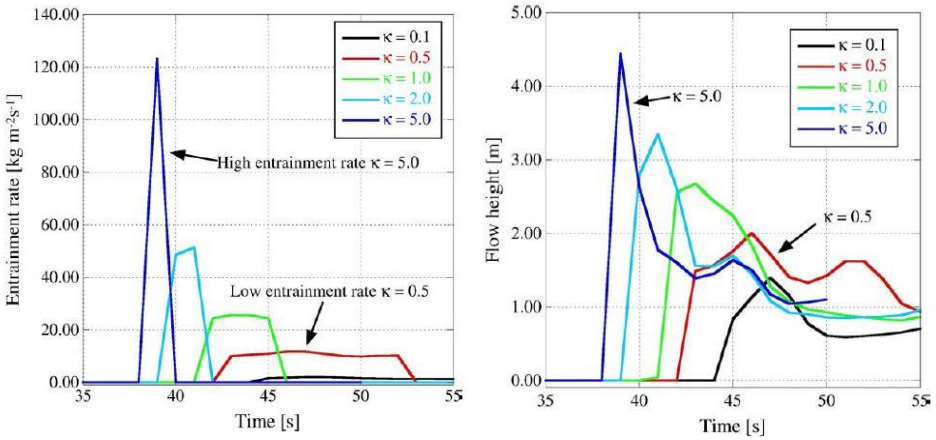

Figure 61 (Left) The effect of the entrainment coefficient on the entrainment rate and (right) on the flow height (after: Christen et al. (2010c))

6.5.2. Run-out Distance

Studies analyzing the sensitivity of the Voellmy rheological parameters on the run-out distance in 1D and 2D modeling of mass movements have been previously conducted (Borstad & McClung, 2009; Brideau et al., 2006; Hürlimann et al., 2008). Their findings conclude that the friction coefficient μ (Mu) affects the run-out distance more than the turbulent coefficient ξ (Xi), and that the turbulent coefficient mainly influences the velocity of the flow.

However, in this study the run-out distance was overall more sensitive to the turbulent coefficient ξ (Xi) than the friction coefficient μ (Mu) (Figure 53). The turbulent coefficient ξ acts as a drag force which directly affects the momentum and velocity of the flow, and for this reason given the name "velocity dependent coefficient". Furthermore, the change in velocity and energy of the flow depends highly on the topography and the channel slope, as has been discussed in Section 6.4. The irregularities in the topography including the decreasing of the turbulent coefficient ξ, causes the run-out to be sensitive to the turbulent coefficient. If the turbulent coefficient ξ were to increase, it would increase the velocity of the flow and cause the flow to be more frictional, thus increasing the effect of the friction coefficient μ (Figure 53).

There was a lack of time to carry out a sensitivity analysis of the velocity to the friction parameters. The emphasis was instead put on debris flow heights in this research, due to the fact that the elements at risk in the Faucon catchment were affected by the muddy cement like debris depositing next to or inside the houses and not by the actual velocity or impact of the debris flow on these elements at risk.

6.5.3. Maximum Debris Flow Height

As mentioned in the previous section, the maximum debris flow height was assessed in this research because of the affect it had in the past on the elements at risk. The financial costs of clean-up of the muddy deposits at Domaine de Bérard and the R.D. 900 Bridge were high and the debris cut off the main route for traffic within the whole valley for several hours.

The maximum debris flow height at the V.C. 3 Bridge is only slightly more sensitive to the turbulent coefficient ξ than the friction coefficient μ (Figure 54). There is a possibility that due to the decrease in velocity caused by the decrease in turbulent coefficient, that the height is also affected. It is however peculiar how the slight decrease in the friction coefficient causes decrease in the debris flow height (Figure 54). A possible reason is that the velocity increases due to the lower friction on the flow causing the height to slightly decrease. As was mentioned before the height reacts to the changes in velocity and slope.

Thus, the heights depend also on the topography. If there are sudden decreases in slope as mentioned previously in this chapter, the velocity can drastically decrease while at the same time increasing the height. This is possibly the cause of the irregularities found in the change of the debris height in the sensitivity analysis (Figure 54).

6.6. Spatial Probability

The probability was calculated using the output of the sensitivity analysis, which are the 53 modeled run-outs. The trend in the spatial run-out and debris height probability seems logic (Figure 55, 56 and 57). A longer run-out distance or a higher debris flow height has a lower probability of occurrence than a shorter run-out or a lower height. However the actual probabilities seem high, like a 91% chance of a debris flow reaching the fan apex. The reason for these high probabilities is the number of debris flows modeled and the parameter values chosen. Due to a lack of time more runs could not be carried out.

This study has first calibrated the model based on past events and on the basis of the calibrated input parameters, a systematic sampling scheme starting at the calibrated value was applied. If sampling occurs from a specific calibrated point, than it cannot be considered random. The uncertainty of the input parameters is therefore determined by the calibrated parameters.

If the Voellmy parameter values would have been sampled randomly including the probability for a single parameter value from a probability density function, instead of using a systematic sampling method (0.06, 0.08, 0.1…etc.) from the calibrated value, than a more accurate probability could have been found. Also the number of modeled runs can be increased in future studies to get a better probability.

A Monte-Carlo method can be applied in the future to randomly sample the parameter values including the uncertainty of the parameters and applying them to a numerical model. This would produce hundreds or even thousands of run-outs for a whole range of parameters. The parameters would not have to be kept constant in such a method due to the vast number of runs that can be conducted. Such a study could also give indications of parameters having influence on other parameters and if there is any statistical relationship between them. Due to the lack of time and material in this research, a random generation of input parameters including the assessment of their uncertainty could not be conducted. Therefore, it is highly advised to look at the uncertainties of the parameters when approaching debris flow modeling in a stochastic manner.

7. CONCLUSIONS AND RECOMMENDATIONS

7.1. Conclusions

The main objective of this thesis was to model the run-out and debris height of a channeled debris flow located within the Barcelonnette basin, in order to evaluate the possible ranges of the areas affected by the run-out, to characterize the ranges of the input parameters in the modeling and to assess the probability of the output. The sub-objectives and the conclusions drawn from them are stated as follows:

1. To assess the applicability of the Voellmy rheology applied by the RAMMS software, originally designed for snow avalanches, to model debris flow run-outs in channelized environments.

   This study has shown that the Voellmy rheology imbedded in the RAMMS dynamic modeling software can be applied to model channelized debris flow run-outs successfully, assuming that the user knows which input parameter values are needed and has gathered knowledge on the environmental setting and the past debris flow events in the area.

2. To calibrate the model input parameters in order to obtain debris flow run-outs and heights based on the past events in the Faucon catchment

   The method of applying calibration criteria has shown to be a successful approach for obtaining the calibrated input parameters, thus narrowing down the possibility of having more than one combination of input parameters giving the same output. The resulting calibrated model has been able to accurately reproduce the run-out distance within the ranges of the past events at the catchment. The under prediction of the model to the debris heights is due to the change in channel geometry since the last debris flow event. However, it can be concluded that the construction carried out on the channel after 2003 are considered to be adequate for protecting the village from debris flows with the same deposit volumes as those in 1996 and 2003.

3. To determine the sensitivity of the RAMMS dynamic model with respect to the various input parameters

   The total deposit volume of the debris flow modeled in RAMMS is most sensitive to the entrainment coefficient K. The run-out distance and the maximum debris flow height of the modeled debris flow is most sensitive to changes in the turbulent coefficient ξ followed by the friction coefficient μ. This is based on the irregularities found in the topography which have influenced the velocity of the debris flow in its channel.

4. To study the effect of the DEM used as input in the run-out model

   The study has found that the DEM accuracy greatly affects the topography of the area and the geometry of the debris flow channel. This directly affects the behavior of the debris flow in terms of velocity and debris flow height. A rapid decrease of the channel slope causes a decrease in velocity and run-out distance leading to an increase in the deposit height at the head of deposited debris flow. If the channel is simply not being depicted in the DEM, than the DEM must be

adjusted in order to recreate the actual topography, otherwise using the DEM would lead to unrealistic results.

5. To obtain the spatial probability of the modeled debris flow run-out and deposit height

   The spatial probability of a debris flow reaching the elements at risk at the village of Domaine de Bérard is estimated at 75% and is based on an initiation volume of 16,728.4 m³ with 53 modeled run-outs including their corresponding input parameter ranges. The probability of the debris flow reaching a height of 4 m is 26% at the apex and only 2% at the village of Domaine de Bérard.

The RAMMS dynamic model with the embedded Voellmy rheology seems very useful to accurately model debris flow run-outs. This powerful modeling tool, if incorporated into a full scale risk assessment can possibly give very good results. The output of the probability of the initiation (temporal and spatial) can be incorporated into modeling software like RAMMS to assess the spatial run-out probability. The output intensity parameters associated with the run-out probability can then be used to assess the vulnerability of the elements at risk on the debris fan. Thus, powerful modeling software like RAMMS which has shown to be capable of modeling run-outs accurately can be used as a stepping stone between the probability of initiation and the vulnerability assessment within the risk assessment framework.

7.2. Recommendations

- A LIDAR DEM can be very useful as input into the RAMMS software in order to accurately model the channelized debris flows at the Faucon catchment in the future. This does not only apply to the Faucon area or the RAMMS software, but also to any 2D modeling software trying to model channelized debris flows over long run-out distances.

- It is advised to thoroughly analysis the change in slope of the debris flow channel in the DEM and the effect of this slope on the changes in the velocities of the flow. This is important when using RAMMS in specific or other 2D rheological continuum models in general.

- When dealing with modeling of channelized debris flows and their extent onto debris fans or other flat areas, high resolution imagery can be of great use to show where exactly the debris flow strikes the elements at risk. The more accurate this data is, the better the hazard assessment will be.

- The grid resolution chosen for modeling these types of debris flows in RAMMS can be increased to a 5 or even a 1 m grid cell resolution in order to generate more detail in the extent of the deposits at the debris fan. However, the user must be aware of the increase in calculation times.

- Future studies can use a Monte-Carlo approach to obtain the uncertainties of the rheological input parameters used in 2D numerical continuum modeling. The parameter uncertainty can be further applied in the hazard or risk assessment of landslides. However, one must find a practical solution to automatically enter the high number of randomly generated parameter values into the modeling process. RAMMS as it is would not be suitable for that, as it is currently not possible to automate the input procedure for the parameters, using some sort of batch file approach. It can be recommended to the model developers to make such an approach possible, and develop some kind of Monte Carlo simulation interface for the model.

- RAMMS is capable of producing other intensity parameters that have not been thoroughly assessed in this research, like the velocity and impact pressure. Future studies using RAMMS can test the sensitivity of these outputs to the rheological parameters.

- The compiled data in this thesis can be used to find relationships between other types of outputs like the total surface extent of the run-out, the vertical travel distance and the change in the energy of the flow (momentum, kinetic energy) versus the input parameters or the initiation volume.

- Further study is needed on how the entrainment process in RAMMS exactly affects the entrainment and deposit volume outputs. It may be possible to study entrainment and depositional features in the transport zone (levees, scouring) after a debris flow has taken place, at least to determine the areas of entrainment even if the volume is unknown.

- The data acquired in this thesis can be used as the spatial component of a hazard assessment. However, it is advised to increase the number of runs based on a stochastic method to optimize the spatial probability and to find the uncertainties of the input parameters.

LIST OF REFERENCES

ArcGIS Resource Center. (2010). How Topo to Raster works. Retrieved December 1st, 2010, from http://help.arcgis.com/en/arcgisdesktop/10.0/help/index.html#/How_Topo_to_Raster_works/009z0000007m000000/

Ayotte, D., & Hungr, O. (2000). Calibration of a runout prediction model for debris-flows and avalanches. In G. F. Wieczorek & N. D. Naeser (Eds.), *Debris-Flow Hazards Mitigation: Mechanics, Prediction, and Assessment, Proc. 2nd International DFHM Conference* (pp. 505-514). Taipei, Taiwan.

Bartelt, P., Salm, B., & Gruber, U. (1999). Calculating dense-snow avalanche runout using a Voellmy-fluid model with active/passive longitudinal straining. *Journal of Glaciology, 45*(150), 242-254.

Beguería, S., van Asch, T. W. J., Malet, J.-P., & Gröndahl, S. (2009). A GIS-based numerical model for simulating the kinematics of mud and debris flows over complex terrain. *Natural Hazards and Earth System Science, 9*(6), 1897-1909.

Borstad, C. P., & McClung, D. M. (2009). Sensitivity analyses in snow avalanche dynamics modeling and implications when modeling extreme events. *Canadian Geotechnical Journal, 46*(9).

Brideau, M. A., Stead, D., Millard, T., & Patton, G. (2006). Runout Characteristics of Open Slope Landslides in Harvested Terrain on Vancouver Island: Preliminary Results of an Integrated Field-Dynamic Modelling Based Study, *Sea to Sky; Canadian Geotechnical Society Conference 2006* (pp. 342 - 350). Vancouver, BC.

Brunsden, D. (1999). Some geomorphological considerations for the future development of landslide models. *Geomorphology, 30*(1-2), 13-24.

Calvo, B., & Savi, F. (2009). A real-world application of Monte Carlo procedure for debris flow risk assessment. *Computers & Geosciences, 35*(5), 967-977.

Cesca, M., & D'Agostino, V. (2006). Comparison between FLO-2D and RAMMS in debris-flow modelling: a case study in the Dolomites *International Conference on Monitoring, simulation, prevention and remediation of Dense and Debris Flows II 60*, 197-206.

Chen, H., & Lee, C. F. (2004). Geohazards of slope mass movement and its prevention in Hong Kong. *Engineering Geology, 76*(1-2), 3-25.

Christen, M., Bartelt, P., & Kowalski, J. (2010a). Back calculation of the In den Arelen avalanche with RAMMS: interpretation of model results. *Annals of Glaciology, 51*(54), 161-168.

Christen, M., Buehler, Y., Bartelt, P., & Schumacher, L. (2010b). RAMMS User Manual v1.01. Retrieved August 30th, 2010, from http://ramms.slf.ch/ramms/index.php?option=com_content&view=article&id=53&Itemid=70

Christen, M., Kowalski, J., & Bartelt, P. (2010c). RAMMS: Numerical simulation of dense snow avalanches in three-dimensional terrain. *Cold Regions Science and Technology, 63*(1-2), 1-14.

Cruden, D. M., & Varnes, D. J. (1996). Landslide types and process. In A. K. Turner & R. J. Schuster (Eds.), *Landslides: Investigation and Mitigation, Special Report 247* (pp. 36–75).

Dai, F. C., Lee, C. F., & Ngai, Y. Y. (2002). Landslide risk assessment and management: an overview. *Engineering Geology, 64*(1), 65-87.

DNV. (2011). Understanding Debris Flows. Retrieved January 26th, 2011, from http://www.dnv.org/article.asp?c=1031

Düzgün, H., & Özdemir, A. (2006). Landslide risk assessment and management by decision analytical procedure for Dereköy, Konya, Turkey. *Natural Hazards, 39*(2), 245-263.

Flageollet, J.-C., Maquaire, O., Martin, B., & Weber, D. (1999). Landslides and climatic conditions in the Barcelonnette and Vars basins (Southern French Alps, France). *Geomorphology, 30*(1-2), 65-78.

Gorsevski, P. V., Gessler, P. E., Boll, J., Elliot, W. J., & Foltz, R. B. (2006). Spatially and temporally distributed modeling of landslide susceptibility. *Geomorphology, 80*(3-4), 178-198.

Gostner, W., Bezzola, G. R., Schatzmann, M., & Minor, H.-E. (2008). Water-Related Natural Disasters: Strategies to Deal With Debris Flows: The Case of Tschengls, Italy. In E. Wiegandt (Ed.), *Mountains: Sources of Water, Sources of Knowledge* (Vol. 31, pp. 221-241): Springer Netherlands.

Griffiths, D. V., Huang, J., & Fenton, G. A. (2008). Probabilistic Stability Analysis of Shallow Landslides using Random Fields. *International Association for Computer Methods and Advances in Geomechanics (IACMAG)*, 3014-3020.

Hubbard, D. W. (2007). *How to Measure Anything: Finding the Value of Intangibles in Business*: John Wiley & Sons.

Hungr, O., & Evans, S. G. (1996). Rock avalanche runout prediction using a dynamic model. In K. Senneset (Ed.), *Landslides, Proceedings of the 7th International Symposium on landslides, Trondheim, Norway* (Vol. 1, pp. 233–238). Rotterdam: A.A. Balkema.

Hungr, O., Evans, S. G., Bovis, M. J., & Hutchinson, J. N. (2001). A review of the classification of landslides of the flow type. *Environmental & Engineering Geoscience, 7*(3), 221-238.

Hungr, O., Corominas, J., & Eberhardt, E. (2005). Estimating landslide motion mechanism, travel distance and velocity. In O. Hungr, R. Fell, R. Couture & E. Eberhardt (Eds.), *Landslide Risk Management* (pp. 99-128). London: Taylor and Francis.

Hürlimann, M., Rickenmann, D., Medina, V., & Bateman, A. (2008). Evaluation of approaches to calculate debris-flow parameters for hazard assessment. *Engineering Geology, 102*(3-4), 152-163.

Hutchinson, J. N. (1988). General Report: Morphological and geotechnical parameters of
landslides in relation to geology and hydrogeology. In C. Bonnard (Ed.), *Proceedings, Fifth International Symposium on Landslides* (Vol. 1, pp. 3-35): Rotterdam: Balkema.

IGN. (2006). *Carte de Randonee, Aiguille de Chambeyron, Cols de Larche et de Vars*. Paris: Institut Geographique National.

Imran, J., Harff, P., & Parker, G. (2001). A numerical model of submarine debris flow with graphical user interface. *Computers & Geosciences, 27*(6), 717-729.

Intermap Technologies. (2010). Retrieved December 1st, 2010, from http://www.intermap.com/

Iverson, R. M. (1997). The physics of debris flows. *Reviews of Geophysics, 35*(3), 245-296.

Jakob, M., Anderson, D., Fuller, T., Hungr, O., & Ayotte, D. (2000). An unusually large debris flow at Hummingbird Creek, Mara Lake, British Columbia. *Canadian Geotechnical Journal, 37*, 1109-1125.

Jakob, M. (2005). Debris-flow hazard analysis. In M. Jakob & O. Hungr (Eds.), *Debris-flow Hazard and Related Phenomena* (pp. 411-443). Chichester: Springer-Praxis.

Jakob, M., & Hungr, O. (2005). *Debris-flow Hazards and Related Phenomena*. Chichester: Springer-Praxis.

Kowalski, J. (2008). Two-Phase Modeling of Debris Flows. PhD Thesis, Swiss Federal Institute of Technology, Zurich.

Kronfellner-Kraus, G. (1985). Quantitative estimation of torrent erosion. *International Symposium on Erosion, Debris Flow and Disaster Prevention* (pp. 107-110). Tsukuba, Japan.

Kuriakose, S. L., van Beek, L. P. H., & van Westen, C. J. (2010). Comparison of physically based models for debris flow initiation – A case study in the Tikovil River basin of the Western Ghats of Kerala, India. *Computers and Geosciences (Under review)*.

Liu X., Zhang, Z., Peterson, J., & Chandra, S. (2007). The effect of LIDAR dat density on DEM accuracy *Proceedings of the International Congress on Modelling and Simulation 'MODSIM07', 10 -13 December* (pp. 1363-1369). Christchurch, New Zealand.

Liu, C. N. (2008). Landslide Hazard Mapping Using Monte Carlo Simulation- a Case Study in Taiwan. In H. Liu, A. Deng & J. Chu (Eds.), *Geotechnical Engineering for Disaster Mitigation and Rehabilitation* (pp. 189-194): Springer Berlin Heidelberg.

Malet, J. P., Laigle, D., Remaître, A., & Maquaire, O. (2005). Triggering conditions and mobility of debris flows associated to complex earthflows. *Geomorphology, 66*(1-4), 215-235.

Malet, J. P. (2010). Data Access - Barcelonnette area. Retrieved October 1st, 2010, from http://eost.u-strasbg.fr/omiv/data_access_Barcelonnette.html

Maquaire, O., Malet, J. P., Remaître, A., Locat, J., Klotz, S., & Guillon, J. (2003). Instability conditions of marly hillslopes: towards landsliding or gullying? The case of the Barcelonnette Basin, South East France. *Engineering Geology, 70*(1-2), 109-130.

Nettleton, I. M., Martin, S., Hencher, S., & Moore, R. (2005). Debris flow types and mechanisms. In M. G. Winter, F. Macgregor & L. Shackman (Eds.), *Scottish Road Network Landslides Study* (pp. 45-67). Edinburgh: The Scottish Executive.

Pirulli, M., Scavia, C., & Hungr, O. (2004). Determination of rock avalanche run-out parameters through back analyses. In W. A. Lacerda, M. Ehrlich, S. A. B. Fontoura & A. S. F. Sayão (Eds.), *Proceedings of the 9th International Symposium on Landslides, Rio de Janeiro* (pp. 1361-1366). London: Balkema.

Pirulli, M., Bristeau, M., -O, Mangeney, A., & Scavia, C. (2007). The effect of the earth pressure coefficients on the runout of granular material. *Environmental Modelling & Software, 22*(10), 1437-1454.

Quan Luna, B. (2007). Assessment and modelling of two lahars caused by "Hurricane Stan" at Atitlan, Guatemala, October 2005. M.Sc. Thesis, University of Oslo, Oslo.

Quan Luna, B., van Westen, C. J., Jetten, V., Cepeda, J., Stumpf, A., Malet, J.-P., et al. (2010). A preliminary compilation of calibrated rheological parameters used in dynamic simulations of landslide run - out. In J.-P. Malet, T. Glade & N. Casagli (Eds.), *Mountain risks : bringing science to*

society : proceedings of the Mountain Risks International Conference, Firenze, Italy (pp. 255-260). Strasbourg: CERG.

Remaître, A., Malet, J.-P., Maquaire, O., Ancey, C., Laigle, D., & Locat, J. (2003). Torrential hazard assessment using a debris-flow runout model. The case of the Faucon stream. *Fast Slope Movements-Prediction and Prevention for Risk Mitigation*, 445–452.

Remaître, A., Malet, J.-P., Maquaire, O., Ancey, C., & Locat, J. (2005a). Flow behaviour and runout modelling of a complex debris flow in a clay-shale basin. *Earth Surface Processes and Landforms, 30*(4), 479-488.

Remaître, A., Malet, J.-P., & Maquaire, O. (2005b). Morphology and sedimentology of a complex debris flow in a clay-shale basin. *Earth Surface Processes and Landforms, 30*(3), 339-348.

Remaître, A. (2006). Morphologie et dynamique des laves torrentielles : application aux torrents des Terres Noires du bassin de Barcelonnette (Alpes du Sud). PhD Thesis, University of Caen Basse-Normandie, Caen, France.

Remaître, A., van Asch, T. W. J., Malet, J.-P., & Maquaire, O. (2008). Influence of check dams on debris-flow runout intensity. *Natural Hazards and Earth System Sciences, 8*, 1403-1416.

Remaître, A., Malet, J.-P., & Maquaire, O. (2009). Sediment budget and morphology of the 2003 Faucon debris flow (South French Alps): scouring and channel-shaping processes. In J.-P. Malet, A. Remaître & T. A. Boogard (Eds.), *Proceedings of the International Conference 'Landslide Processes: from geomorpholgic mapping to dynamic modelling'* (pp. 75-80). Strasbourg: CERG.

Remaître, A., & Malet, J.-P. (2010). The effectiveness of torrent check dams to control channel instability: example of debris-flow events in clay shales. In C. C. Garcia & M. A. Lenzi (Eds.), *Check dams, morphological adjustements and erosion control in torrential streams* (pp. 211-237). New York: Nova Science Publishers Inc.

Rickenmann, D. (1999). Empirical Relationships for Debris Flows. *Natural Hazards, 19*(1), 47-77.

Rickenmann, D. (2005). Runout prediction methods. In M. Jakob & O. Hungr (Eds.), *Debris-flow Hazard and Related Phenomena* (pp. 305-324). Chichester: Springer-Praxis.

Rickenmann, D., Laigle, D., McArdell, B., & Hübl, J. (2006). Comparison of 2D debris-flow simulation models with field events. *Computational Geosciences, 10*(2), 241-264.

Salm, B. (1993). Flow, flow transition and runout distances of flowing avalanches. *Annals of Glaciology, 18*, 221-226.

Savage, S. B., & Hutter, K. (1989). The motion of a finite mass of granular material down a rough incline. *Journal of Fluid Mechanics, 199*(-1), 177-215.

Scotto di Santolo, A., & Evangelista, A. (2009). Some observations on the prediction of the dynamic parameters of debris flows in pyroclastic deposits in the Campania region of Italy. *Natural Hazards, 50*(3), 605-622.

Soeters, R., & van Westen, C. J. (1996). Slope instability recognition, analysis, and zonation. *In: Landslides, investigation and mitigation / ed. by. A.K. Turner and R.L. Schuster. Washington, D.C. National Academy Press, (Transportation Research Board, National Research Council, Special Report ; 247)*, pp. 129 - 177.

Sosio, R., Crosta, G. B., & Hungr, O. (2008). Complete dynamic modeling calibration for the Thurwieser rock avalanche (Italian Central Alps). *Engineering Geology, 100*(1-2), 11-26.

Sovilla, B., Burlando, P., & Bartelt, P. (2006). Field experiments and numerical modelling of mass entrainment in snow avalanches. *Journal of Geophyscial research, 111*, 16 p.

Uzielli, M., Duzgun, S., & Vangelsten, B. V. (2006). A first-order Second-moment framework for probabilistic estimation of vulnerability of landslides. *Geohazards, 24, 2006, ECI Confrence on Geohazards, Lillehammer, Norway*.

van Westen, C. J. (2010). *Multi-Hazard risk assessment: RiskCity, distance education*. Enschede, The Netherlands: ITC.

Varnes, D. J. (1978). Slope movement types and processes. *In: Special Report 176: Landslides: Analysis and Control (Eds: Schuster, R. L. & Krizek, R. J.), Transportation and Road Research Board, National Academy of Science, Washington D. C.*, pp.11-33.

von Bertalanffy, L. (1968). *General systems theory*. New York: Braziller.

WP/WLI. (1995). A suggested method for describing the rate of movement of a landslide. *Bulletin of the International Association of Engineering Geology, 52*, 75-78.

Zeller, J. (1985). Schutz vor Hochwassershäden und Rutshungen im Gebirge; ein Überlick. *Schweizerische Zeitschrifte für Forstwesen, 127*, 129-137.

APPENDIX I

Aerial and ground photography of the aftermath of the 2003 debris flow event at the Faucon catchment

The initiation zone

Damage to check dams at the entrainment zone

Debris flow deposits at the Apex Bridge

Debris flow deposits near the V.C. 3 Bridge

The village of Domaine de Bérard effected by the debris flow

Water continues to flow within the debris flow deposits near Domaine de Bérard

Clearing the debris at the R.D. 900 Bridge

Debris deposit height at Domaine de Bérard

APPENDIX II

Fieldwork observations at the debris fan area

Point 30

Discription: Outflow point of torrent into the Ubaye, 132 m from bridge 1
photo: 285-292
video:
UTM:
East: 316299 m
North: 4918475 m

Elevation: 1167 m

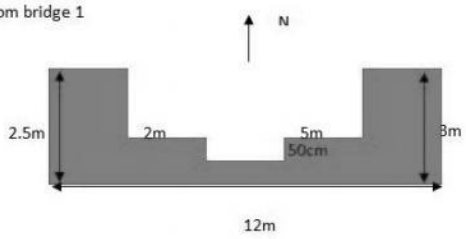

Point 31

Discription: 55m from outflow point, inside torrent close to Ubaye
photo: 293-296
video:
UTM:
East: 316250 m
North: 4918527 m

Elevation: 1176 m

Point 32

Discription: Bridge 1
photo: 297-306
video:
UTM:
East: 316209 m
North: 4918566 m

Elevation: 1182 m

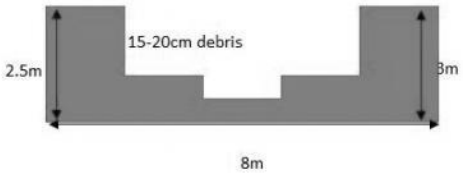

Point 33

Discription: On top of artificial dike, next to Domaine de Berard. 45.5m from Bridge 1
photo: 307-315
video:
UTM:
East: 316146 m
North: 4918577 m

Elevation: 1190 m

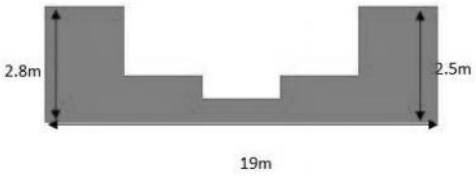

Point 34

Discription: On top of Domaine de Berard torrent Levee (artificial)
258m from bridge 1
photo: 316-319
video:
UTM:
East: 315970 m
North: 4918658 m

Elevation: 1202 m

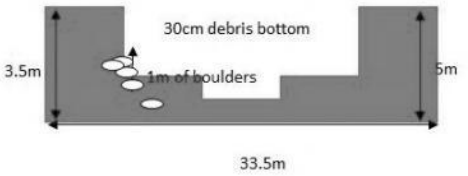

Point 35

Discription: Bridge 2
Distance Bridge 1 - Bridge 2 = 299m
photo: 320-323
video:
UTM:
East: 315929 m
North: 4918680 m

Elevation: 1203 m

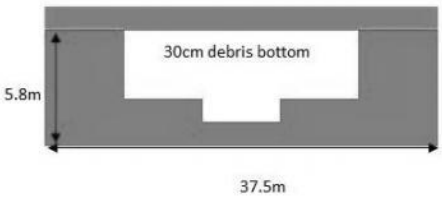

Point 36

Discription: Stream braiding inside diked debris zone, artifical heaped mounds on west levee. Road on east side next to levee. Debris slighty thicker
Distance to Bridge 2 = 110m

photo: 324-333
video:
UTM:
East: 315820 m
North: 4918727 m

Elevation: 1224 m

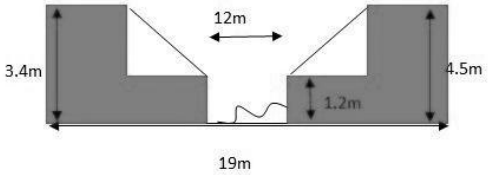

Point 37

Discription: On the artificial levee of debris fan torrent
Distance Bridge 2 = 295m

photo: 334-341
video:
UTM:
East: 315650 m
North: 4918776 m

Elevation: 1230 m

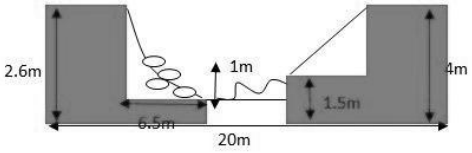

Point 38

Discription: On diked levee
130m from bridge 3

photo: 343-349
video:
UTM:
East: 315342 m
North: 4918931 m

Elevation: 1261 m

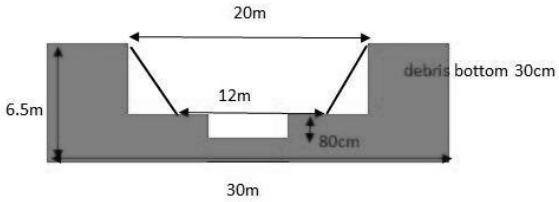

Point 39

Discription: Bridge 3, Border of Apex. Little incision, not much debris, 20cm thick.

photo: 360-364
video:
UTM:
East: 315276 m
North: 4919024 m

Elevation: 1290 m

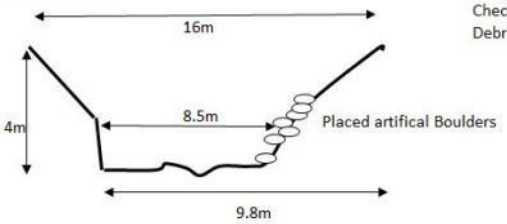

Checkdams next to bridge 3
Debris levees 40 cm

APPENDIX III

A quick start guide of the RAMMS user interface to model run-outs

1. First adding the RAMMS preference directories. These directories should contain the files for the DEM, aerial and satellite images or topographic maps.

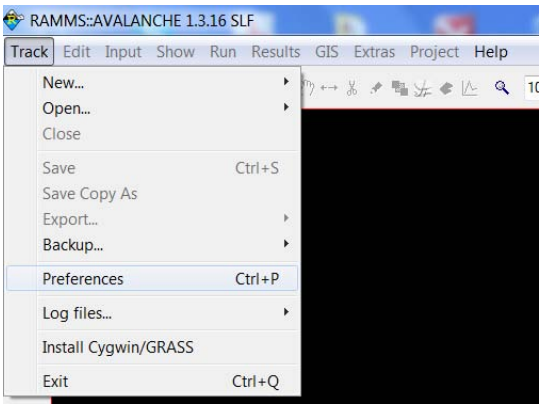

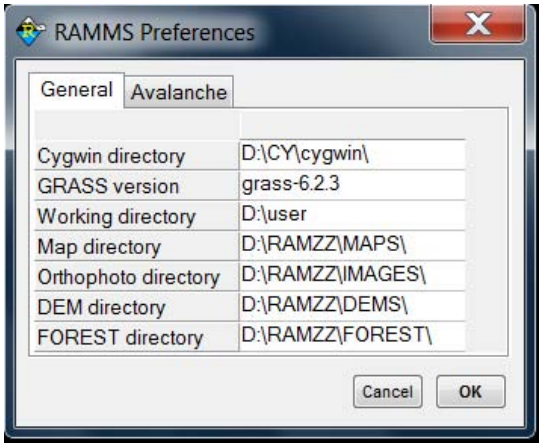

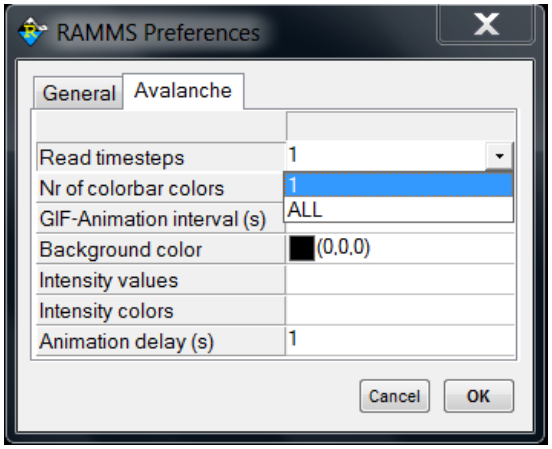

2. Starting a new RAMMS project

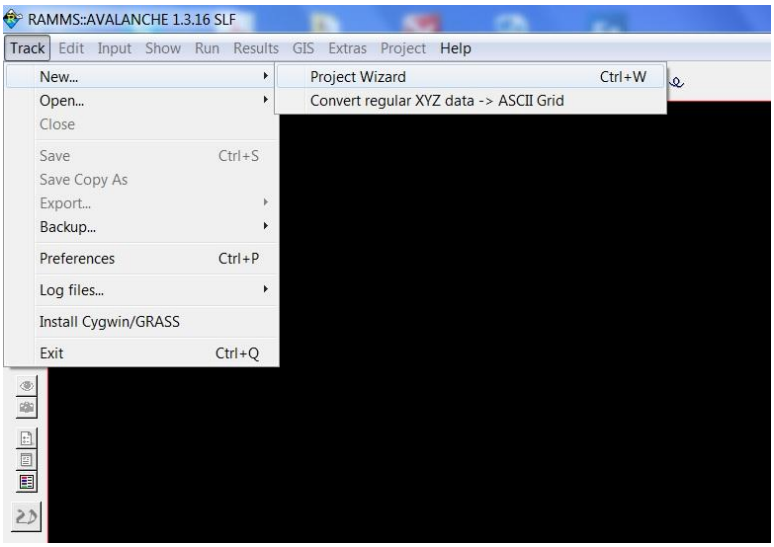

2.1. Assigning a new Project name

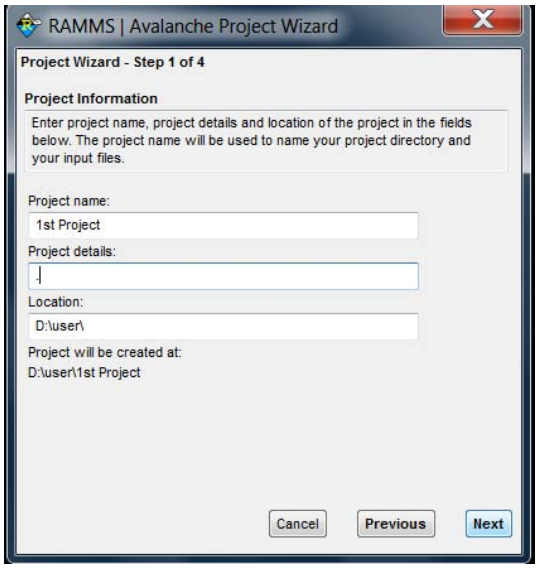

2.2. Adding the DEM from a local directory. The DEM must be imported in the ASCII grid format.

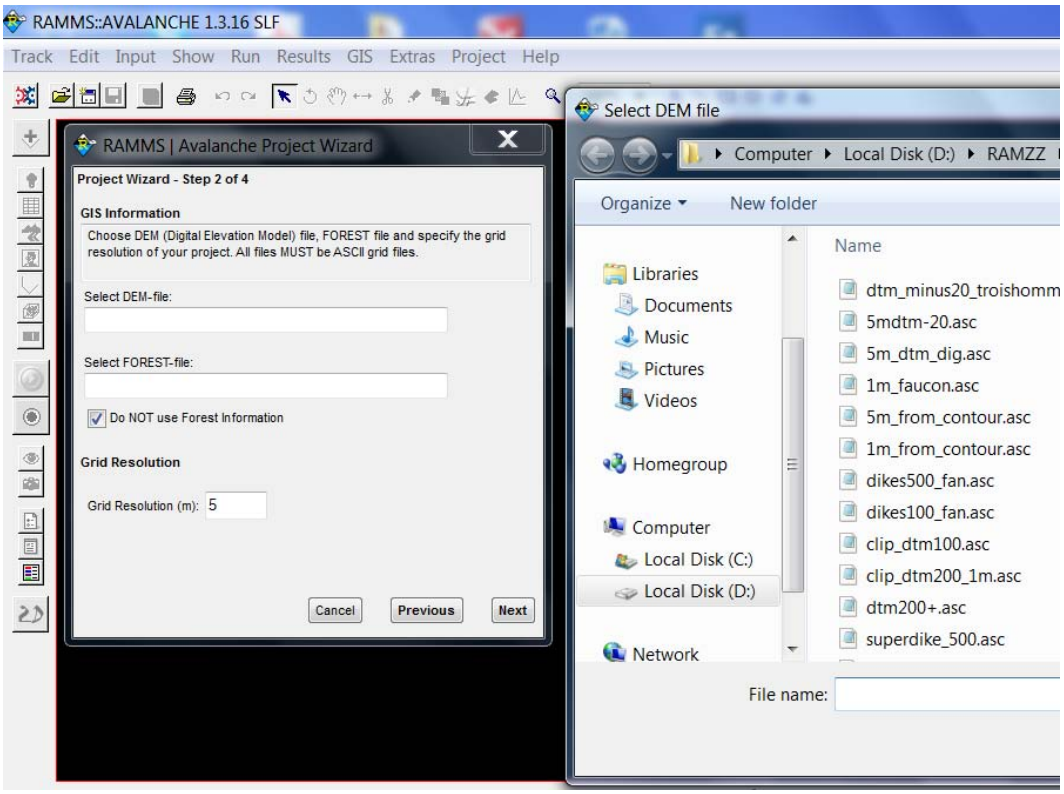

2.3. Assigning the project boundary either using the boundary of the DEM or using a user specificed boundary. A project summary is then shown and the user can continu to create the project.

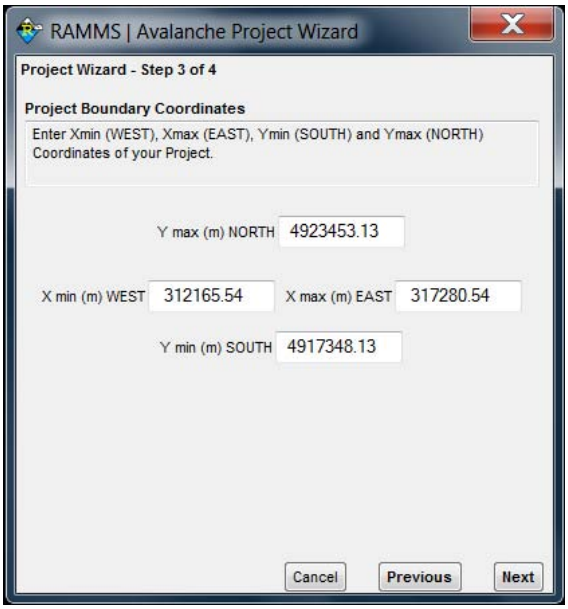

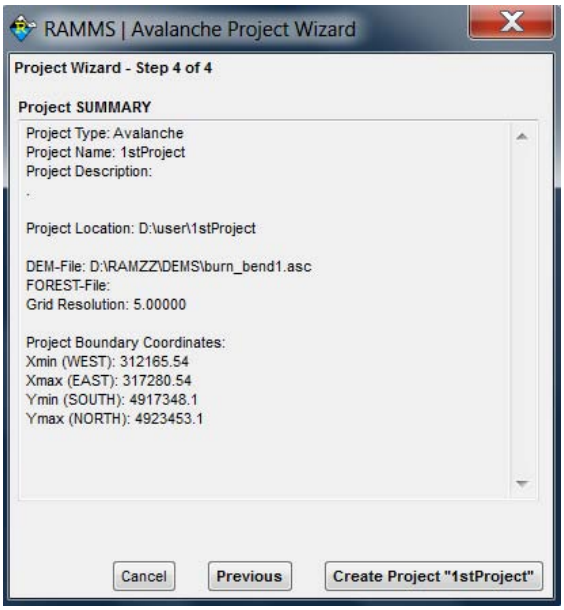

2.4. RAMMS will import the DEM. This can take a few minutes and the time depends on the DEM size and resolution

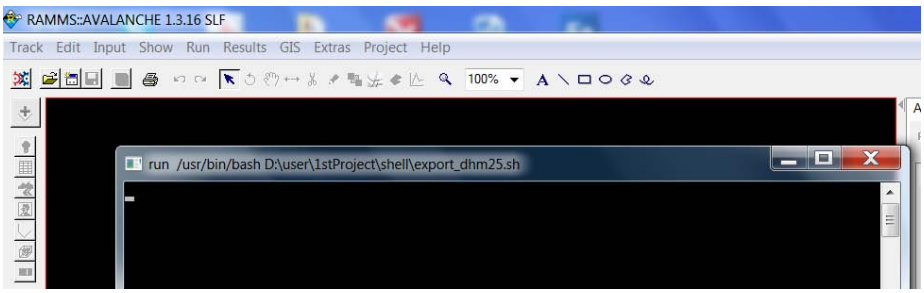

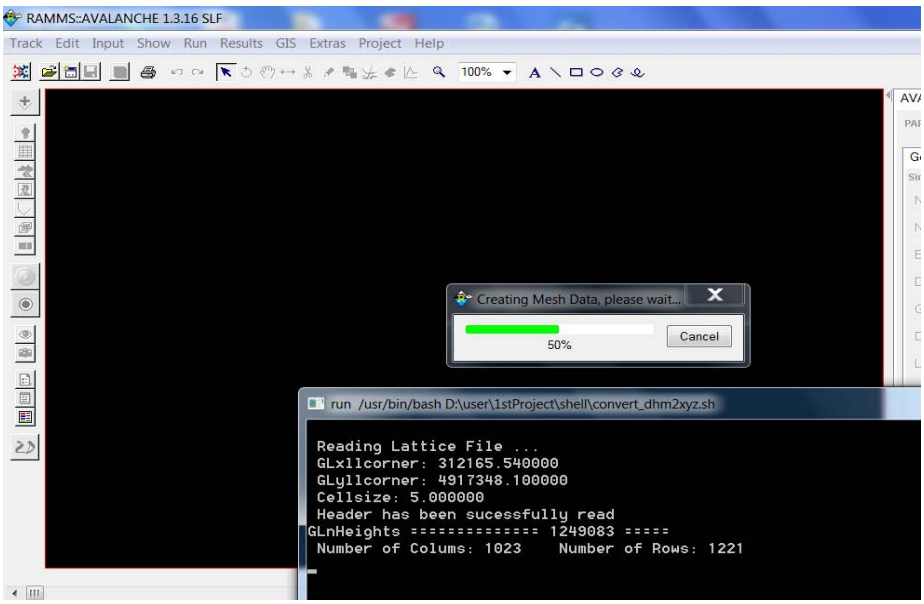

2.5. The user is asked for the location of the maps and images after the DEM has been imported

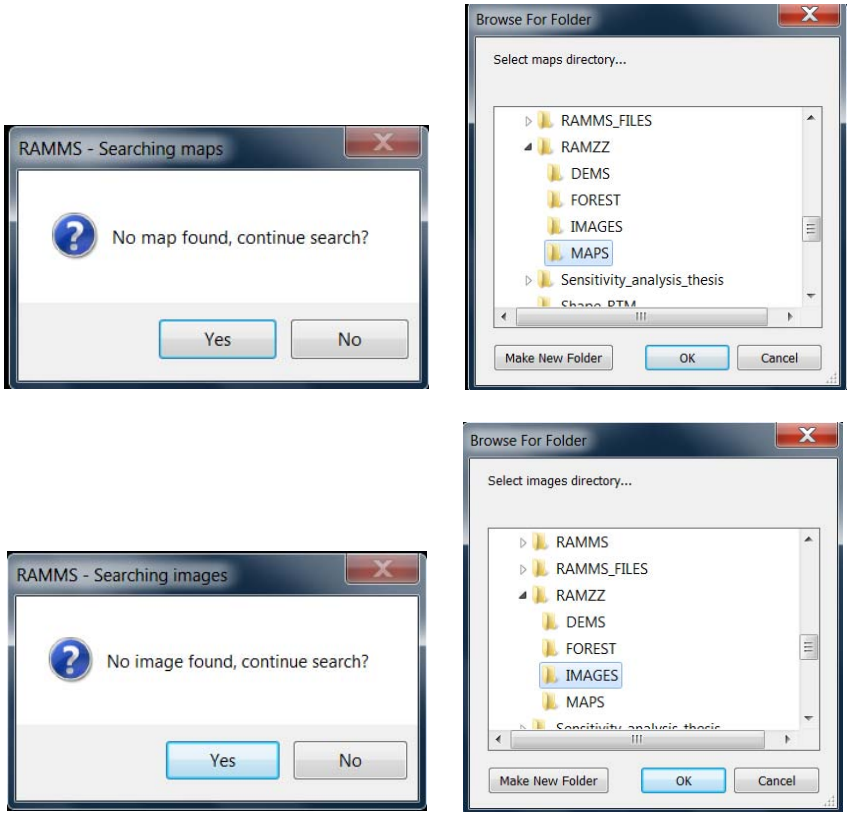

3. The 3D representation of the DEM and the drapped image after the necessary files have been imported

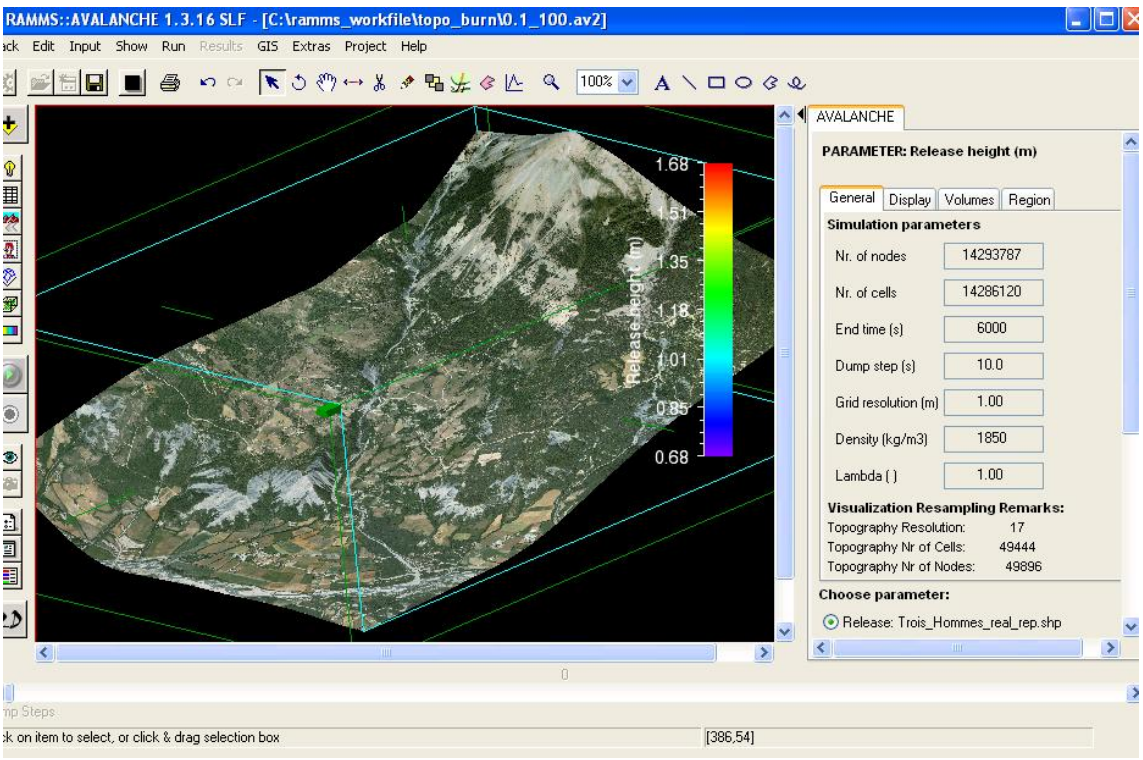

4. Switching to the 2D view to start the assigning of a new calculation domain for the initial modeling

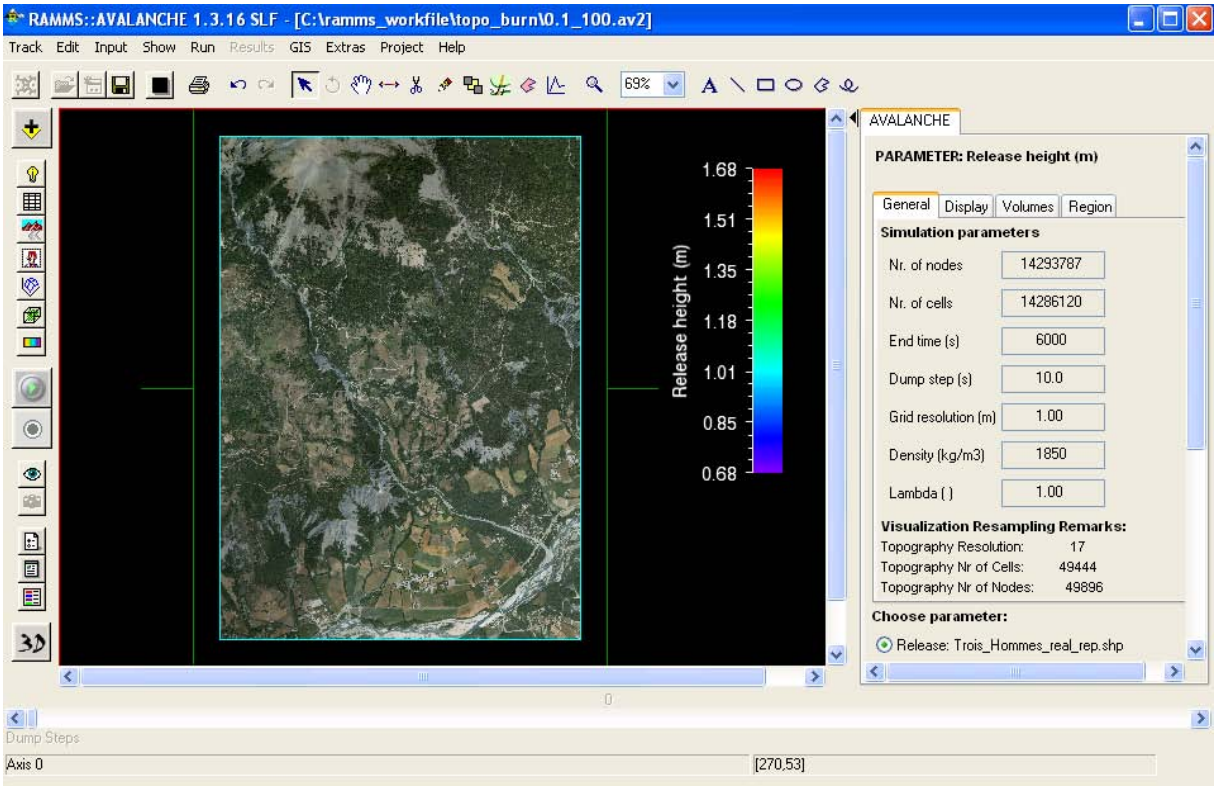

5. Drawing the new domain and chosing a new domain filename

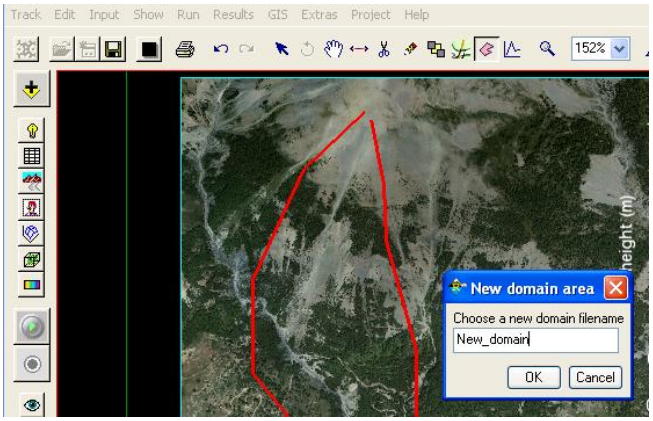

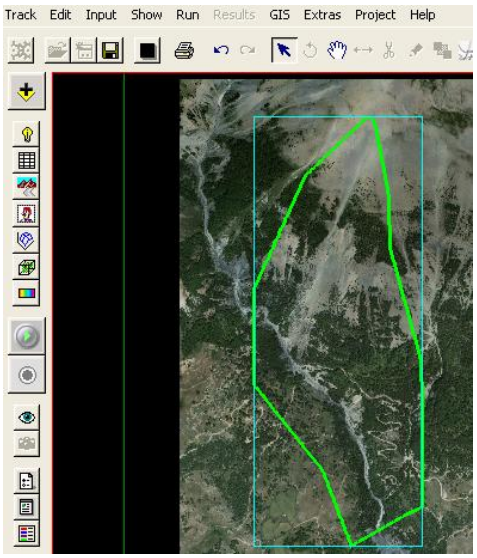

6. Drawing a new release area and assigning a new release filename

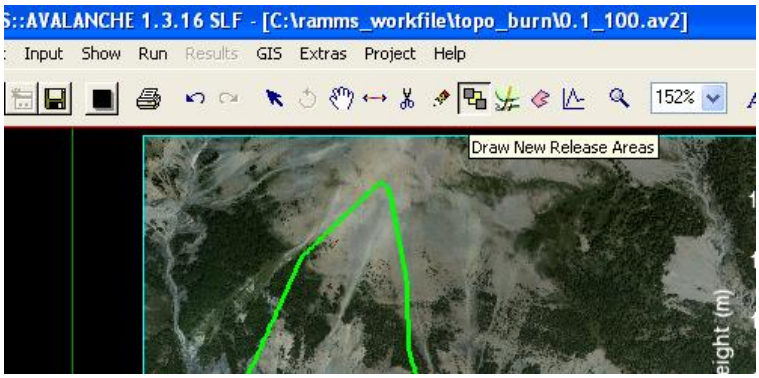

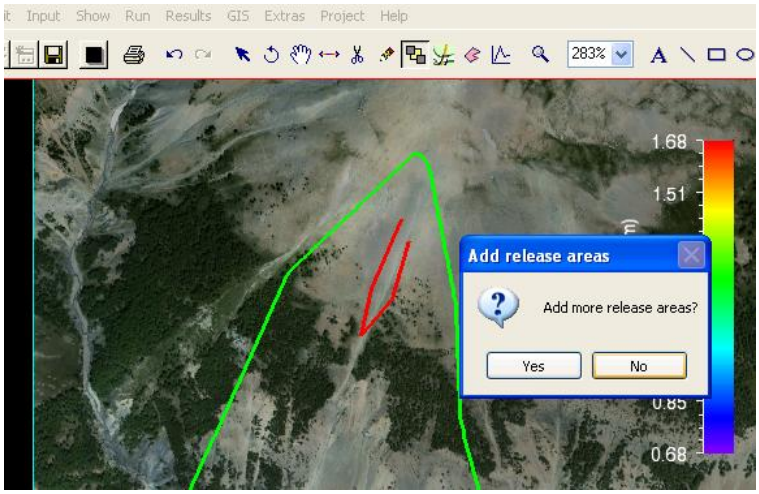

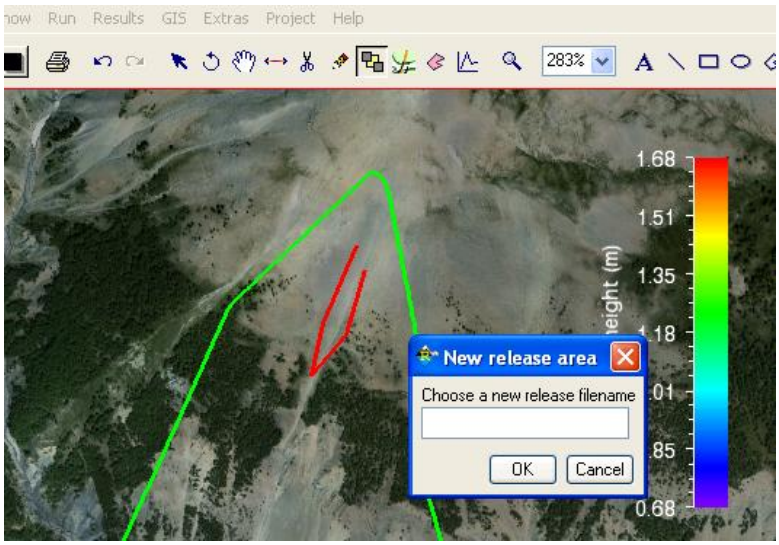

7. Choosing an appropriate release height (this can also be done in step 9)

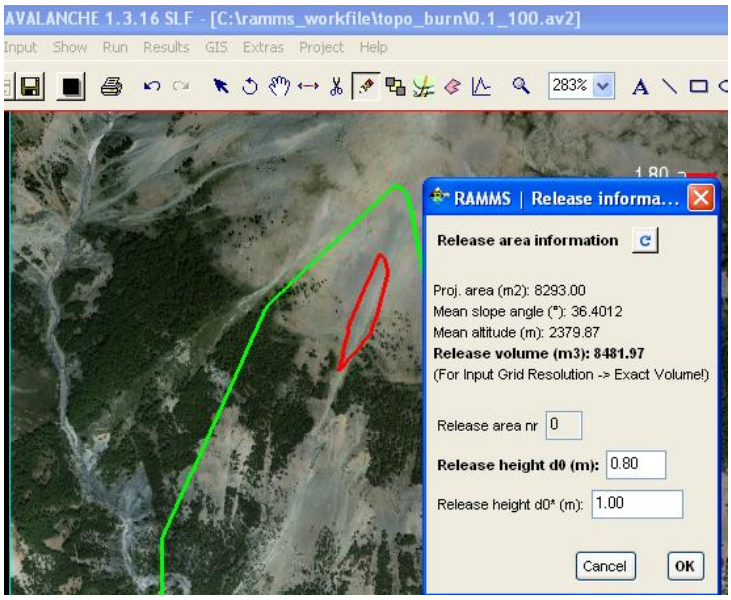

8. Starting a new avalanche calculation run. The user specificies an output name for the run and the simulation parameters are chosen: grid resolution, end time, number of dump steps, the density of the chosen release area and the Lambda (earth pressure coefficient). Numerical scheme is kept to second order.

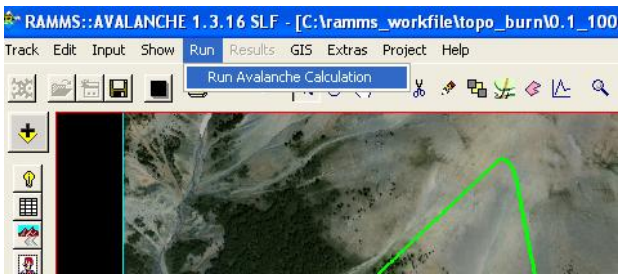

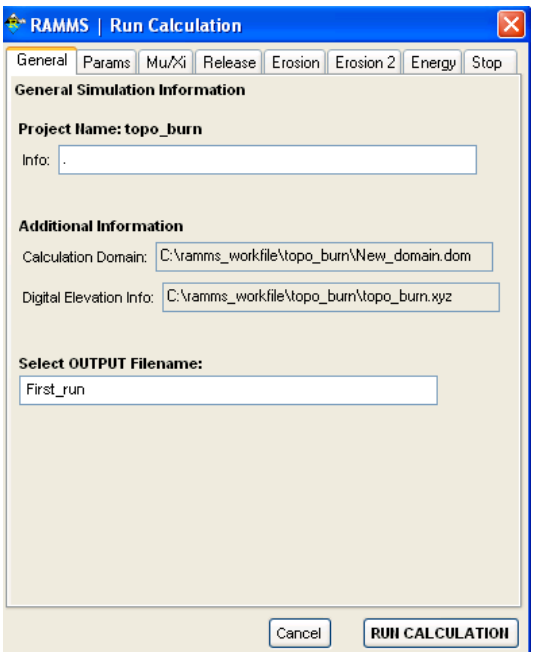

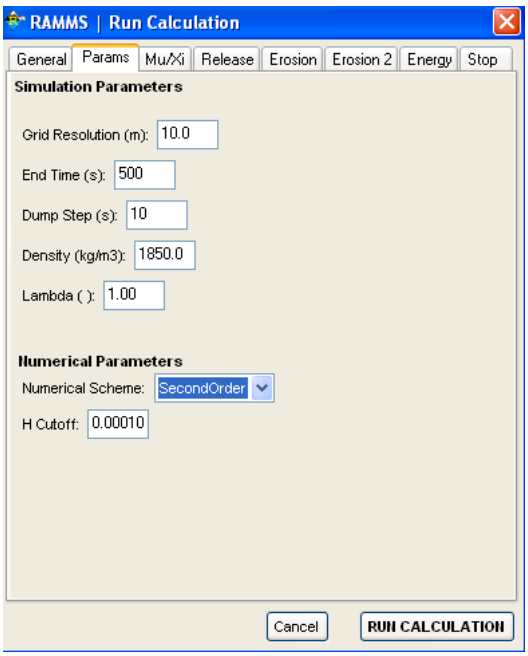

9. Assigning the friction parameters or friction polygons and release heights. The estimated release volume can be update after assigning a new height.

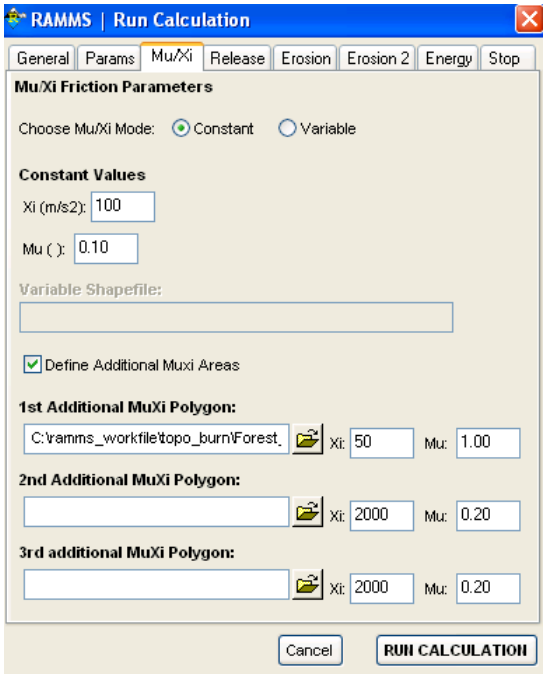

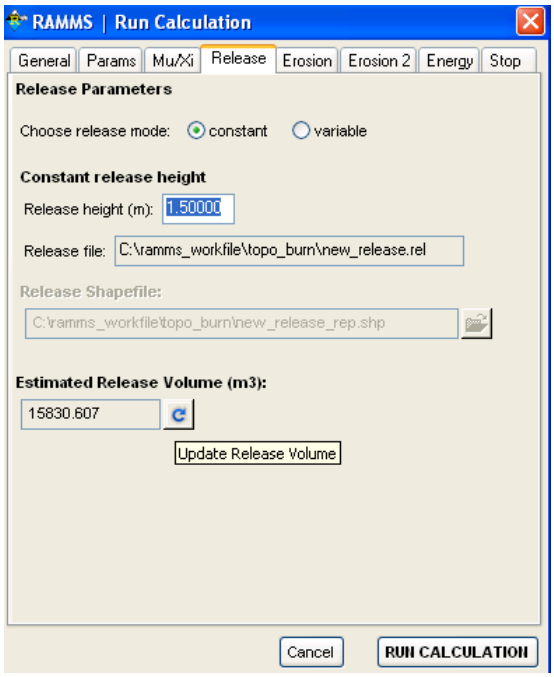

10. Choosing entrainment heights either using the 3 layer method or user defined entrainment polygons

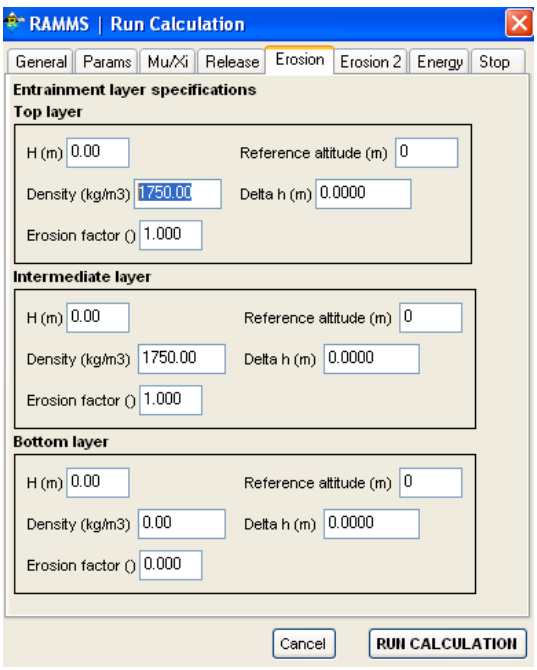

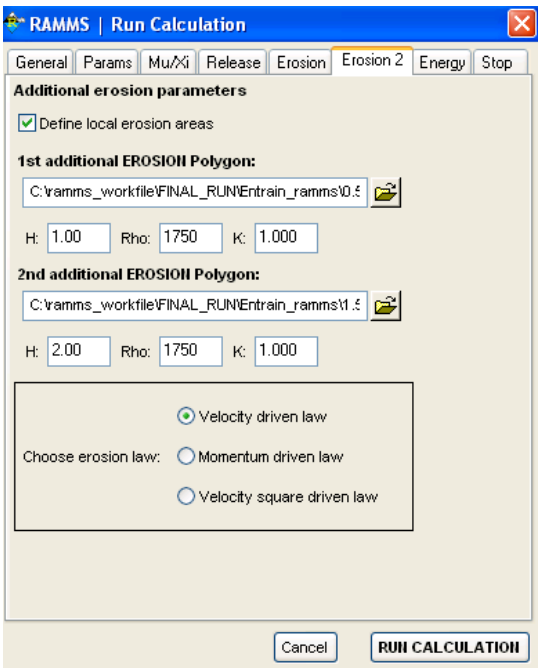

11. Using the Random Kinetic Energy (RKE) model (optional) and specifying the stop criteria of the model

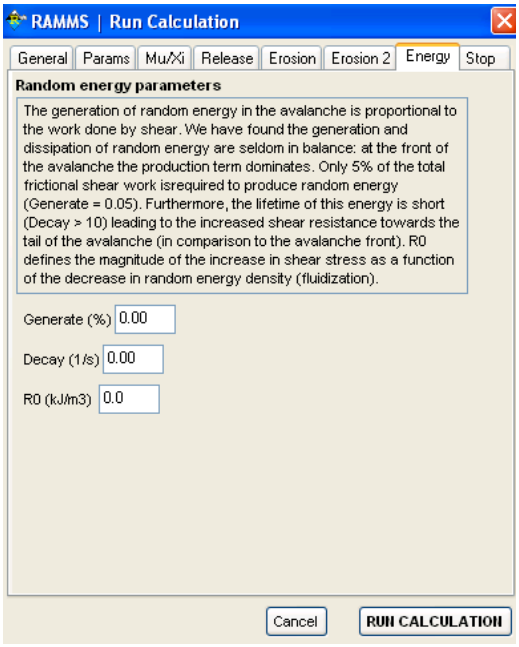

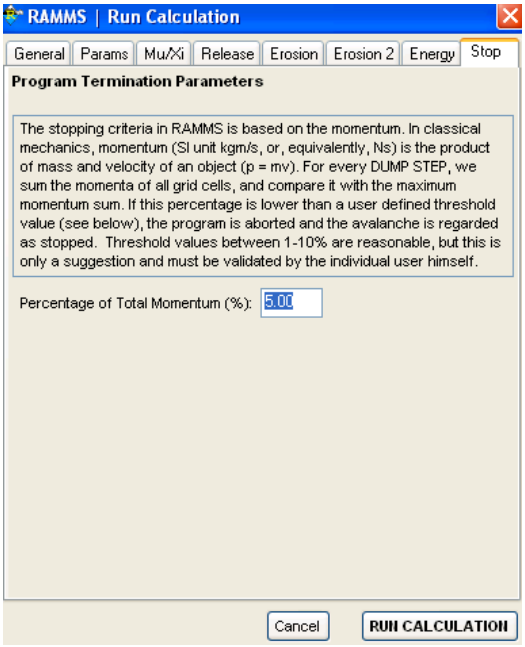

12. Once the calculation starts, RAMMS will start to calculate the flow at each dump step

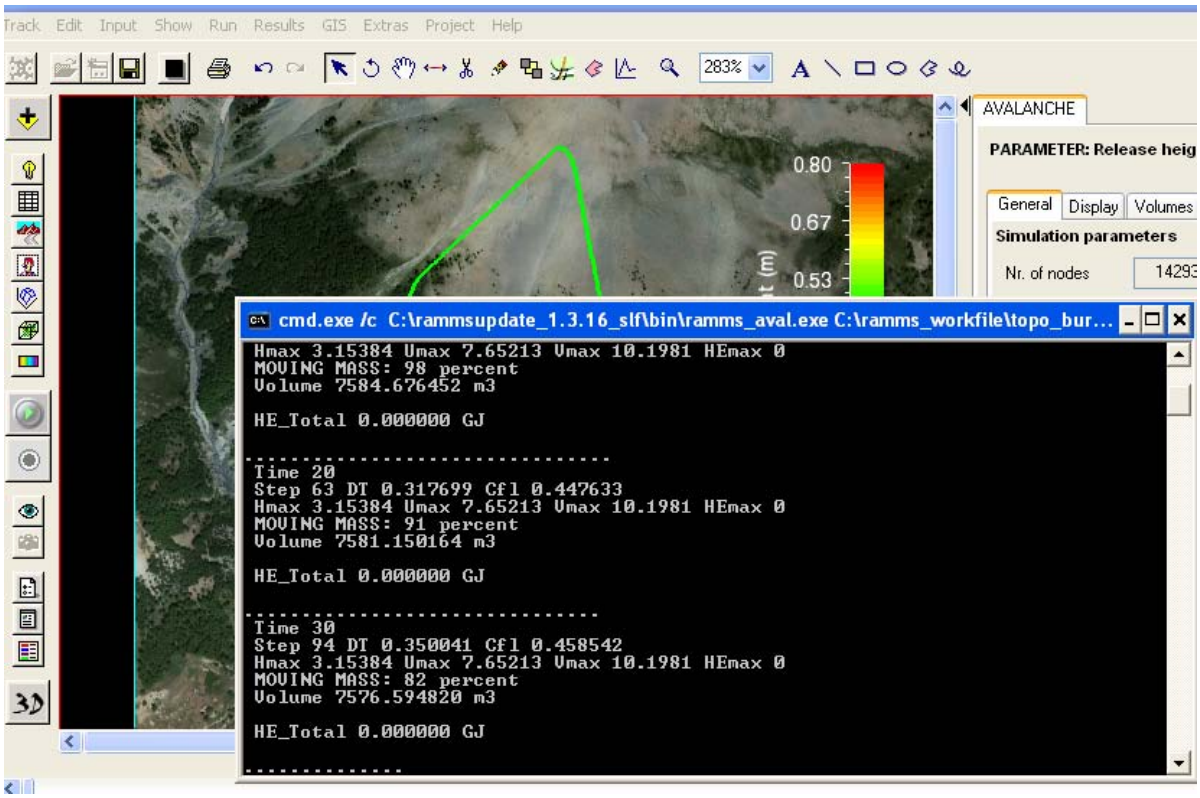

13. RAMMS starts reading the simulation after it has finished calculating the flow and then produces an output logfile

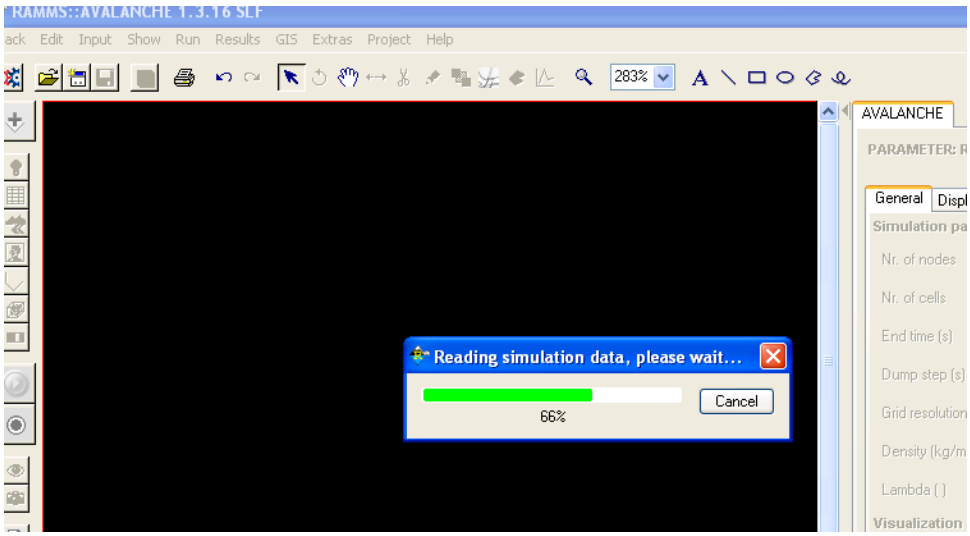

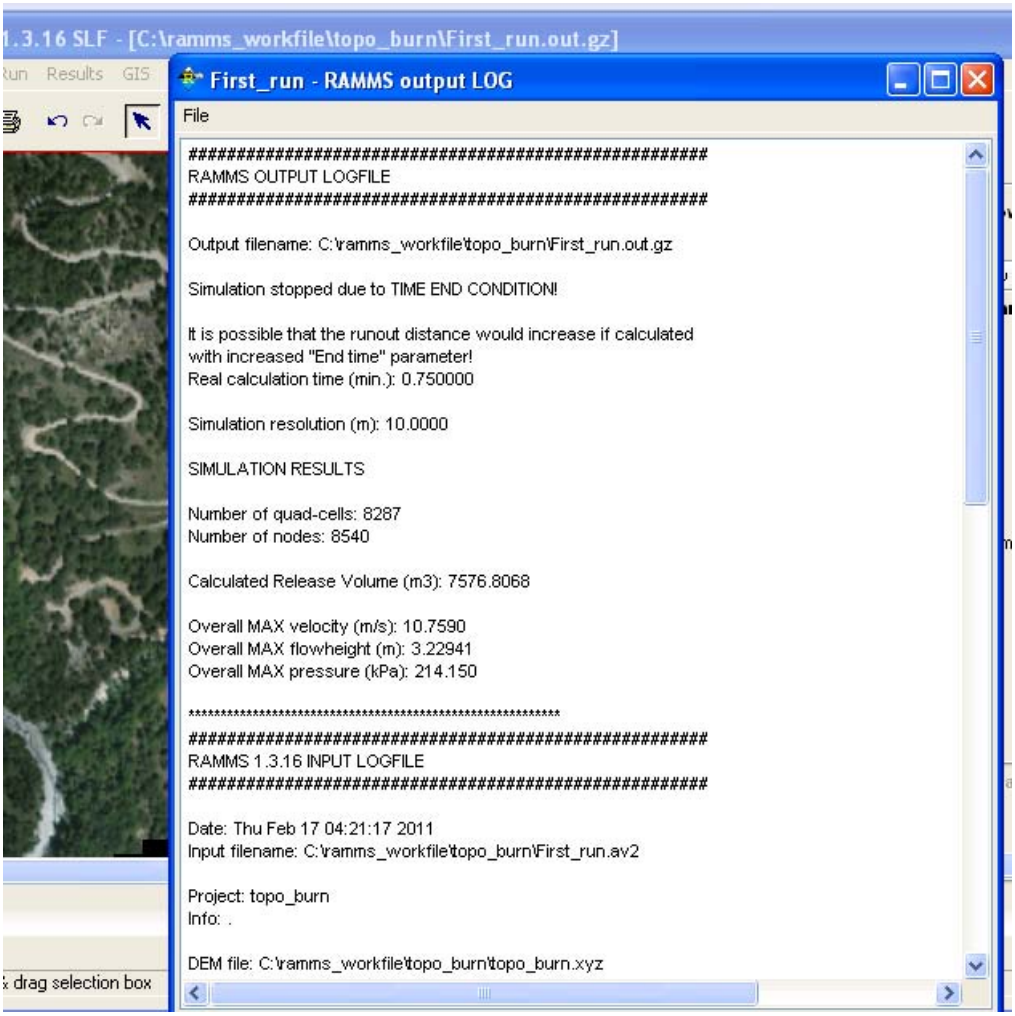

14. The calculation domain is represented in 3D at dump step = 0. By sliding the dump step bar at the bottom of the interface, the flow can be viewed at each dump step.

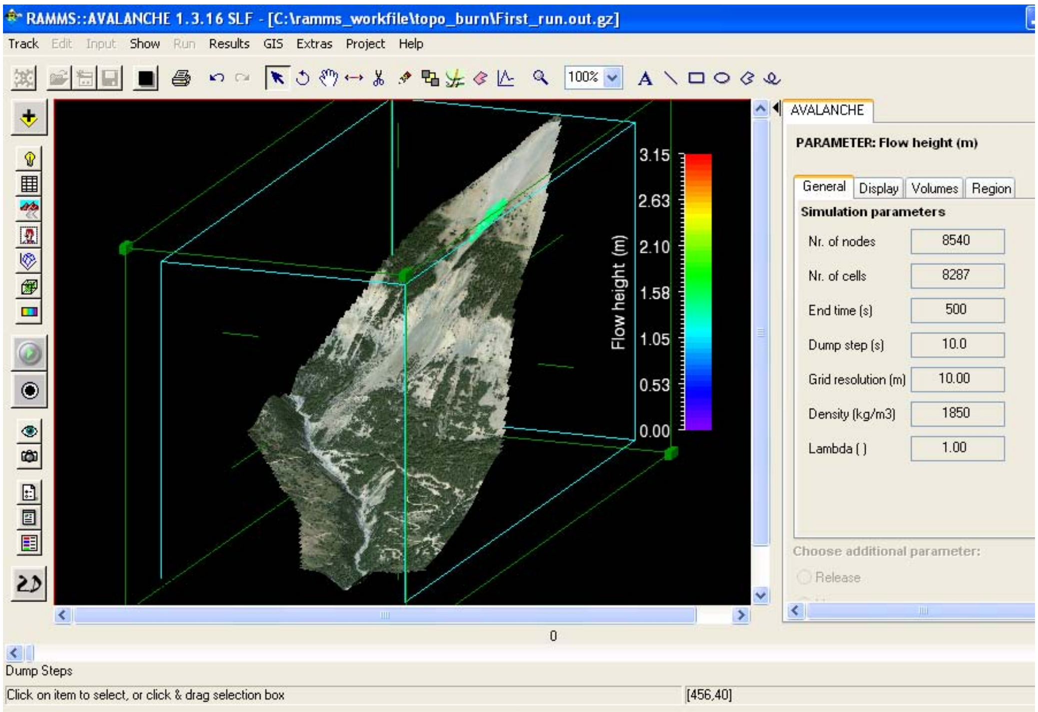

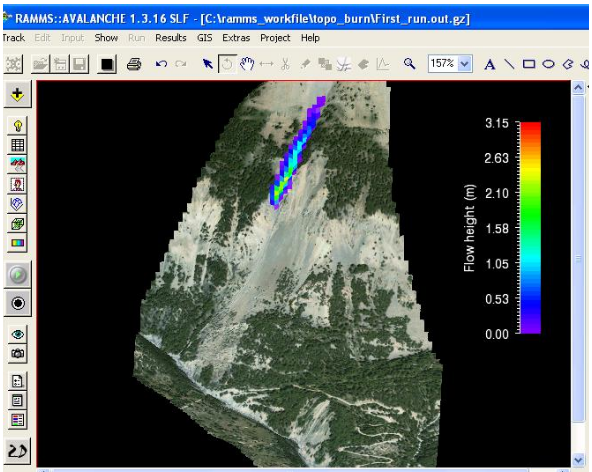

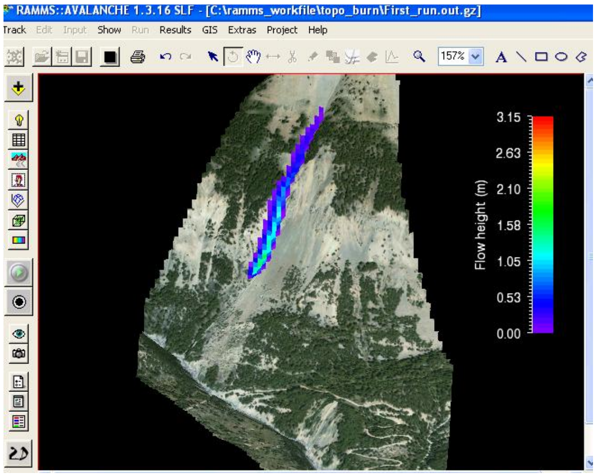

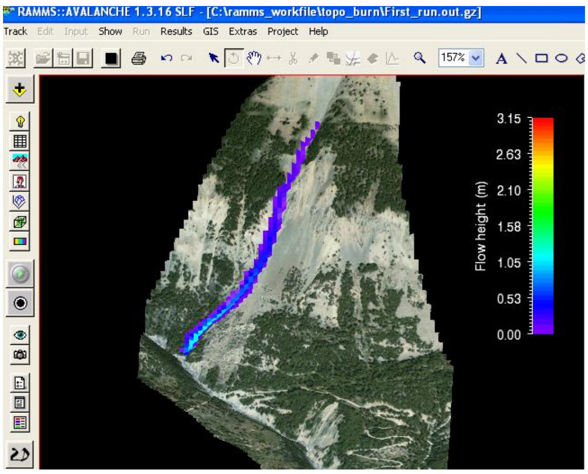

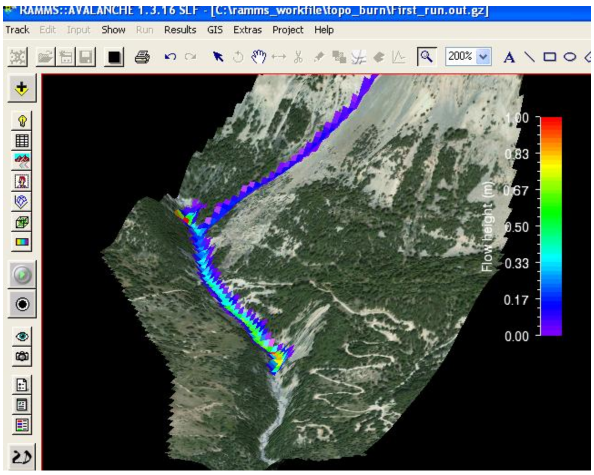

15. The maximum flow height can be viewed, chosen from the Results drop down menu.

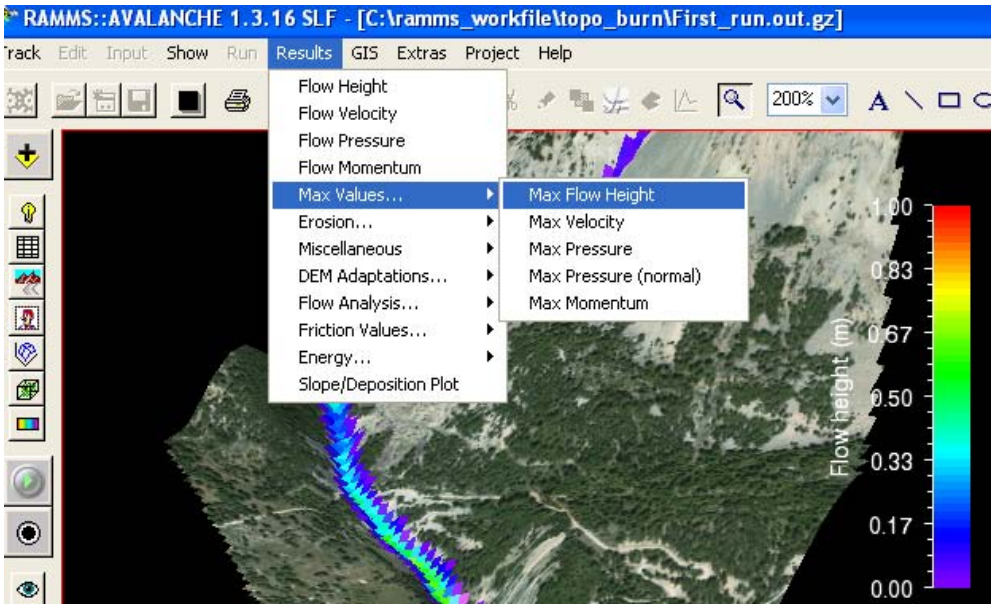

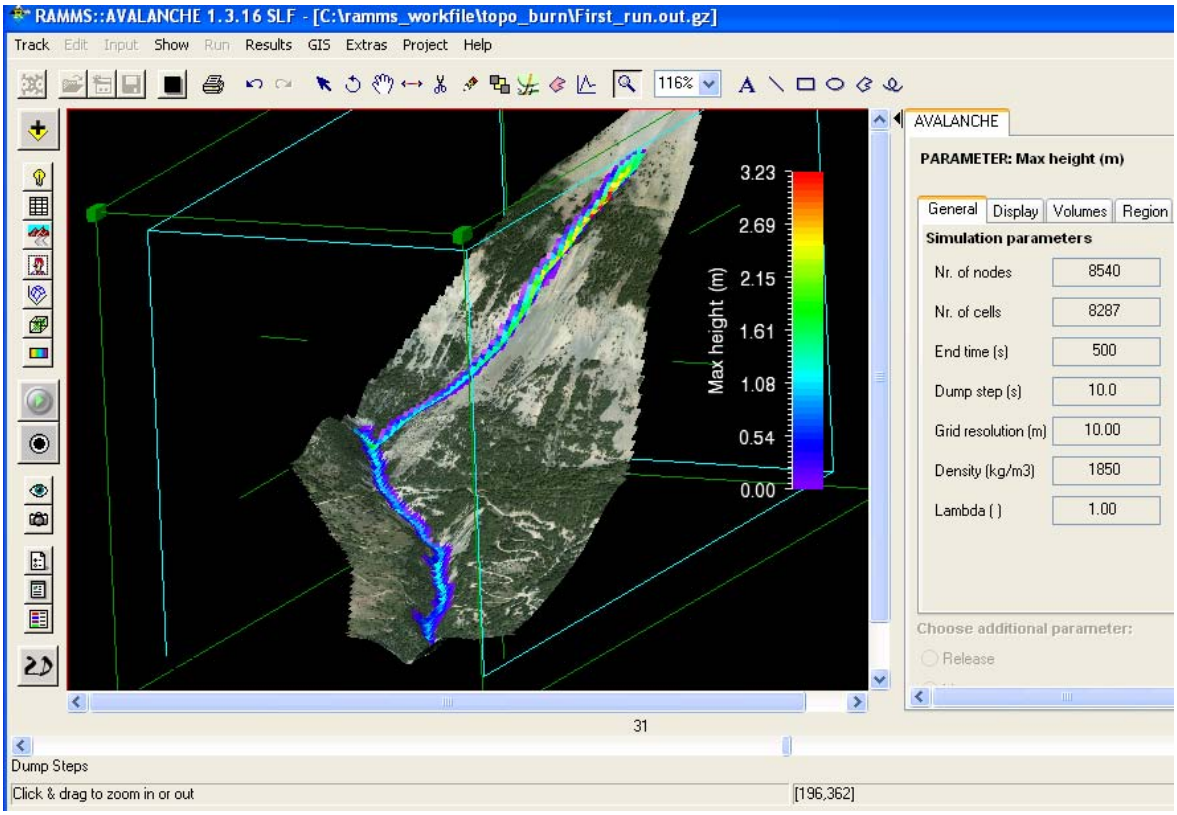

16. By switching to the 2D view, profiles and cross-sections can be drawn and assessed

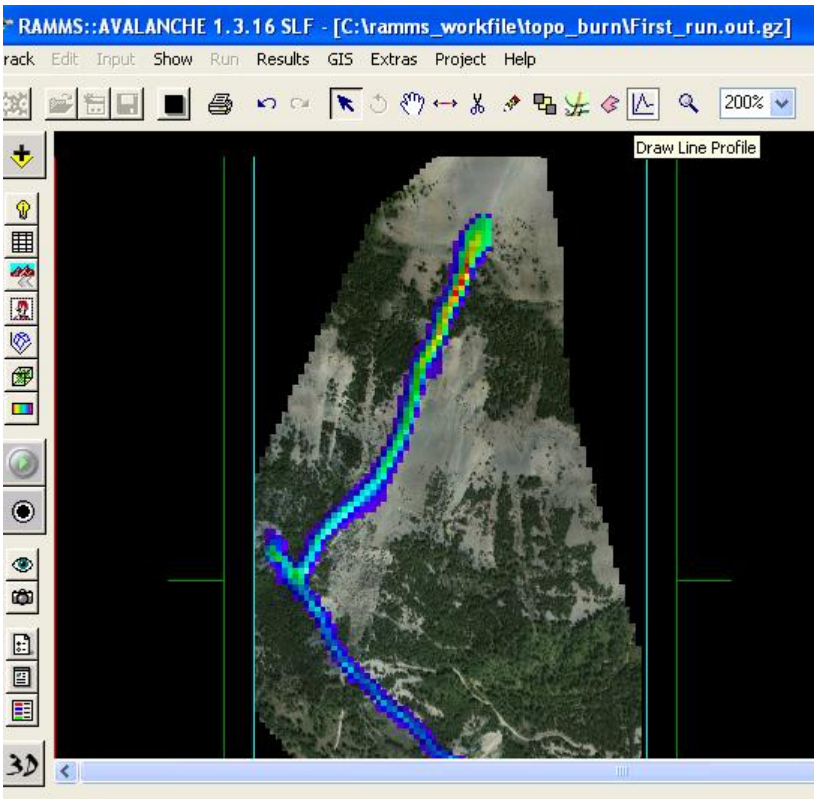

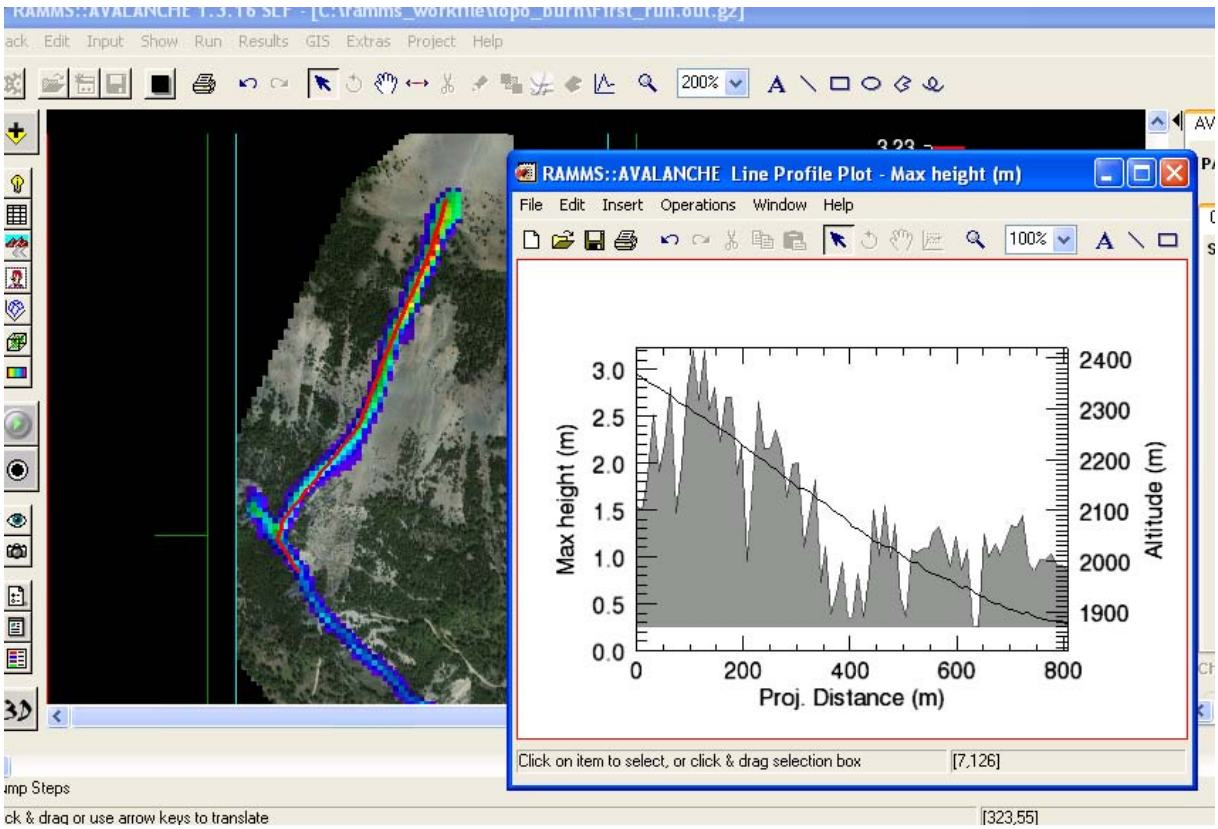

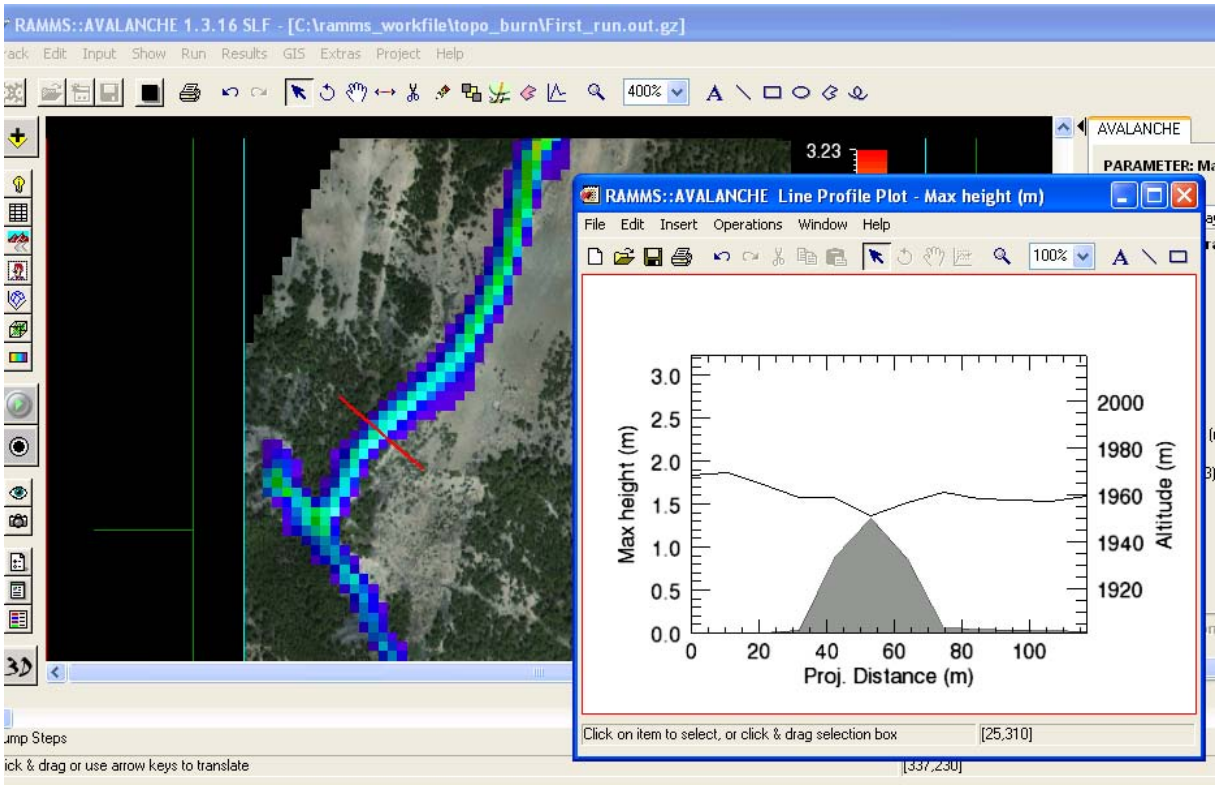
RAMMS::AVALANCHE 1.3.16 SLF - [C:\ramms_workfile\topo_burn\First_run.out.gz]
Edit Input Show Run Results GIS Extras Project Help
400%
3.23
AVALANCHE
RAMMS::AVALANCHE Line Profile Plot - Max height (m)
File Edit Insert Operations Window Help
100%
Max height (m)
3.0
2.5
2.0
1.5
1.0
0.5
0.0
0
20
40
60
80
100
Proj. Distance (m)
2000
1980
1960
1940
1920
Altitude (m)
Click on item to select, or click & drag selection box
[25,310]
[337,230]

APPENDIX IV

The 53 modeled run-outs and their corresponding outputs

Mu	Mu (%)	Runout (m)	Runout (%)	Initiation volume (m^3)	Deposit volume (m^3)	Deposit volume (%)	Max velocity apex (m/s)	Max height apex (m)	Max velocity VC3 (m/s)	Max height VC3 (m)	Max height VC3 (%)	Overall max velocity (m/s)	Overall max height (m)
0.01	-83.33	4970.00	5.74	16728.40	62973.60	-31.39	9.70	3.39	6.33	3.06	10.94	18.64	5.56
0.02	-66.67	4965.00	5.64	16728.40	71590.20	-22.00	9.19	3.34	5.59	3.10	12.30	21.38	7.89
0.03	-50.00	4925.00	4.79	16728.40	77585.40	-15.47	7.41	2.30	3.78	2.59	-6.27	21.22	7.92
0.04	-33.33	4815.00	2.45	16728.40	58474.30	-36.29	7.18	2.11	3.11	2.16	-21.93	20.69	7.75
0.05	-16.67	4755.00	1.17	16728.40	57117.70	-37.77	7.00	2.00	2.47	2.06	-25.44	20.63	7.83
0.06	0.00	4765.00	0.00	16728.40	91780.40	0.00	7.19	3.38	2.59	2.76	0.00	17.98	6.75
0.07	16.67	4515.00	-3.94	16728.40	55111.20	-39.95	6.77	2.25	1.14	1.83	-33.58	18.40	6.60
0.08	33.33	4311.00	-8.28	16728.40	54169.40	-40.98	6.43	2.69	0.81	1.19	-56.78	18.19	6.63
0.09	50.00	4215.00	-10.32	16728.40	72020.90	-21.53	5.90	3.96	0.00	0.00	-100.00	18.13	6.74
0.10	66.67	4034.00	-14.17	16728.40	68021.30	-25.89	6.10	3.98	0.00	0.00	-100.00	17.98	6.75
0.15	150.00	3565.00	-24.15	16728.40	47820.20	-47.90	5.51	4.89	0.00	0.00	-100.00	18.05	7.41
0.16	166.67	3448.00	-26.64	16728.40	48157.10	-47.53	0.00	0.00	0.00	0.00	-100.00	18.08	7.49
0.20	233.33	3036.00	-35.40	16728.40	59398.90	-35.28	0.00	0.00	0.00	0.00	-100.00	17.87	8.46

Xi (m/s^2)	Xi (%)	Runout (m)	Runout (%)	Initiation volume (m^3)	Deposit volume (m^3)	Deposit volume (%)	Max velocity apex (m/s)	Max height apex (m)	Max velocity VC3 (m/s)	Max height VC3 (m)	Max height VC3 (%)	Overall max velocity (m/s)	Overall max height (m)
100.00	-80.00	2961.00	-37.86	16728.40	48616.40	-47.03	0.00	0.00	0.00	0.00	-100.00	9.95	4.67
125.00	-75.00	3384.00	-28.98	16728.40	45050.20	-50.92	0.00	0.00	0.00	0.00	-100.00	12.03	5.84
150.00	-70.00	3586.00	-24.74	16728.40	48277.30	-47.40	3.77	2.66	0.00	0.00	-100.00	12.41	5.54
200.00	-60.00	3828.00	-19.66	16728.40	55225.80	-39.83	4.22	2.39	0.00	0.00	-100.00	13.40	5.84
250.00	-50.00	3806.00	-20.13	16728.40	53284.10	-41.94	5.52	2.50	0.00	0.00	-100.00	17.01	8.43
300.00	-40.00	4290.00	-9.97	16728.40	51880.20	-43.47	5.77	3.88	1.42	1.27	-53.89	15.73	6.69
350.00	-30.00	4311.00	-9.53	16728.40	56121.40	-38.85	6.26	2.14	1.29	1.49	-45.90	16.44	6.25
400.00	-20.00	4399.00	-7.68	16728.40	56775.10	-38.14	6.47	2.43	1.50	1.84	-33.24	19.43	7.96
450.00	-10.00	4573.00	-4.03	16728.40	56669.80	-38.26	6.79	2.43	1.67	1.91	-30.75	18.02	6.64
500.00	0.00	4765.00	0.00	16728.40	91780.40	0.00	7.19	3.38	2.59	2.76	0.00	17.98	6.75
550.00	10.00	4805.00	0.84	16728.40	97778.40	6.54	7.41	3.41	2.84	2.74	-0.92	19.22	6.85
600.00	20.00	4835.00	1.47	16728.40	89472.10	-2.52	7.82	3.56	3.11	2.75	-0.39	22.11	8.11
650.00	30.00	4845.00	1.68	16728.40	87836.00	-4.30	7.71	3.05	3.03	2.63	-4.64	21.89	7.92
700.00	40.00	4875.00	2.31	16728.40	92428.50	0.71	8.43	4.64	3.75	3.01	9.18	22.51	7.95
800.00	60.00	4895.00	2.73	16728.40	92772.70	1.08	9.09	3.99	3.89	3.08	11.46	22.85	8.02

K	K (%)	Runout (m)	Runout (%)	Initiation volume (m^3)	Deposit volume (m^3)	Deposit volume (%)	Max velocity apex (m/s)	Max height apex (m)	Max velocity VC3 (m/s)	Max height VC3 (m)	Max height VC3 (%)	Overall max velocity (m/s)	Overall max height (m)
0.00	-100.00	3438.00	-27.85	16728.40	16728.40	-81.77	0.00	0.00	0.00	0.00	-100.00	18.33	4.89
0.10	-90.00	4022.00	-15.59	16728.40	22558.30	-75.42	5.40	0.86	0.00	0.00	-100.00	18.33	4.93
0.20	-80.00	4182.00	-12.24	16728.40	32597.00	-64.48	5.87	0.90	0.00	0.00	-100.00	18.33	4.97
0.30	-70.00	4300.00	-9.76	16728.40	45007.40	-50.96	6.11	1.26	1.18	1.12	-59.36	18.33	5.09
0.40	-60.00	4357.00	-8.56	16728.40	54716.00	-40.38	6.63	1.81	1.38	1.62	-41.39	19.87	6.14
0.50	-50.00	4538.00	-4.76	16728.40	63839.80	-30.44	7.08	2.15	1.71	2.05	-25.91	18.33	5.57
0.60	-40.00	4618.00	-3.08	16728.40	69689.70	-24.07	6.97	2.46	1.98	2.24	-18.80	18.33	5.89
0.70	-30.00	4410.00	-7.45	16728.40	44959.80	-51.01	6.66	1.55	1.39	1.63	-40.91	20.75	7.14
0.80	-20.00	4527.00	-4.99	16728.40	50019.60	-45.50	6.89	1.77	1.47	1.77	-35.89	18.33	6.39
0.90	-10.00	4573.00	-4.03	16728.40	53280.70	-41.95	6.97	2.27	1.72	1.87	-32.15	20.92	7.74
1.00	0.00	4765.00	0.00	16728.40	91780.40	0.00	7.19	3.38	2.59	2.76	0.00	17.98	6.75
1.50	50.00	4765.00	0.00	16728.40	61659.00	-32.82	7.08	2.94	2.24	2.25	-18.46	21.32	8.48
2.00	100.00	4815.00	1.05	16728.40	68923.40	-24.90	7.51	3.82	2.53	2.51	-9.05	21.44	8.77
2.50	150.00	4855.00	1.89	16728.40	73341.80	-20.09	8.03	4.65	2.74	2.74	-0.77	21.03	8.84
3.00	200.00	4875.00	2.31	16728.40	78121.20	-14.88	8.40	5.36	3.03	2.95	7.04	20.28	9.01
3.50	250.00	4882.00	2.46	16728.40	77365.70	-15.71	8.60	5.51	3.14	3.06	10.73	19.93	9.08
4.00	300.00	4895.00	2.73	16728.40	75566.90	-17.67	8.89	5.86	3.28	3.08	11.62	19.48	9.09
4.50	350.00	4895.00	2.73	16728.40	80710.20	-12.06	8.90	6.35	3.41	3.19	15.69	18.87	9.07
5.00	400.00	4895.00	2.73	16728.40	79433.40	-13.45	8.95	6.49	3.43	3.18	15.14	18.83	9.11

Lambda	Lambda (%)	Runout (m)	Runout (%)	Initiation volume (m^3)	Deposit volume (m^3)	Deposit volume (%)	Max velocity apex (m/s)	Max height apex (m)	Max velocity VC3 (m/s)	Max height VC3 (m)	Max height VC3 (%)	Overall max velocity (m/s)	Overall max height (m)
0.30	-70.00	4935.00	3.57	16728.40	94958.30	3.46	7.17	5.22	3.82	2.18	-21.02	19.49	7.89
0.40	-60.00	4915.00	3.15	16728.40	94583.80	3.05	6.81	5.12	3.42	3.30	19.39	19.30	8.00
0.50	-50.00	4885.00	2.52	16728.40	96702.70	5.36	8.03	4.50	2.92	3.23	17.07	19.16	7.90
0.60	-40.00	4865.00	2.10	16728.40	98826.40	7.68	8.00	4.83	3.15	3.34	21.08	18.94	7.75
0.70	-30.00	4855.00	1.89	16728.40	99860.70	8.80	6.76	6.41	3.18	3.38	22.30	18.77	8.35
0.75	-25.00	4845.00	1.68	16728.40	104102.20	13.43	8.07	4.66	3.10	3.22	16.51	18.65	8.80
0.80	-20.00	4845.00	1.68	16728.40	100606.70	9.62	8.10	4.85	3.16	3.34	20.96	18.55	7.98
0.90	-10.00	4755.00	-0.21	16728.40	86463.00	-5.79	5.63	3.63	2.13	2.47	-10.49	18.39	6.20
1.00	0.00	4765.00	0.00	16728.40	91780.40	0.00	7.19	3.38	2.59	2.76	0.00	17.98	6.75